
GENERATIVE MOLECULAR DESIGN WITH STEERABLE AND GRANULAR SYNTHESIZABILITY CONTROL

A PREPRINT

Jeff Guo^{1,2*}
jeff.guo@epfl.ch

Víctor Sabanza Gil^{1,2*}
victor.sabanzagil@epfl.ch

Zlatko Jončev¹
zlatko.joncev@epfl.ch

Jeremy S. Luterbacher^{1,2}
jeremy.luterbacher@epfl.ch

Philippe Schwaller^{1,2}
philippe.schwaller@epfl.ch

*Equal contribution

¹ École Polytechnique Fédérale de Lausanne (EPFL)

² National Centre of Competence in Research (NCCR) Catalysis

Correspondence to {jeff.guo, philippe.schwaller}@epfl.ch

June 10, 2025

ABSTRACT

Synthesizability in small molecule generative design remains a bottleneck. Existing works that *do* consider synthesizability can output predicted synthesis routes for generated molecules. However, there has been minimal attention in addressing the *ease* of synthesis and enabling flexibility to incorporate desired reaction constraints. In this work, we propose a small molecule generative design framework that enables *steerable* and *granular* synthesizability control. Generated molecules satisfy arbitrary multi-parameter optimization objectives with predicted synthesis routes containing pre-defined allowed reactions, while optionally avoiding others. One can also enforce that *all* reactions belong to a pre-defined set. We show the capability to mix-and-match these reaction constraints across the most common medicinal chemistry transformations. Next, we show how our framework can be used to valorize industrial waste, transforming waste byproducts into *de novo* generated molecules targeting any arbitrary objective function. Going further, we demonstrate how granular control over synthesizability constraints can loosely mimic virtual screening of ultra-large make-on-demand libraries. Using only a single GPU, we generate and dock 15,000 molecules to identify promising candidates in ChEMSPACE's Freedom space 4.0 constituting 142 billion make-on-demand molecules (assessing only 0.00001% of the library). Generated molecules satisfying the reaction constraints have > 90% exact match rate. Lastly, we benchmark our framework against recent synthesizability-constrained generative models and demonstrate the highest sample efficiency even when imposing the additional constraint that all molecules must be synthesizable from a single reaction type. The main theme is demonstrating that a pre-trained *generalist* molecular generative model can be *incentivized* to generate property-optimized small molecules under challenging synthesizability constraints through reinforcement learning. The code is available at: <https://github.com/schwallergroup/saturn>.

Contents

1	Introduction	4
2	Methods	7
3	Experimental Setup	9
4	Framework Development Results	11
4.1	Development Experiments	11
4.1.1	Enforcing the Presence of Specified Reactions	11
4.1.2	Enforcing that the Synthesis Routes <i>Only</i> Contain Specified Reactions	16
4.1.3	Reaction Co-emergence and Avoiding Undesired Reactions	19
4.1.4	<i>Incentivizing</i> Shorter Synthesis Routes: Navigating the Pareto-front	21
5	Valorizing (Industrial) Waste into <i>De Novo</i> Molecules	24
6	Generative (Ultra-large-scale) Virtual Screening: Overcoming Library Scaling	27
7	Benchmarking Against Previous Synthesizability-constrained Generative Models	32
7.1	Efforts for Fair Benchmarking	32
7.2	Benchmarking Design Decisions	33
7.3	Benchmarking Results	34
7.3.1	RGFN	35
7.3.2	SynFlowNet	37
7.3.3	RxnFlow	39
7.3.4	SynFormer	40
7.4	Post-benchmark General Observations	41
8	Conclusion	43
A	Saturn: Architecture and Reinforcement Learning Algorithm	46
B	Saturn PubChem Pre-training	47
C	Rxn-INSIGHT: Reaction Name Definitions	48
D	Rxn-INSIGHT vs. NameRxn	48
E	Benchmarking Experiments Additional Details	49
F	Waste Valorization Additional Details	50
G	Additional Example Synthesis Routes	51
H	Reaction-based Enumeration to Seed Generative Experiments	51

I	Experiments with 40M Building Blocks	51
J	Development Enforce Block Experiments	52

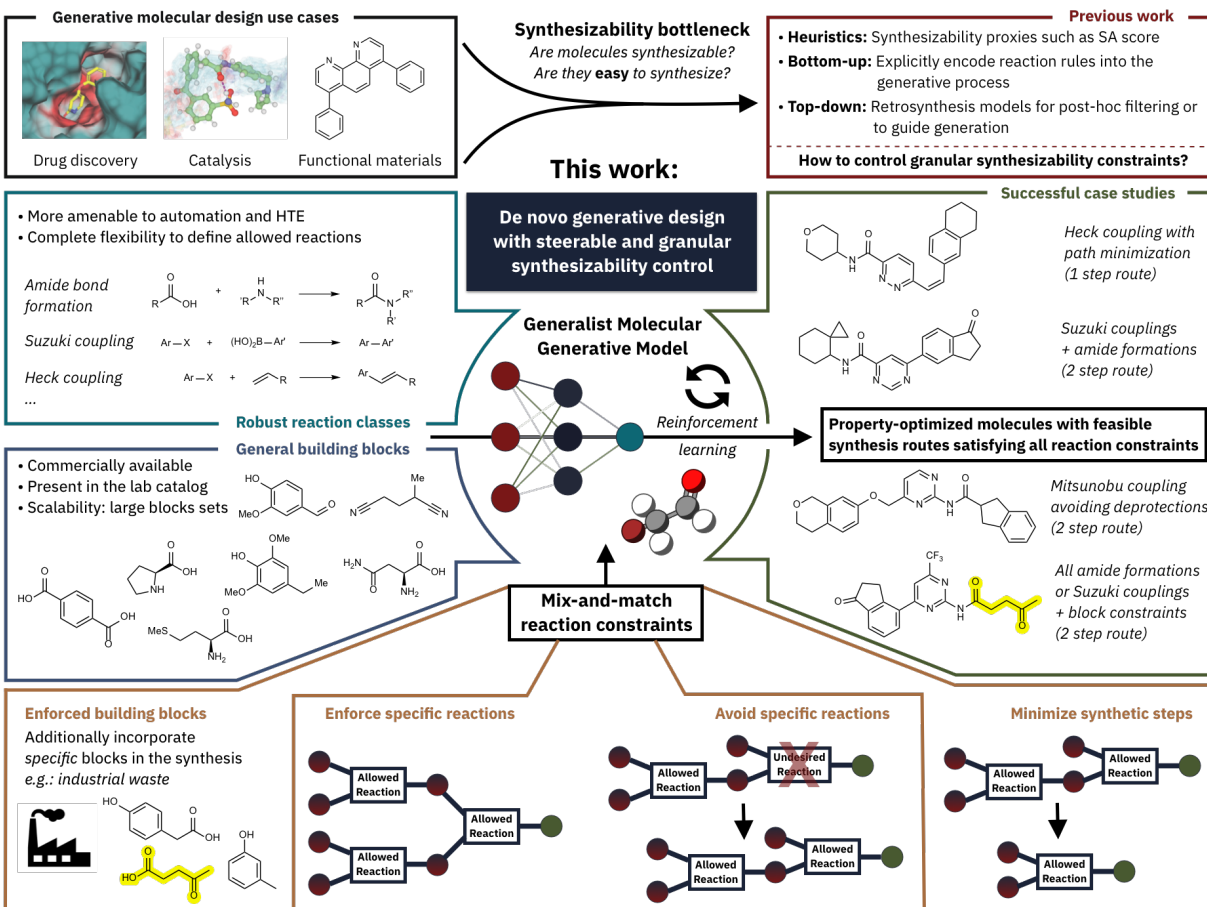


Figure 1: Overview of the framework and all reaction constraints that can be imposed. All generated molecules have a predicted synthesis route. Within these routes, reaction constraints include enforcing specific building blocks are used, enforcing specific reactions, avoiding specific reactions, and minimizing the number of synthetic steps. Molecular generation can mix-and-match these constraints which enables *steerable and granular*. The molecule SVG in the middle was created using Molecule Icon Generator¹.

1 Introduction

Designing and validating molecules are the two fundamental components of molecular discovery. Historically, domain experts’ ingenuity (which remains paramount) guided the design process, a remarkable example of which is the blockbuster drug atorvastatin (sold as Lipitor) to treat high cholesterol². A key development in the last decade to augment domain experts’ decision-making is enhanced capabilities of *in silico* molecular design, which has been enabled by increasingly accessible compute. In the pharmaceutical industry, every prioritized molecule for experimental validation now undergoes significantly more *in silico* validation³, in light of improved predictive accuracy for properties of interest. An ubiquitous example is the prediction of binding affinity using molecular dynamics simulations^{4–6}. This is a natural progression as synthesis remains the major bottleneck so greater confidence in the designed compounds can mitigate risk and accelerate experimental validation⁷. Correspondingly, the ability to run ultra-large-scale molecular docking has enabled virtual screening (VS) of “make-on-demand” libraries (10^7 – 10^{10} in size⁸), which can mitigate synthesizability challenges as these libraries are often enumerated using well-known reactions⁹. These workflows continue to achieve widespread success^{10–25} and are expected to improve with more compute and larger libraries. However, while compute is becoming cheaper, ultra-large-scale libraries are growing exponentially, making screening endeavors potentially prohibitively costly²⁶. Building on the idea of grounding molecular design with well-known reactions, *in silico* “on-the-fly” enumeration methods using selected reactions also have a rich history^{23,27–37} and has potential to avoid screening ultra-large libraries by intentional expansion.

More recently and since the first examples in 2016^{38–42}, machine learning (ML)-based generative molecular design has rapidly increased in adoption. In 2024, there were more published case studies (in academia and industry) achieving experimental validation than in the cumulative years before^{43–45}. However, while promising, the same challenge of synthesizability remains a limitation^{46–48}. Without the constraint of curated reactions, generated molecules can pose significant synthesis challenges that, while not necessarily *impossible* to synthesize, can make it practically disadvantageous over existing VS and enumeration methods. Correspondingly, many existing approaches aim to address this synthesizability bottleneck in the context of generative design. One approach is to pre-train specifically on synthesizable molecules which *implicitly* learns a distribution of these molecules^{46,49}. This enables generating new likely-to-be synthesizable molecules. In this work, we focus instead on the paradigm where a notion of synthesizability is *explicitly* considered or optimized for. We categorize three general approaches to this end:

(1) Synthesizability Heuristics. One approach is tailoring the generation to optimize for heuristics, e.g, assessing synthesizability based on the presence or absence of commonly observed fragments in previously synthesized molecules⁵⁰. These heuristics^{50–60} can function as a noisy proxy for synthesizability and have been the most common approach as they are computationally inexpensive to compute. Moreover, *any* generative model can be tasked to optimize for these heuristics without changes to the underlying model formulation.

(2) Bottom-up Synthesizability-constrained. While synthesizability heuristics are and will continue to be practically useful, more recent works explicitly address synthesizability by *constraining* the generative process. We broadly define *bottom-up* approaches, which in the most general sense, combine available ‘building blocks’, i.e., commercially available reagents, with known reactions. Since the generative process itself is *constrained*, we will refer to these models as synthesizability-constrained generative models^{60–81}. More specifically, existing approaches commonly define a set of permitted reactions and the generative process only combines together pairs of molecules that are reaction-compatible. These approaches bear similarity to reaction-based enumeration but avoid explicit exhaustive enumeration and can thus be more efficient.

(3) Top-down Retrosynthesis. Assessing synthesizability predates generative models, and the idea of “retrosynthesis” was pioneered by E. J. Corey in the 70’s^{82,83}. Retrosynthesis is the process of decomposing a target molecule into a set of building blocks that form a synthesis route back to the target molecule. Since 2017, many ML methods for multi-step retrosynthesis have been released and are enabled by coupling search algorithms^{84–89} to reactivity outcome prediction models^{90–118}. It follows that the last general approach to incorporating synthesizability in generative molecular design is to either: 1) use these retrosynthesis models as a *post-hoc filter*^{39,46,60,71,72,75,119–121} or 2) *explicitly tailor* molecular generation where these retrosynthesis models successfully output a predicted synthesis route^{49,60,122–125}. This last approach can offer many advantages:

1. *Modularity*: By de-coupling the generative and synthesizability aspects, advancements in retrosynthesis models directly benefit the generative model without any changes to the model formulation. Retrosynthesis models can also be freely swapped.
2. *Flexibility*: Does not require re-training the generative model, and the building blocks and reactions sets of the retrosynthesis models can be freely expanded or shrunk.
3. *Chemistry Expertise Incorporation*: Comparing retrosynthesis models and synthesizability-constrained generative models, the former can potentially offer a more rigorous assessment of synthesizability as the search algorithms can mimic synthetic chemists, such as by temporarily adding molecular complexity in order to yield a larger complexity decrease later¹²⁶.

In this work, we introduce *steerable and granular* synthesizability control in small molecule generative design:

Generating molecules satisfying arbitrary multi-parameter optimization objectives while being synthesizable by user-specified permitted reaction classes or specific reactions, while optionally avoiding others. The synthesis routes can also optionally be enforced to incorporate a small set of user-specified building blocks.

We show that our proposed framework is a general approach and is *malleable*, enabling tailored generation towards diverse and stringent synthesizability constraints. Compared to:

1. Bottom-up approaches (enumeration and generative-based), our framework only needs to assess a limited number of candidates before optimal molecules can be generated (sample-efficient)
2. Ultra-large-scale VS which requires massively parallelized compute clusters, our framework can be run with a single GPU-equipped computer. Our model, out-of-the-box, can also be tasked to perform essentially *retrieval* of optimal molecules from these libraries in a sample-efficient manner

Steerable and granular control over the synthesizability of generated molecules is more amenable to robotic synthesis automation. Such platforms are often specialized to perform specific reactions and/or handle specific reagent types^{127–134} and enhanced synthesizability compatibility is an important step towards autonomous molecular discovery^{135,136}. We note that recent algorithms have been proposed to promote compatibility of a set of generated molecules for parallel synthesis^{137,138}. This is done by constraining the number of unique reaction classes required to synthesize a batch of molecules, under the assumption that reactions belonging to the same class, can be performed in parallel. Building on this idea, we will show in the Results section that our framework can *directly* generate property-optimized molecules that have predicted synthesis routes involving a single user-specified reaction class, e.g., all generated molecules can be synthesized using *only* amide coupling reactions.

Lastly, very recently, Iktos proposed molecular generation with reaction constraints in a series of two papers^{60,80}. In the earlier work⁶⁰, it is stated that their retrosynthesis model, Spaya¹¹², can return predicted synthesis routes allowing specific reactions. This feedback is used to fine-tune their generative model which is an RNN (LSTM¹³⁹) with hill-climbing adapted from Neil et al.¹⁴⁰. This capability was only explicitly shown in their follow-up work⁸⁰ with a case study to generate molecules that have one-step predicted syntheses using Suzuki coupling. We cannot compare to these works since the retrosynthesis code is proprietary. Here, we present an end-to-end open-source framework capable of steering molecular generation under diverse, stringent, and granular reaction constraints (Figure 1).

2 Methods

In this section, we describe each component of the framework: **Saturn**¹⁴¹ (our previously reported generative model), **Syntheseus**¹⁴² (an interface for retrosynthesis models), **Reaction Classification** (to label reaction classes and names), and **Reward Formulation** (how we make variable and granular degrees of synthesizability constraints learnable). Our entire framework is end-to-end open-source.

Saturn: Molecular Generative Model. Saturn¹⁴¹ is a language-based molecular generative model using the Mamba¹⁴³ architecture and pre-trained on the PubChem¹⁴⁴ dataset in the SMILES¹⁴⁵ format (see Appendix B for pre-training details). Next, this pre-trained model is tuned with reinforcement learning (RL) to achieve goal-directed generation, i.e., tailoring the generation of molecules towards user-specified property objectives. The specific RL algorithm is Augmented Memory¹⁴⁶, which we previously proposed by building on REINVENT’s algorithm^{40,147,148}, which in turn is a variant of REINFORCE¹⁴⁹. Notably, Saturn is an unconditional, i.e., pre-training with unlabeled data and unconstrained, i.e., generation always proceeds token-by-token with no inductive biases. We show that *incentivizing* general-purpose models with a *sample-efficient* and *malleable* algorithm can successfully tackle challenging molecular design objectives. We refer to Appendix A for details about the Mamba architecture and RL algorithm.

Syntheseus: Multi-step Retrosynthesis Framework. Given a target molecule, retrosynthesis models propose a directed graph (*synthesis route*) with nodes and edges representing molecules and reactions, respectively. In this work, we use Syntheseus¹⁴² which is a wrapper around single-step retrosynthesis models and search algorithms, allowing mix-and-match formulations to tackle multi-step retrosynthesis. Unless otherwise stated, we use the eMolecules stock (denoted B_{stock}) representing commercially available molecules (23,077,162 in size). The specific version of eMolecules stock is from Chen et al.⁸⁶ and originally downloaded in Nov. 2019. We create an "Enforced Stock" denoted ($B_{enforced}$) by randomly sampling 100 molecules from eMolecules with the following criteria:

1. $150 \leq MW \leq 200$
2. No Stereochemistry
3. No aliphatic carbon chains > 2
4. No charged atoms
5. If a ring is present, then size = [5, 6]
6. Must contain at least 1 nitrogen, oxygen, or sulfur atom

We used these criteria to represent simple building blocks but other criteria could have been used, such as inexpensive blocks or blocks derived from industrial byproducts, as we will show in Section 5. Through Syntheseus, we use the MEGAN graph-edits⁹⁷ model re-trained by the Syntheseus authors on USPTO-50k^{150,151}. The search algorithm is Retro*⁸⁶ with a search time limit of 180 seconds or when the first route is found, whichever occurs first. We chose MEGAN due to its fast inference for method development and future work could integrate more proficient models, such as Chimera¹¹⁷ developed by the Syntheseus authors.

Reaction Classification. Syntheseus outputs a synthetic route resulting from the application of a single-step retrosynthesis model and a search algorithm. We adopt a straightforward approach to label these synthesis routes with reaction class and name information. Every *chemical transformation* from Syntheseus output is represented by a reaction SMILES. We use Rxn-INSIGHT¹⁵² which takes as input reaction SMILES and performs 10-class classification using bond-electron matrices, with the reaction class nomenclature following Carey et al.¹⁵³. Next, the reaction name is retrieved by matching to a set of 527 reaction SMIRKS¹⁵⁴. In this way, every Syntheseus route output is augmented with reaction class and name information. We note that labeling the reaction *class* with Rxn-INSIGHT adds a non-negligible amount of time to the generative experiments due to the need for atom mapping¹⁵⁵ and can be mitigated in two ways: (1) Leveraging multi-GPU nodes which we do not explore (due to GPU limitations and to showcase a framework that *any* GPU-enabled setup can run) or (2) Using a template-based retrosynthesis model with pre-labeled templates (such as the templates from Hartenfeller et al.²⁸ and Button et al.²⁹). The latter would remove the need to label chemical transformations, as they would be directly outputted. However, we opted to *not* use this solution as template-free models would be incompatible and we wanted a general solution. Moving forward, it is conceivable that the "creativity" of template-free models can be desirable as we acquire more reaction data^{61,156}. Template-free models can also complement current template-based methods and offer their own advantages¹¹⁷. In the Results section, we perform all experiments using Rxn-INSIGHT, thus constituting an end-to-end open-source framework. We also implement NameRxn¹⁵⁷ from NextMove Software as a proprietary solution for reaction labeling that is available with licensing (from NextMove Software). Two important characteristics if NameRxn were used is that: (1) The reaction labeling nomenclature differs from Rxn-INSIGHT and (2) NameRxn is much faster than Rxn-INSIGHT, such that the labeling time *is* negligible. Our framework can freely toggle between Rxn-INSIGHT and NameRxn as the reaction

labeling tool. See Appendix D for a detailed discussion on the nuances between Rxn-INSIGHT and NameRxn when used in our framework.

Reward Formulation. Previously, we coupled Saturn with Syntheseus to generate molecules satisfying various degrees of synthesizability. By running an explicit retrosynthesis search on every generated molecule, we showed that Saturn can generate property-optimized molecules with a predicted synthesis route⁴⁹, while also optionally enforcing the presence of user-specified building blocks¹²⁵. Here, we extend these capabilities to also enforce or avoid user-specified reaction classes or even *specific* reactions. In the previous section, we described how Syntheseus output can be labeled with reaction information, whereby every reaction involved has an associated name string, e.g., Mitsunobu reaction. We introduce a simple binary reward, such that the model receives a perfect reward (1.0) if the user-specified reaction *constraint* is met and 0.0 otherwise. We write *constraint* to encompass the following:

1. **‘Enforce Reaction’**: The user-specified reactions are incorporated (≥ 1) in the synthesis routes.
2. **‘Avoid Reaction’**: The user-specified reactions are *not* present in the synthesis routes.
3. **‘Enforce all Reactions’**: All reactions belong to the user-specified reactions set.

Note that one could enforce the presence of certain reactions while simultaneously avoiding others, as we will show in the Results section. Moreover, the ‘Enforce all Reactions’ constraint implies that other reactions are avoided.

Next, we comment on the binary reward formulation, which raises concerns around reward sparseness. In earlier work⁴⁹, we took the same binary reward approach to learning general synthesizability, i.e., receive perfect reward (1.0) if there is *any* predicted synthesis route. In our follow-up work¹²⁵, we formulated the TANGO reward function to tackle the task of constrained synthesizability (i.e., does the synthesis route also contain user-specified building blocks?) TANGO is a dense reward function and is necessary for robust learning in the block-constrained synthesizability setting as the binary formulation (equivalent to brute-force) is unreliable. We argue that the reward landscape imposed by the problem setting of reaction constraints can be less sparse than constrained synthesizability because retrosynthesis is a *one-to-many* problem. Given the same target molecule, there are generally multiple synthesis routes which also often contain > 1 reaction in each (multi-step synthesis). One can imagine that if the reaction constraint is only to enforce the presence of, e.g., an amide coupling, it only needs to be present in one of the many reactions in the set of synthesis routes (though in practice, we only consider a single synthesis route as we terminate retrosynthesis search when a single solution is found). Therefore, we hypothesized that this problem setting has *enough* solutions that the reward is not too sparse, such that a binary reward formulation is tolerable. As expected, under such a formulation, we see that certain reaction classes that may be less frequent, are more difficult to learn, e.g., Heck reaction (C-C coupling). In Appendix H, we explored preliminary reaction-based enumeration at the start of a generative experiment to seed the model with molecules that satisfy the reaction constraints, e.g., if the constraint were to enforce the presence of a Heck reaction, we can enumerate molecules using a Heck reaction template to guide initial learning. In general, we found this approach sometimes beneficial but that letting the model *freely explore*, resulted in higher quality generated molecules. We further discuss this in the Conclusion section.

Finally, from an implementation perspective, all reaction constraints are defined as ‘multipliers’, which either multiply the reward by 1.0 (constraint(s) satisfied) or 0.0 (constraint(s) not satisfied). In this way, we can apply reward shaping on top of the multipliers to *incentivize* other constraints that may be of interest, such as the TANGO reward for constrained block-synthesizability or route length penalization to generate molecules that can be synthesized with shorter synthesis routes. This enables users to enforce any of the reaction constraints discussed above and also optionally enforce the use of specific building blocks and/or incentivize shorter synthesis routes. Collectively, this constitutes *steerable and granular* synthesizability control over generated molecules.

3 Experimental Setup

In this section, we outline the shared experimental setup parameters, metrics, and introduce the outline of the Results section.

Experiment Parameters. Every experiment was run across 5 seeds (0–4 inclusive) with a 15,000 oracle budget and we also report the wall times. We did not tune any hyperparameters throughout the entire paper and all performance is out-of-the-box. The specific Saturn *fixed* hyperparameters are batch size 64 and 2 rounds of Augmented Memory¹⁴⁶. Lastly, we use the pre-trained Saturn model on the PubChem¹⁴⁴ dataset for all experiments (see Appendix B for pre-training details).

General Multi-parameter Optimization Objective. For method development, we fixed a specific multi-parameter optimization (MPO) objective relevant to drug discovery and adapted from our previous work^{49,125}. The components of the objective function are:

1. **Docking:** Minimize QuickVina2-GPU^{158–160} docking scores against ATP-dependent Clp protease proteolytic subunit (ClpP)¹⁶¹.
2. **QED:** Maximize the quantitative estimate of drug-likeness (QED)¹⁶² score.
3. **Hydrogen-bond Donors:** Constrain the number of hydrogen bond donors < 4 . This constraint differs from our previous work and the rationale is two-fold: (1) To make the optimization objective slightly more challenging and (2) Constraining hydrogen-bond donors can improve ADME properties^{163,164}.
4. **Synthesizability:** Various degrees of synthesizability based on predicted synthesis routes from Synthesus¹⁴² and reaction labels from Rxn-INSIGHT¹⁵². We re-iterate that the use of Rxn-INSIGHT makes the framework end-to-end open-source.

Throughout this work, we also formulated other MPO objectives, but these are experiment-specific and we defer details to the respective Results sections.

Metrics. The general evaluation metrics are summarized in Table 1.

Table 1: Summary of general evaluation metrics. The mean and standard deviation are reported across all 5 (0–4 inclusive) seeds. For the **Molecule Set Quality (Pooled)** metrics, all molecules across the 5 seeds are pooled, de-duplicated, and statistics reported.

Category	Metric (averaged or pooled across all 5 seeds)
Synthesizability	Non-synth: retrosynthesis model does not return a synthesis route
	Synth: synthesis route returned but not all constraints are met
	Synth (constraints): synthesis route returned and all constraints satisfied
	Rxn Steps: # reaction steps amongst all Synth (constraints)
	Enforced Blocks (reported if applicable): # unique enforced blocks amongst all Synth (constraints)
Molecule Set Quality (Pooled)	N Successful Runs: # seeds (out of 5) with ≥ 1 Synth (constraints)
	QuickVina2-GPU Docking Scores ^{158–160} : < -10 is considered favourable following previous work ⁷¹
	QED ¹⁶² : Quantitative estimate of drug-likeness
	Ligand Efficiency: Docking score divided by # heavy atoms
	Bemis–Murcko Scaffolds ¹⁶⁵ : # unique Bemis–Murcko scaffolds
	IntDiv1 ¹⁶⁶ : Pairwise Morgan fingerprint similarity (radius=2, nBits=1024)
Compute	#Circles ¹⁶⁷ : Sphere packing number (0.75 similarity threshold)
	Oracle Calls: # unique generated molecules scored by the objective function. <i>This is fixed at 15,000.</i>
	Wall Time: Compute time on a shared NVIDIA L40S GPU cluster

These metrics are used in all method development experiments and were chosen for a comprehensive coverage to answer the following questions:

1. Do generated molecules satisfy all user-specified reaction constraints?
2. Are generated molecules property-optimized?

A robust method should achieve both characteristics and we will highlight in the Results section cases where the reaction constraints impose a challenging Pareto-front, such that property optimization is diminished. We report both **Oracle Calls** and **Wall Time** to comment on *resource usage*. Given a fixed oracle budget, the wall time differs across models, across reward functions, e.g., if a larger building block stock were used for retrosynthesis as the search time would vary, and across GPU types. Oracle calls may also impose additional costs such as API costs. All Tanimoto similarity calculations are computed with Morgan fingerprints with radius 2 and 1024 bits. Finally, for certain experiments, other metrics are used, either to compare with previous work or to comment on experiment-specific characteristics. We defer details to the respective Results sections. Finally, we note that all wall times are reported in Appendix D to manage table sizes and also to accompany it with a discussion on Rxn-INSIGHT compared to NameRxn for reaction labeling.

Outline of Experiments. The experiments are divided into four sections as follows:

1. **Method Development:** Steering molecular generation under varying reaction constraints.
2. **Valorizing (Industrial) Waste:** Leveraging TANGO¹²⁵ and the capabilities introduced in this work to valorize industrial waste into *de novo* property-optimized generated molecules.
3. **Generative Virtual Screening:** Demonstrating how imposing reaction constraints can steer molecular generation to mimic virtual screening of ultra-large make-on-demand libraries.
4. **Benchmarking:** Performance comparison to recent synthesizability-constrained models while imposing additional reaction constraints made possible in this work.

4 Framework Development Results

All experiments were performed on a single NVIDIA L40S GPU with 48 GB GPU memory. Saturn¹⁴¹ and Syntheus¹⁴² using MEGAN⁹⁷ together take up to 5.5 GB GPU memory while QuickVina2-GPU¹⁵⁸⁻¹⁶⁰ takes 20 GB GPU memory (given the docking ‘exhaustiveness’ parameter used). Therefore, if CPU-docking were used, e.g., Glide from Schrödinger¹⁶⁸, the entire workflow can be run even on an 8 GB GPU memory card.

4.1 Development Experiments

In this section, we show that generation can be steered towards molecules having synthesis routes enforcing the *presence* of a user-specified reaction, containing *only* a set of user-specified reactions, and avoiding user-specified reactions. We will demonstrate this capability with and without the additional constraint of enforcing that the synthesis routes contain specific building blocks. These enforced blocks are from the 100 blocks randomly sampled from the eMolecules (23,077,162 in size) commercially available stock. To promote practicality of the specific reactions to enforce, we selected common medicinal chemistry reactions based on data analysis from Brown and Bostrom¹⁶⁹: amide bond-forming (**Amide**), Suzuki-Miyaura C-C coupling (**Suzuki**), the **Mitsunobu** reaction, Heck C-C coupling (**Heck**), and the **Wittig** reaction.

4.1.1 Enforcing the Presence of Specified Reactions

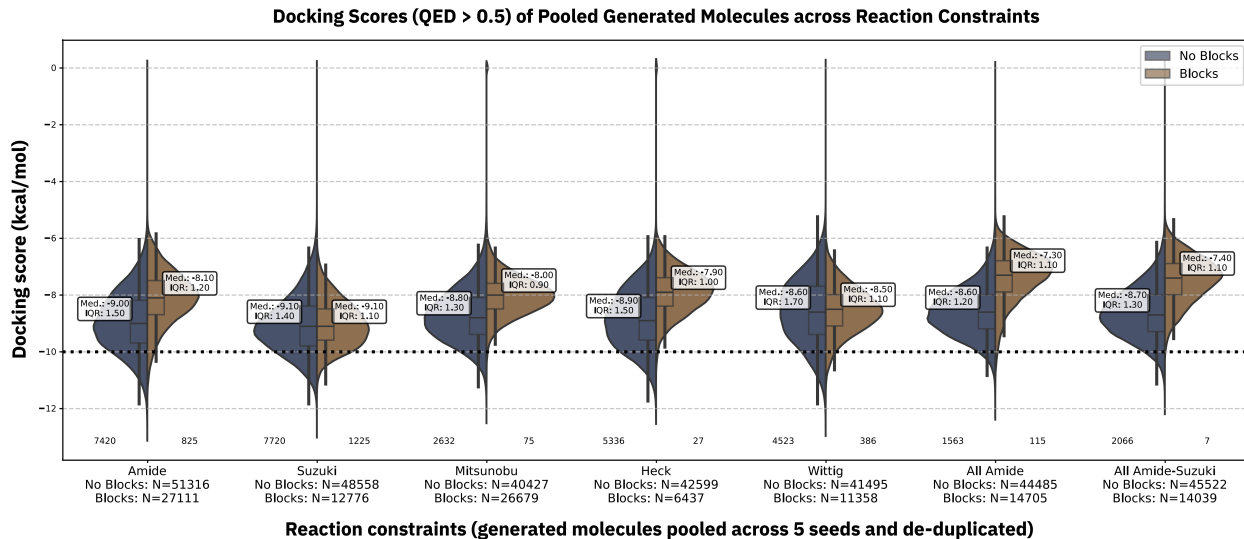


Figure 2: Docking scores of generated molecules filtered for QED > 0.5 across various reaction constraints with and without also enforcing blocks. The molecules are pooled across all 5 seeds (0–4 inclusive) and de-duplicated. N denotes the total number of molecules and annotated on the x-axis labels. The total number of molecules with docking scores < -10 are annotated just above the x-axis.

Tables 2 and 3 show the metrics for enforcing reaction presence with and without also enforcing building blocks, respectively. The docking score distributions are shown in Figure 2 which convey that also enforcing blocks is a considerably more difficult task, resulting in less optimized docking scores and less molecules satisfying all the constraints (reaction and block). We summarize the results and **bold the metric that supports the observation**:

- All reaction constraints are learnable within the oracle budget - **Synth (constraints)**
- Generated molecules are property-optimized - **Docking Score Intervals**
- Amide is the easiest constraint to learn and has the lowest number of reaction steps - **Synth (constraints)** and **Rxn Steps**
- Enforcing blocks increases optimization difficulty with fewer generated molecules satisfying the reaction constraint and the docking scores are worse - **Synth (constraints)** and **Docking Score Intervals**
- When enforcing blocks, only several unique enforced blocks are used *in the top 5% (by reward) molecules* - **# Enforced Blocks** and was observed in the original TANGO¹²⁵ work, where more block diversity could be achieved by purging the enforced block set of these specific blocks and/or aggregating results across seeds

- Amide top generated molecules are generally more diverse than molecules generated under other reaction constraints, and all the diversity metrics are lower when additionally enforcing building block presence - **# LE, BMS, IntDiv1, # Circles (0.75)**

Figure 3 shows example synthesis routes which are all chemically plausible. Generated molecules exhibit drug-like structural features as QED was optimized, which generally enforces Lipinski-compliance¹⁷⁰. We comment on some interesting examples. In the case of enforcing amide bond formation presence, the generated molecule is obtained in 3 steps (amide formation followed by deprotection of the Boc-protected amine to undergo a second amide coupling). This synthesis yields a high scoring molecule (docking score: -12.4, QED: 0.90, HBD: 1) using straightforward chemistry. When enforcing the presence of the Mitsunobu reaction, a 4-steps convergent synthesis is displayed. This route comprises a stereoselective reduction followed by an aryl-alkyl Mitsunobu coupling to react with the product of a Boc-deprotection to form an amide bond. The resulting optimized molecule (docking score -11.4, QED: 0.91, HBD: 1) exemplifies one of the advantages of our framework: the generation of convergent synthesis extracted from chemistry-specific retrosynthesis software instead of linear routes, which is a limitation in some synthesizability-constrained generative models^{71,72,75}. On the other hand, a pitfall of the retrosynthesis model is observed: in the second synthetic step (Mitsunobu reaction), the stereochemistry of the product is incorrect, as Mitsunobu reactions in this case requires an overall inversion on the reacting stereocentre. This issue arises as a consequence of incomplete template extraction, which does not consider the stereo-specificity of the reaction (however, the transformation is still considered as feasible). Lastly, when enforcing the presence of a Wittig reaction, we observe a convergent synthesis starting from a Horner-Wadsworth-Emmons (HWE) reaction involving a phosphonate and a ketone. The HWE reaction is a special variant of the Wittig reaction, and in this case it is labeled as the latter due to Rxn-INSIGHT’s¹⁵² template name definition (see Appendix C for additional discussion on template names and classification model’s issues). The resulting molecule possesses a good docking score, and in the building block constrained case (Figure 4), it additionally incorporates the enforced methyl cyclopentanecarboxylate in the route.

Table 2: **Enforcing reaction presence.** The enforced reaction is present in ≥ 1 step(s) of the predicted route. The mean and standard deviation across 5 seeds are reported. **N** denotes the number of replicates (out of 5) that have at least one generated molecule satisfying all reaction constraints. The total number of molecules in each docking score interval pooled across all 5 seeds is denoted by **M** (only molecules satisfying all reaction constraints are considered). Within each of these docking score intervals, the **QED**, number of hydrogen-bond donors (**HBD**), ligand efficiency (**LE**), number of Bemis-Murcko scaffolds (**BMS**), internal diversity (**IntDiv1**), and number of circles (**#Circles (0.75)**) are annotated. The oracle budget was fixed at 15,000.

Enforced	Synthesizability			Rxn Steps	Docking Score Intervals for Synth (constraints)		
	Non-synth	Synth	Synth (constraints)		DS < -10	-10 < DS < -9	-9 < DS < -8
Amide (N=5)	2427 \pm 382	12576 \pm 383	10640 \pm 534	2.19 \pm 1.40	-10.55 \pm 0.42 (M=7428) 0.87 \pm 0.07 (QED) 1.06 \pm 0.24 (HBD) 0.39 \pm 0.03 (LE) 6319 (BMS) 0.737 (IntDiv1) 22 (#Circles)	-9.52 \pm 0.28 (M=16824) 0.89 \pm 0.07 1.07 \pm 0.27 0.37 \pm 0.03 12423 0.758	-8.58 \pm 0.29 (M=16187) 0.88 \pm 0.09 1.14 \pm 0.38 0.35 \pm 0.04 12815 0.781 78
Suzuki (N=5)	3369 \pm 436	11637 \pm 438	10078 \pm 401	3.00 \pm 1.32	-10.49 \pm 0.36 (M=7788) 0.86 \pm 0.08 1.00 \pm 0.36 0.40 \pm 0.03 7258 0.758 17	-9.52 \pm 0.28 (M=18568) 0.87 \pm 0.08 1.00 \pm 0.43 0.37 \pm 0.03 17053 0.766 52	-8.61 \pm 0.28 (M=15037) 0.85 \pm 0.11 0.94 \pm 0.56 0.35 \pm 0.04 12389 0.788 105
Mitsunobu (N=5)	3860 \pm 1353	11148 \pm 1352	8861 \pm 1321	3.17 \pm 1.48	-10.38 \pm 0.29 (M=2659) 0.84 \pm 0.09 0.89 \pm 0.42 0.38 \pm 0.02 2486 0.720 11	-9.48 \pm 0.27 (M=13152) 0.85 \pm 0.11 0.88 \pm 0.45 0.36 \pm 0.03 10913 0.742 28	-8.57 \pm 0.28 (M=16435) 0.82 \pm 0.15 0.86 \pm 0.51 0.33 \pm 0.04 13332 0.771 49
Heck (N=5)	3993 \pm 675	11014 \pm 674	8691 \pm 970	3.29 \pm 1.38	-10.47 \pm 0.35 (M=5372) 0.86 \pm 0.08 0.97 \pm 0.48 0.40 \pm 0.03 5218 0.755 11	-9.52 \pm 0.28 (M=13284) 0.86 \pm 0.08 1.04 \pm 0.45 0.37 \pm 0.03 11833 0.777 19	-8.57 \pm 0.28 (M=13774) 0.85 \pm 0.09 1.06 \pm 0.53 0.34 \pm 0.04 11930 0.787 35
Wittig (N=5)	4478 \pm 929	10528 \pm 931	8491 \pm 664	3.64 \pm 1.46	-10.58 \pm 0.42 (M=4554) 0.78 \pm 0.08 0.84 \pm 0.46 0.37 \pm 0.02 3181 0.680 12	-9.50 \pm 0.28 (M=10078) 0.82 \pm 0.09 0.95 \pm 0.40 0.36 \pm 0.03 8339 0.780 31	-8.55 \pm 0.29 (M=12702) 0.83 \pm 0.10 0.94 \pm 0.40 0.34 \pm 0.04 10310 0.807 47

Table 3: **Enforcing reaction and block presence.** The enforced reaction is present in ≥ 1 step(s) of the predicted route. The mean and standard deviation across 5 seeds are reported. **N** denotes the number of replicates (out of 5) that have at least one generated molecule satisfying all reaction constraints. The total number of molecules in each docking score interval pooled across all 5 seeds is denoted by **M** (only molecules satisfying all reaction constraints are considered). Within each of these docking score intervals, the **QED**, number of hydrogen-bond donors (**HBD**), ligand efficiency (**LE**), number of Bemis-Murcko scaffolds (**BMS**), internal diversity (**IntDiv1**), and number of circles (**#Circles (0.75)**) are annotated. The oracle budget was fixed at 15,000.

Reaction	Synthesizability			Rxn Steps	Docking Score Intervals			Enforced Blocks in Top 5% Molecules
	Non-synth	Synth	Synth (constraints)		DS < -10	-10 < DS < -9	-9 < DS < -8	
Amide (N=5)	3036 \pm 171	11969 \pm 173	6041 \pm 722	2.33 \pm 1.28	-10.47 \pm 0.35 (M=828) 0.82 \pm 0.07 (QED) 1.10 \pm 0.30 (HBD) 0.40 \pm 0.03 (LE) 762 (BMS) 0.630 (IntDiv1) 4 (Circles)	-9.44 \pm 0.27 (M=3301) 0.84 \pm 0.07 1.12 \pm 0.33 0.37 \pm 0.03 2969 0.732 6	-8.49 \pm 0.28 (M=9698) 0.85 \pm 0.07 1.13 \pm 0.35 0.33 \pm 0.03 7634 0.710 7	5/100
Suzuki (N=4)	3354 \pm 532	11654 \pm 533	2841 \pm 1698	2.71 \pm 1.26	-10.33 \pm 0.24 (M=1278) 0.71 \pm 0.09 0.85 \pm 0.48 0.37 \pm 0.03 1199 0.679 2	-9.52 \pm 0.28 (M=5485) 0.74 \pm 0.09 0.91 \pm 0.47 0.35 \pm 0.03 4839 0.714 7	-8.60 \pm 0.28 (M=4638) 0.78 \pm 0.10 0.94 \pm 0.44 0.32 \pm 0.04 4044 0.750 5	4/100
Mitsunobu (N=5)	4762 \pm 1292	10245 \pm 1288	5648 \pm 1800	3.17 \pm 1.51	-10.37 \pm 0.30 (M=79) 0.75 \pm 0.12 0.85 \pm 0.48 0.35 \pm 0.02 75 0.530 3	-9.34 \pm 0.24 (M=1644) 0.81 \pm 0.10 0.85 \pm 0.46 0.34 \pm 0.02 1490 0.683 4	-8.46 \pm 0.27 (M=11593) 0.84 \pm 0.10 0.87 \pm 0.44 0.33 \pm 0.03 9705 0.735 4	4/100
Heck (N=5)	3963 \pm 649	11044 \pm 642	1295 \pm 1598	2.78 \pm 1.27	-10.27 \pm 0.16 (M=27) 0.84 \pm 0.08 1.00 \pm 0.00 0.43 \pm 0.02 23 0.571 2	-9.36 \pm 0.25 (M=411) 0.83 \pm 0.08 1.07 \pm 0.25 0.39 \pm 0.04 299 0.645 5	-8.47 \pm 0.27 (M=2188) 0.80 \pm 0.07 1.11 \pm 0.32 0.34 \pm 0.04 1852 0.717 6	4/100
Wittig (N=5)	4504 \pm 454	10501 \pm 450	2320 \pm 1757	3.63 \pm 1.62	-10.40 \pm 0.28 (M=400) 0.72 \pm 0.08 0.82 \pm 0.60 0.34 \pm 0.02 399 0.551 3	-9.43 \pm 0.27 (M=2585) 0.74 \pm 0.08 0.92 \pm 0.73 0.33 \pm 0.03 2307 0.696 7	-8.55 \pm 0.28 (M=5380) 0.77 \pm 0.09 1.09 \pm 0.81 0.33 \pm 0.04 4280 0.756 7	5/100

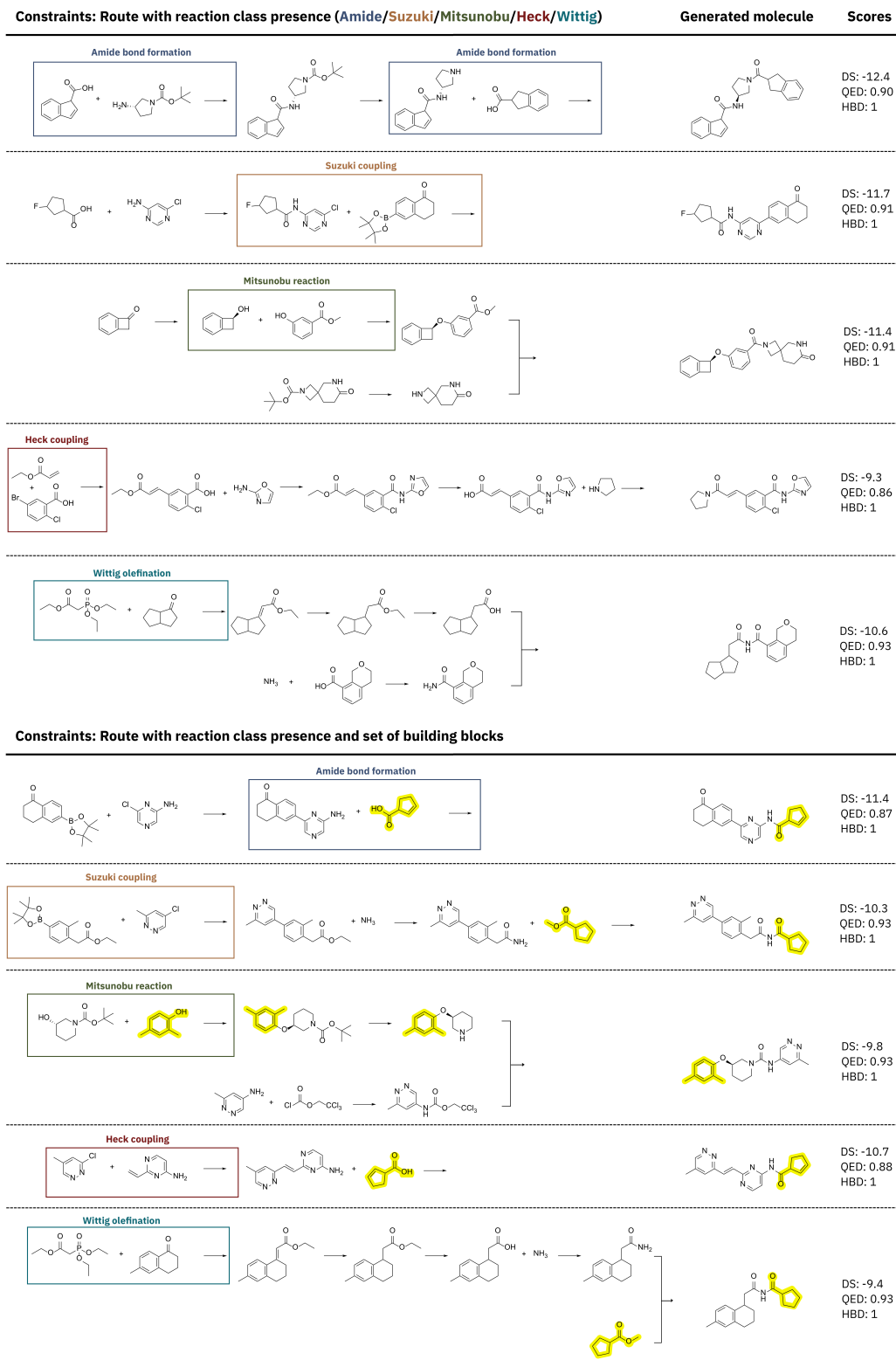


Figure 3: Example synthesis routes of generated molecules under various reaction presence constraints. **Left:** Enforcing reaction presence. **Right:** Enforcing reaction and building block presence. A box is used to denote the specific reaction satisfying the constraint. If also enforcing building block presence, the specific enforced building block is highlighted and its substructure also shown in the generated molecule. Property values of the generated molecules are annotated.

4.1.2 Enforcing that the Synthesis Routes *Only* Contain Specified Reactions

In the previous section, we showed that generation can be steered to incorporate specified reactions. This can be useful as certain reactions install specific functional groups that can be particularly desirable depending on the application, e.g., amide bonds are stable due to resonance¹⁷¹. However, as we move towards increasing automation and ease of synthesis, it is highly advantageous to narrow the number of reaction types that need to be performed to promote parallel syntheses^{137,138}. Accordingly, we chose two of the most common medicinal chemistry reactions (amide and Suzuki couplings)¹⁶⁹ and enforce generated molecules to be synthesizable using *only* these reactions. Tables 4 and 5 show the metrics with and without also enforcing building blocks, respectively. The docking score distributions are shown in Figure 2 which continues to convey that also enforcing blocks is a considerably more difficult task, resulting in less optimized docking scores. Here, this is even more apparent than when enforcing only the presence of specified reactions. We again summarize the results and **bold the metric that supports the observation**:

- Both reaction constraints are learnable within the oracle budget - **Synth (constraints)**
- The number of reaction steps is generally shorter than when enforcing only the *presence* of amide couplings (as in the previous section) - **Rxn Steps**
- The docking scores are worse than when only enforcing the *presence* of amide couplings - **Docking Score Intervals**
- When enforcing blocks, only several unique enforced blocks are used again - **# Enforced Blocks**
- Less optimal molecules are generated, although the diversity is similar to the case when enforcing only the reaction presence. When enforcing blocks, the diversity and number of optimal molecules decrease. **# LE, BMS, IntDiv1, # Circles (0.75)**

From the results, we can also see the emergence of a Pareto-front, though not a particularly surprising one: on average, molecules that can be synthesized with less steps have worse docking scores. One can verify this by cross-referencing the **Rxn Steps** and the number of generated molecules (**M**) with a docking score < -10. For a specific example, compare the docking score < -10 metrics when enforcing only the presence of amide reactions in Table 2 and now enforcing *only* amide couplings in Table 4. When enforcing only the presence of amide couplings, more generated molecules possess a docking score < -10. It is well known that larger molecules can achieve better docking scores^{172,173}. On average, fewer reaction steps yield smaller molecules, which in turn, imposes a trade-off on docking scores (though because we also optimize for QED, this effect is not more pronounced. Had we not constrained QED, then more reaction steps can freely lead to larger and larger molecules). We further explore and elucidate the implications of this behaviour in the subsequent sections.

Figure 4 shows example synthesis routes. When enforcing only amide and Suzuki couplings, we show an example route where these reactions are sequentially performed. We further note that under this double reaction constraint settings, most generated molecules have synthesis routes containing amide couplings as it is the most common reaction. Overall, this section demonstrates that generation can be steered towards property-optimized molecules that have predicted synthesis routes only incorporating user-specified reactions.

Table 4: **Enforcing all reactions are from the specified set.** The enforced reaction(s) is present in all step(s) of the predicted route. The mean and standard deviation across 5 seeds are reported. **N** denotes the number of replicates (out of 5) that have at least one generated molecule satisfying all reaction constraints. The total number of molecules in each docking score interval pooled across all 5 seeds is denoted by **M** (only molecules satisfying all reaction constraints are considered). Within each of these docking score intervals, the **QED**, number of hydrogen-bond donors (**HBD**), ligand efficiency (**LE**), number of Bemis-Murcko scaffolds (**BMS**), internal diversity (**IntDiv1**), and number of circles (**#Circles (0.75)**) are annotated. The oracle budget was fixed at 15,000.

Enforced	Synthesizability			Rxn Steps	Docking Score Intervals		
	Non-synth	Synth	Synth (constraints)		DS < -10	-10 < DS < -9	-9 < DS < -8
Amide (N=5)	1998 \pm 276	13016 \pm 277	9890 \pm 467	1.21 \pm 0.82	-10.35 \pm 0.27 (M=1564) 0.89 \pm 0.06 (QED) 1.11 \pm 0.33 (HBD) 0.41 \pm 0.02 (LE) 1301 (BMS) 0.759 (IntDiv1) 15 (#Circles)	-9.45 \pm 0.26 (M=12230) 0.91 \pm 0.05 1.09 \pm 0.29 0.39 \pm 0.03 8585 0.770	-8.56 \pm 0.28 (M=19377) 0.90 \pm 0.06 1.09 \pm 0.30 0.36 \pm 0.03 14849 0.780 51
Amide-Suzuki (N=5)	2008 \pm 177	13000 \pm 174	9790 \pm 129	1.29 \pm 0.85	-10.35 \pm 0.27 (M=2073) 0.88 \pm 0.07 1.09 \pm 0.29 0.40 \pm 0.02 1918 0.752 21	-9.46 \pm 0.27 (M=13042) 0.90 \pm 0.06 1.09 \pm 0.30 0.39 \pm 0.03 9929 0.773 29	-8.57 \pm 0.28 (M=18934) 0.90 \pm 0.07 1.10 \pm 0.31 0.36 \pm 0.03 14340 0.785 59

Table 5: **Enforcing all reactions are from the specified set and enforcing blocks.** The enforced reaction(s) is present in all step(s) of the predicted route. The mean and standard deviation across 5 seeds are reported. **N** denotes the number of replicates (out of 5) that have at least one generated molecule satisfying all reaction constraints. The total number of molecules in each docking score interval pooled across all 5 seeds is denoted by **M** (only molecules satisfying all reaction constraints are considered). Within each of these docking score intervals, the **QED**, number of hydrogen-bond donors (**HBD**), ligand efficiency (**LE**), number of Bemis-Murcko scaffolds (**BMS**), internal diversity (**IntDiv1**), and number of circles (**#Circles (0.75)**) are annotated. The oracle budget was fixed at 15,000.

Reaction	Synthesizability			Rxn Steps	Docking Score Intervals			Enforced Blocks in Top 5% Molecules
	Non-synth	Synth	Synth (constraints)		DS < -10	-10 < DS < -9	-9 < DS < -8	
Amide (N=5)	2920 \pm 242	12087 \pm 242	3947 \pm 1156	1.45 \pm 1.04	-10.37 \pm 0.26 (M=115) 0.79 \pm 0.06 (QED) 1.94 \pm 0.24 (HBD) 0.40 \pm 0.02 (LE) 113 (BMS) 0.539 (IntDiv1) 1 (Circles)	-9.44 \pm 0.28 (M=634) 0.81 \pm 0.06 1.83 \pm 0.38 0.37 \pm 0.03 551 0.597 2	-8.48 \pm 0.27 (M=1643) 0.84 \pm 0.06 1.31 \pm 0.46 0.37 \pm 0.04 1379 0.698 3	2/100
Amide-Suzuki (N=5)	3144 \pm 566	11863 \pm 566	3069 \pm 1691	1.53 \pm 1.01	-10.20 \pm 0.13 (M=7) 0.80 \pm 0.04 1.57 \pm 0.49 0.38 \pm 0.03 7 0.570 2	-9.36 \pm 0.23 (M=450) 0.81 \pm 0.06 1.81 \pm 0.40 0.34 \pm 0.03 429 0.649 3	-8.46 \pm 0.28 (M=2818) 0.84 \pm 0.06 1.64 \pm 0.49 0.33 \pm 0.03 2429 0.719 3	3/100

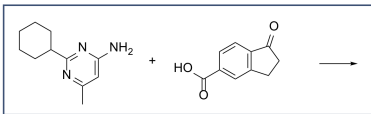
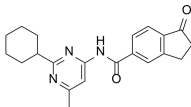
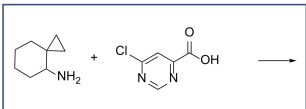
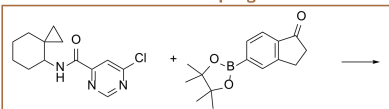
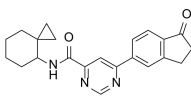
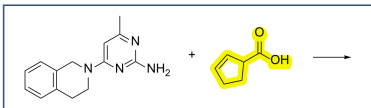
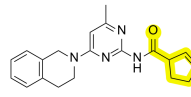
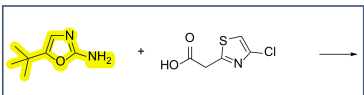
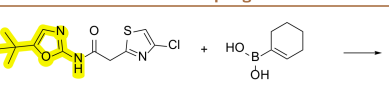
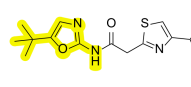
Constraints: Route with all amide bond formation reactions	Generated molecule	Scores	
<p>Amide bond formation</p> 		DS: -11.7 QED: 0.90 HBD: 1	
Constraints: Route with all amide bond formation or Suzuki reactions			
<p>Amide bond formation</p> 	<p>Suzuki coupling</p> 		DS: -11.5 QED: 0.90 HBD: 1
Constraints: Route with all amide bond formation reactions plus presence of building blocks			
<p>Amide bond formation</p> 		DS: -10.7 QED: 0.85 HBD: 2	
Constraints: Route with all amide bond formation or Suzuki reactions plus presence of building blocks			
<p>Amide bond formation</p> 	<p>Suzuki coupling</p> 		DS: -8.9 QED: 0.88 HBD: 1

Figure 4: Example synthesis routes of generated molecules containing *only* the specified reactions. **Left:** Enforcing all reactions. **Right:** Enforcing all reactions and building block presence. All reactions are boxed to denote that they belong to the specified reaction set. If also enforcing building block presence, the specific enforced building block is highlighted and its substructure also shown in the generated molecule. Property values of the generated molecules are annotated.

4.1.3 Reaction Co-emergence and Avoiding Undesired Reactions

In Section 4.1.1, we only enforced the *presence* of specified reactions. Given that the generated molecules were typically not one-step syntheses, e.g., see the example routes in Figure 3, this implies that the synthesis routes contain other reaction classes. A natural question is: *what are these other reactions?*. In this section, we show:

1. The co-emergence of heavily-represented tandem reactions
2. The ability to avoid these co-emergent reactions with minimal adverse effects over the property profiles of generated molecules

The starting point of our investigation analyzes the results from the experiments enforcing the *presence* of Mitsunobu and Wittig reactions. We chose these specific reactions because they are more difficult to enforce than common reactions such as amide coupling reactions. This enables us to demonstrate that granular control over avoiding *multiple* reaction classes is possible even when also enforcing a non-trivial reaction. As we are interested in studying the co-emergence of heavily-represented tandem reactions, all plots in this section show reactions which occur > 500 times in the generated set of molecules and for a given seed run (different seeds can have different output due to generative stochasticity). Figure 5 shows the cumulative reaction class number along the optimization for each experiment, together with a selected example route for each tandem.

Enforcing Mitsunobu. Analyzing the cumulative growth of reactions reveals that Mitsunobu reactions increase in frequency as the generative run progresses, as desired. However, deprotection reactions are heavily-represented which are often necessary for chemoselectivity, i.e., masking certain functional groups so that the next reaction occurs at the desired position (Figure 5a). The use of deprotection reactions in syntheses is undesirable because it leads to longer syntheses while generating more waste and decreasing product yields^{174,175}. Therefore, we run a generative experiment to enforce Mitsunobu reactions while *avoiding deprotections*. Analyzing the reaction frequencies shows that deprotections are effectively eliminated (Figure 5a) with minimal effect on the property profiles of generated molecules. While triaging the synthesis routes for the experiment avoiding deprotections, we noticed that some routes contain nitro-group reduction. Commonly, this reaction is palladium-catalyzed using hydrogen gas. These reaction conditions can sometimes be undesirable as palladium is a relatively expensive metal and the reaction itself can lack chemoselectivity, i.e., reducing other functional groups such as alkenes¹⁷⁶. Palladium is also undesirable in active pharmaceutical ingredients (APIs), even in trace amounts. Therefore, we run a generative experiment to enforce Mitsunobu reactions while *avoiding deprotections and nitro-group reduction*. As desired, nitro-group reduction is effectively eliminated and we see that acylation reactions to form amide bonds become heavily-represented. Interestingly, in the nitro-group reduction synthesis routes, this reduction is performed to access the free amine to perform an amide bond-forming reaction (Figure 5a). When avoiding nitro-group reduction, the model implicitly learns to generate molecules already containing the free amine. Cross-referencing earlier results in Table 3, we see that amide bond-forming reactions are also the easiest to learn due to their commonality. To further demonstrate granular control over synthesizability, we run one more experiment to enforce Mitsunobu reactions while *avoiding deprotections, nitro-group reduction, and acylation reactions to form amides*. Note this set of constraints intentionally avoids the *common* amide reactions, and should be expected to have a large impact on constraining the solution space. In order to continue satisfying the objective function, the model now leverages C-C coupling reactions (see Figure 5a, where a tandem of Mitsunobu and Aldol condensation is featured).

In this section, we increasingly imposed more stringent synthesizability constraints in response to observing undesired reactions. In general, it is difficult to know *a priori* the types of chemistry that a model generates in order to satisfy an objective function. If the synthesis routes contain undesirable reactions, we show that it is straightforward to avoid them. We adopted a purely chemical reactivity perspective to *undesirable* reactions, highlighting potential selectivity problems. However, *undesirable* reactions are not limited to reactivity. Certain reactions may require specific reaction vessels or conditions to perform that a lab may not have access to, or that chemists simply do not want for any reason.

Enforcing Wittig. We continue our investigation and show that enforcing Wittig reactions also leads to deprotection reactions being heavily-represented. Similar to the previous section, we perform an experiment to enforce Wittig reactions while *avoiding deprotections*. The Wittig reaction couples a ylide (phosphorus reagent) with a carbonyl, yielding a product containing an alkene. Interestingly, based on the growth in reaction frequencies (Figure 5b), the model finds it advantageous to reduce the resulting alkene via hydrogenation to satisfy the objective function. Previously, we commented that hydrogenation reactions *may* be undesirable due to potential selectivity problems and reagent cost. Here, however, we do not further impose any reaction constraints. We believe the results, taken together, convey that our framework enables *steerable and granular* synthesizability control, while uncovering emergent combinations of suitable reaction tandems, sometimes unexpectedly.

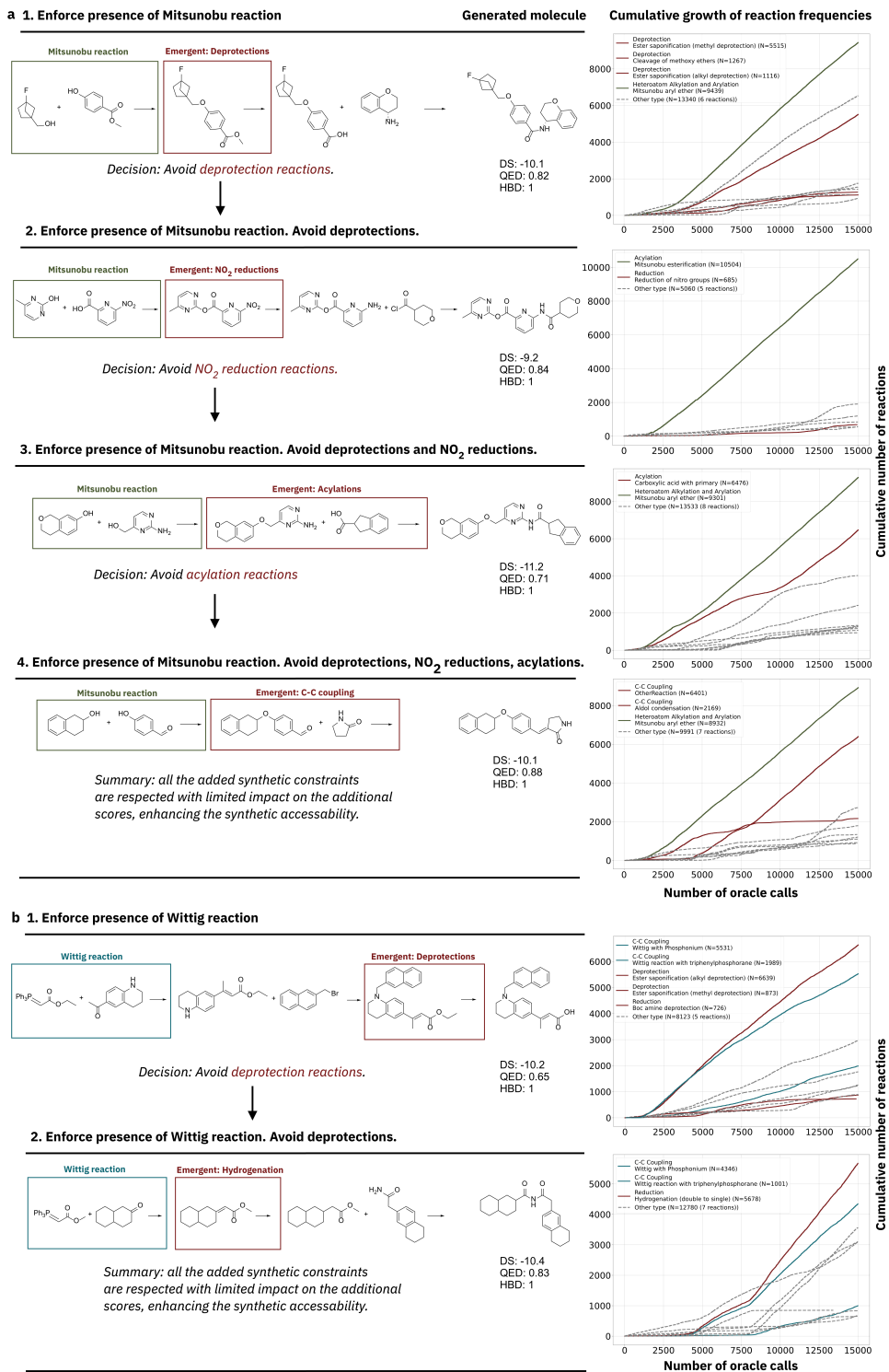


Figure 5: Co-emergence of reaction tandems and the effect of avoiding specific reaction classes. When generating property-optimized molecules, we observe that certain reactions co-emerge in frequency with the *enforced* reaction. These co-emergent reactions may be undesired and we demonstrate the ability to avoid them. **a** and **b** enforce the presence of the Mitsunobu and Wittig reaction, respectively, while avoiding other reactions. In the *Enforce presence of Mitsunobu. Avoid deprotections* example, the reaction is classified as "Mitsunobu esterification" by Rxn-INSIGHT, although specific reaction conditions would be needed to define the transformation (see Appendix C for more details about reaction name classification nuances).

4.1.4 Incentivizing Shorter Synthesis Routes: Navigating the Pareto-front

In Section 4.1.2, we enforced that generated molecules possess synthesis routes containing *only* the specified reactions. In that section, we commented that the synthesis routes when enforcing only amide reactions or amide and Suzuki reactions were often only 1-2 steps. These shorter syntheses imposed a trade-off on docking scores, such that on average, the docking scores were worse than when the syntheses were longer (such as when only enforcing reaction presence in Section 4.1.1). However, the ability to control for shorter synthesis routes has practical benefits, as long as one is aware of the potential trade-offs when doing so. In this section, we describe how shorter synthesis routes can be *incentivized* and discuss the following points:

1. The Pareto-front between synthesis route lengths and docking scores
2. Incentivizing shorter synthesis routes leads to using larger building blocks, and is a predictable emergent behaviour

Incentivize Shorter Synthesis Routes with Reward Shaping. As previously described, reaction constraints are learned via a binary reward, i.e., 1.0 if the constraints are satisfied and 0.0 otherwise. If synthesis route lengths were a concern, one would always want to *minimize* the length. We adopt a straightforward approach by applying a reverse sigmoid reward shaping transformation on top of the binary reward. This reward shaping gives higher reward to shorter paths. Therefore, given that the reaction constraints are satisfied, i.e., the binary reward is 1.0, the final reward signal is multiplied by the length shaped reward, such that the final reward $\in [0, 1]$. We choose two reaction constraints to demonstrate route length minimization:

1. Enforcing Heck reaction presence
2. Enforcing amide reaction presence *and* blocks

We chose these experiments because we noticed that the highest reward molecules generated featured long synthesis routes. We denote these experiments, which were performed in Section 4.1.1 as the *baselines*. In this section, we take these baselines and additionally incentivize route length minimization. Figure 6a shows the average route lengths for each generated batch of molecules as the experiment progresses. In both cases, incentivizing route length minimization leads to shorter routes, on average. Importantly, this is learnable while also enforcing blocks using our previously proposed TANGO¹²⁵ reward function. Figure 6c (right) shows an example synthesis route, confirming that an enforced block is present in the route. From an optimization perspective, both the TANGO and length minimization rewards $\in [0, 1]$, which essentially performs a double reward shaping on top of the binary reward for the reaction constraint. We believe this is interesting because we do not impose any explicit constraints on the generation process and that *incentivization* combined with a robust algorithm can solve challenging MPO objectives.

Trade-off Between Synthesis Route Lengths and Docking Scores. In general, larger molecules possess better docking scores^{172,173} and molecules with longer synthesis routes are often larger. However, in this case, we do not expect that generated molecules would have higher MW between the baseline and the length minimization experiments. This is because QED is part of the objective function, which imposes upper bounds on MW, otherwise decreasing the reward. Figure 6a shows that in the baselines, the docking scores improve (decrease) with longer synthesis routes. We first highlight that even if generated molecules are similar in size, having the freedom to perform additional reactions such as functional group interconversions, deprotections, or reductions which have relatively small impacts on MW, can improve docking scores. Secondly and more importantly, this leads to the question: how can it be that generated molecules have similar MW, yet the length minimization experiments yield notably shorter synthesis routes?

Learning to use Larger Building Blocks. Figure 6a shows that the length minimization experiments yield synthesis routes that are 1-2 steps shorter, on average, compared to the baseline. If the generated molecules have similar MW, the only explanation is that the model learns to generate molecules that can be synthesized using larger building blocks. We verify this in Figure 6b which plots the docking scores of the generated molecules and the number of heavy atoms in the building blocks of their syntheses. We show this across different number of reaction steps for the pooled (across 5 seeds, 0-4 inclusive) top 5% of generated molecules by reward. Note that we report the building blocks number of heavy atoms instead of MW to remove the off-chance that heavy halides skew the statistics, e.g., bromine which has a MW of 79.9. We make three observations:

1. Longer syntheses generally yield lower docking scores, as expected
2. All highest reward (top 5%) generated molecules in the length minimization experiment are 1-2 steps because otherwise, the reward is diminished and the molecules would no longer be the highest rewarding. Cross-referencing the number of heavy atoms in the building blocks, one can see that larger blocks are used, though this is more apparent in the amide and enforced block constraint

3. Amongst all the building blocks used in the top 5% of generated molecules, there is generally a greater percentage > 15 heavy atoms in the path minimization configuration (annotated in Figure 6b)

In contrast, we note that when considering the *entire* generated set, this is not true. This is unsurprising because the model needs to first *learn* to satisfy all these constraints. However, this does not detract from the utility of length minimization, as the highest reward molecules can now be synthesized in fewer steps. Figure 6c contrasts example highest reward generated molecules with and without route minimization. While there is sometimes a trade-off in docking scores, we get in return notably shorter syntheses. Quantitatively, the top 5% (by reward) molecules pooled across 5 seeds (0–4 inclusive) go from 3.97 ± 0.97 (N=2166) to 1.57 ± 0.50 (N=1934) and 3.08 ± 0.84 (N=1411) to 1.05 ± 0.21 (N=1205) for the Heck and amide and enforced block constraints, respectively. Lastly, we note that the purpose of this section is to highlight an interesting observation around implicit learning. If larger building blocks are strictly desired, one could simply optimize for it in the objective function. However, we believe the ability to minimize synthesis route lengths is a more generalizable and practical capability.

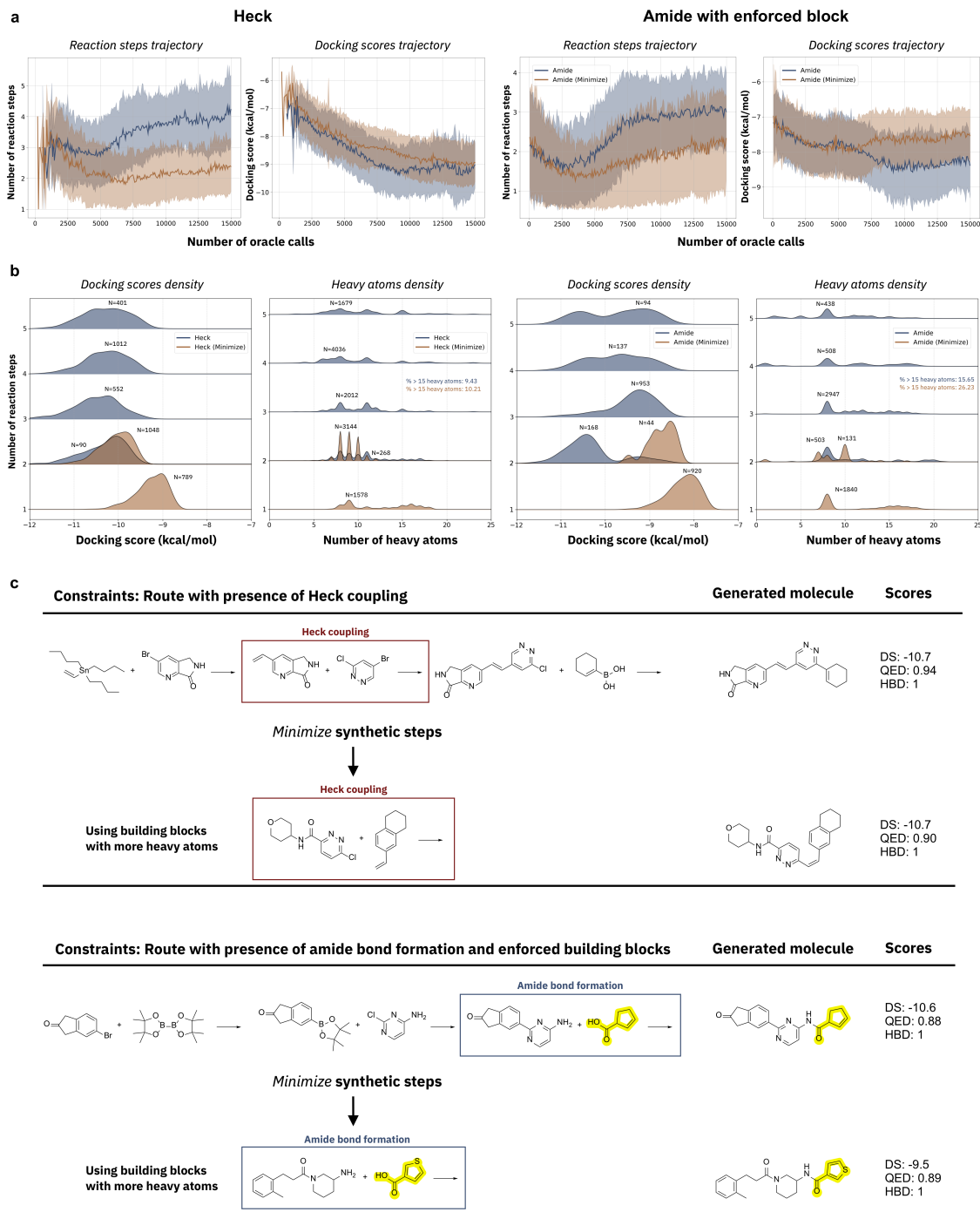


Figure 6: Effect of synthesis route length minimization on two experiments: (1) Enforcing presence of the Heck reaction and (2) Enforcing presence of an amide bond forming reaction and enforcing blocks. **a** the mean and standard deviation across 5 seeds (0–4 inclusive) of the number of reaction steps and docking scores trajectories with and without (baseline) length minimization. Generally, longer synthesis routes yield molecules with better (lower) docking scores. **b** Pooled top 5% (by reward) molecules across the seeds. The left plots show the docking scores distributions of the generated molecules. The right plots show the number of heavy atoms distributions for the building blocks in the synthesis routes of the generated molecules. When minimizing path length, a larger proportion of larger building blocks are used. 1-step results are omitted in the Heck no minimization experiment because the pooled molecules only contained 2 one-step routes. **c** Example synthesis routes of generated molecules with and without route length minimization. Length minimization results in molecules with comparable docking scores with notably shorter synthesis routes.

5 Valorizing (Industrial) Waste into *De Novo* Molecules

Recently, Wołos et al.¹⁷⁷ proposed a forward synthesis model (Allchemy) to find routes from waste molecules to valuable known products. These so-called "waste" molecules are byproducts from chemical industrial processes, and could be better defined as easily accessible building blocks, but for the sake of consistency we will refer to them as "waste". The iterative application of high-quality reaction rules starting from these molecules and subsequent network filtering enabled the discovery and experimental validation of paths to relevant known drugs. This approach opened new possibilities in the application of Computer-Assisted Synthesis Planning (CASP) tools in circular chemistry problems. Despite the impressive results, there are several limitations related to the application of the method in molecular discovery tasks. Firstly, the discovery of new active molecules is limited by the need of biasing the generation toward known drugs and agrochemicals to avoid over-exponential combinatorial explosion. Secondly, the exponential growth of the chemical space requires the computational evaluation of all the generated molecules, which makes the process intractable for large networks if using expensive oracles. We apply our framework to re-frame this problem and abstract it one step higher. Specifically, instead of trying to reconstruct valuable known molecules from industrial waste in a *bottom-up* manner, we aim to design *de novo* molecules optimized for arbitrary objectives using the same waste stock (evaluating the generated molecules in a *top-down* retrosynthetic approach). This block-constraint is enabled by our previously proposed TANGO reward function¹²⁵.

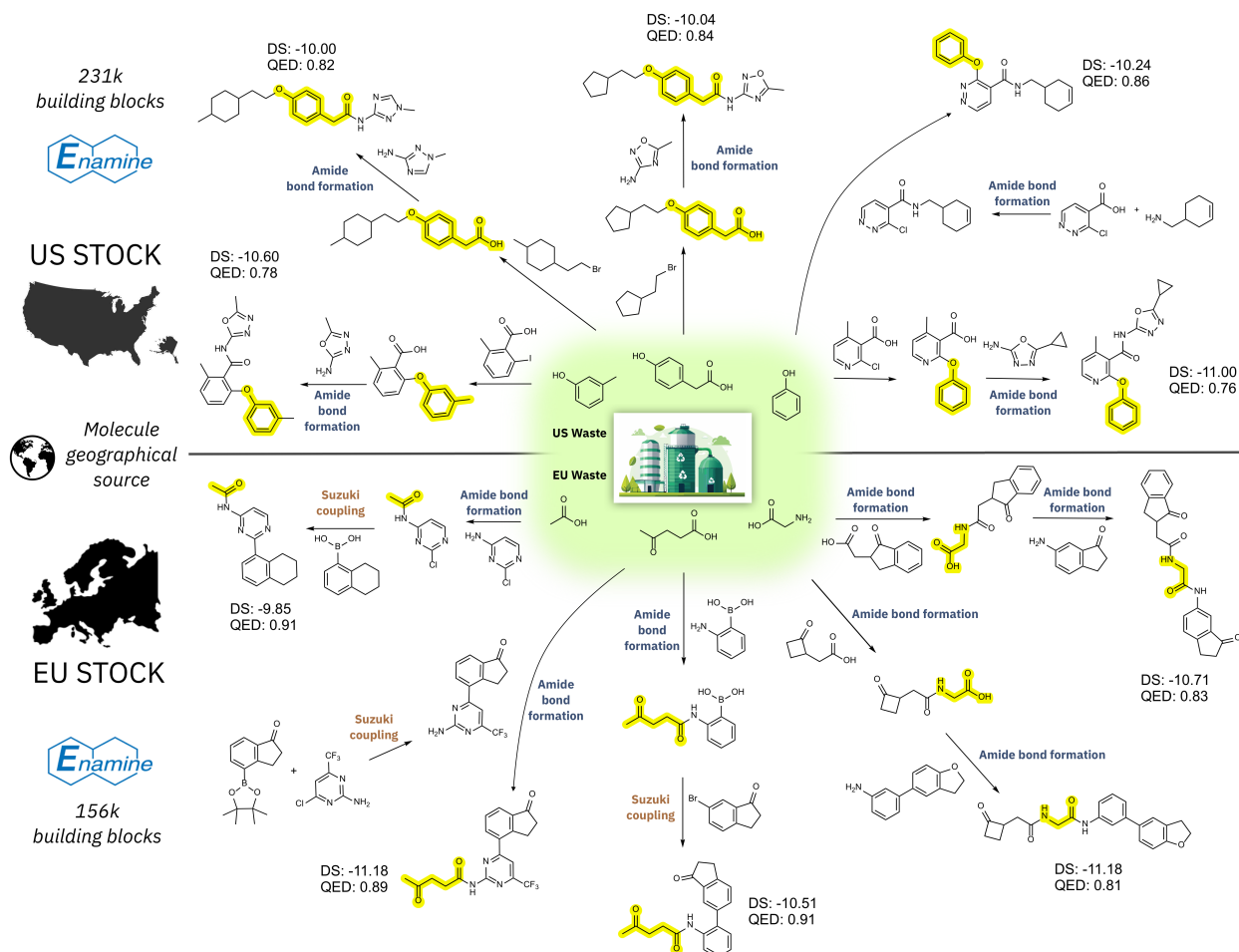
Problem Formulation. In order to build a meaningful optimization objective, we propose an objective function targeting cyclooxygenase-2 (COX2) (PDB ID: 1CX2), a receptor related to the inflammatory response¹⁷⁸. The objective is to design potential inhibitors against COX2 that can be synthesized from industrial waste products. First, we perform pose validation using Gnina¹⁷⁹ by re-docking the 1CX2 co-crystallized ligand (with a somewhat lenient RMSD < 0.75 Å). Next, we assess the capability of Gnina to distinguish between known actives and decoys from the DEKOIS 2.0 dataset¹⁸⁰, based on the docking scores. We obtain an enrichment factor of 28.4 with the top 1% docked molecules (see Appendix F for more details). The generative framework is tasked to enforce the presence of building blocks originating from industrial waste in the proposed synthesis routes. Specifically, we employ two sets of waste molecules of different geographical origin (the US and the EU, according to Wołos et al.¹⁷⁷). For each set, we use the corresponding Enamine catalog (US or EU stock, which contains building blocks that can be delivered within 1-2 days within the US or the EU, respectively) as the building blocks for the retrosynthesis model. This aims to guarantee the geographical availability of all the molecules in the synthesis for accelerated experimental validation, and to guarantee the supply chain in the corresponding location. Additionally, we enforce two sets of synthetic constraints for each waste set. The components of the objective functions are:

- **Docking:** Minimize Gnina¹⁷⁹ docking scores against 1CX2¹⁷⁸. We use Gnina instead of QuickVina2-GPU due to the higher performance of the former in docking tasks.
- **QED:** Maximize QED.
- **Synthesizability oracle:**
 - US waste: Enamine US stock (Feb. 2025, 231,472 molecules) for the retrosynthesis model. Enforce the presence of a US industry waste block, presence of amide coupling, avoid protections or deprotections, minimize the path length.
 - EU waste: Enamine EU stock (Feb. 2025, 156,510 molecules) for the retrosynthesis model. Enforce the presence of an EU industry waste block, enforce that all the reactions in the synthesis routes are amide or Suzuki couplings

For additional details of the docking objective and waste blocks used, see Appendix F.

Results. Table 6 shows the results for each experiment. Our framework successfully finds property-optimized molecules that incorporate the waste building blocks and the synthesis constraints for both US and EU building blocks. On average, the synthesis routes have less than 2 steps, which generally facilitates adherence to green chemistry principles (shorter routes should be favored as an efficiency and atom-economy principle). Although in the EU experiment routes were not optimized for path minimization, the average route length is < 2 steps, showing that under heavy reaction constraints paths can be implicitly minimized (as also remarked in Section 4.1.2 with respect to the average number of steps). In terms of docking quality, the proportion of molecules in the lower docking interval is scarce, and the average docking score is around -1 kcal/mol higher than for the reference ligand (-11.54 kcal/mol). However, this could be improved by increasing the number of oracle calls or by relaxing synthetic constraints. Figure 7 shows selected routes starting or containing 3 different waste molecules from each set. In the US stock, all routes contain an amide formation reaction, and build the final molecule in 2 steps incorporating the selected block (m-cresol, 4-hydroxyphenylacetic acid or phenol). In the case of the EU stock, all the reactions in the synthesis are either amide or Suzuki couplings, and build the final molecule in two steps incorporating the selected waste block (acetic acid, 4-oxopentanoic acid or glycine). In

Constraints: Route with amide bond formation presence, minimal steps, and enforced US waste building blocks



Constraints: Route with all amide bond formation or Suzuki reactions and enforced EU waste building blocks

Figure 7: Waste valorization experiments. In this case study, molecules are generated with optimized docking scores against COX2 (PDB ID: 1CX2) starting or containing industrial waste products. The industrial waste is divided by geographical location (originating from the US and the EU, as classified in Wołos et al.¹⁷⁷) and allowed to react with the Enamine building block stocks available in the corresponding locations (1-2 days delivery). Selected synthesis routes are shown for property-optimized generated molecules containing 3 different waste molecules originating from each location and with specific reaction constraints. In the US stock experiment, the presence of an amide bond formation with minimal synthesis steps is enforced; in the EU experiment, the presence of amide bond formation or Suzuki reactions in all the synthesis steps is enforced.

addition, some of the final molecules incorporate a high percentage of waste-derived carbon atoms, which is a desirable metric when targeting bio-based products. A concrete example is the molecules derived from 4-hydroxyphenylacetic acid in the US waste experiment which contain between 40-44% waste-derived carbon atoms (see Figure 7). It is important to note that the route quality is directly limited by the retrosynthesis model capabilities, e.g., ignorance of reaction selectivity issues. For instance, in the routes starting from glycine, selectivity issues may arise in the amide formation step due to unprotected carboxylic acid groups, and the synthesis may not be feasible without adaptations. This limitation can be mitigated as retrosynthesis models improve and incorporate better feasibility estimations, without requiring changes to the generative framework.

Prospective Biorefinery Application. These experiments show how green chemistry constraints - the use of waste molecules and minimizing the number of reaction steps - can be incorporated into the *de novo* generation of new active molecules. Additional constraints related to diverse sustainability criteria can be explicitly incorporated into the reward

function. For example, a numerical value could be computed in a similar way to the cost formulation in Wołos et al.¹⁷⁷, or by calculating a green chemistry numerical score¹⁸¹ that was recently used to improve the sustainability criteria of the synthetic route¹⁸². This is especially relevant in a biorefinery setting, where multiple molecules are produced from biomass and they must all be valorized to ensure profitability¹⁸³. Our framework could be used to rapidly explore feasible synthesis routes toward new active molecules starting from this biomass feedstock. We hypothesize that our generative framework could be effectively applied to a *de novo* biomass re-purposing task, facilitating a significant step toward circular chemistry. In addition, we showed how the strategic combination of building blocks and waste molecules by geographic source can successfully identify *de novo* molecules that can be easily manufactured in different locations.

Table 6: **Waste valorization results using specific waste block sets.** The mean and standard deviation across 5 seeds are reported. The total number of molecules in each docking score interval pooled across all 5 seeds is denoted by **M**. Within each of these docking score intervals, the **QED** is annotated. The oracle budget was fixed at 15,000.

Experiment	Synthesizability			Rxn Steps	Docking Score Intervals			Enforced Blocks in top 5% molecules
	Non-synth	Synth	Synth (constraints)		DS < -10	-10 < DS < -9	-9 < DS < -8	
US waste (N=5)	4550 ± 749	10460 ± 746	5215 ± 689	2.00 ± 1.09	-10.30 ± 0.25 (M=214) 0.73 ± 0.08	-9.32 ± 0.24 (M=2410) 0.79 ± 0.09	-8.49 ± 0.28 (M=6762) 0.82 ± 0.09	7/35
EU waste (N=5)	8639 ± 1113	6368 ± 1114	2223 ± 1847	1.88 ± 1.14	-10.48 ± 0.38 (M=1942) 0.77 ± 0.08	-9.49 ± 0.29 (M=3337) 0.80 ± 0.08	-8.56 ± 0.29 (M=2436) 0.82 ± 0.08	3/26

6 Generative (Ultra-large-scale) Virtual Screening: Overcoming Library Scaling

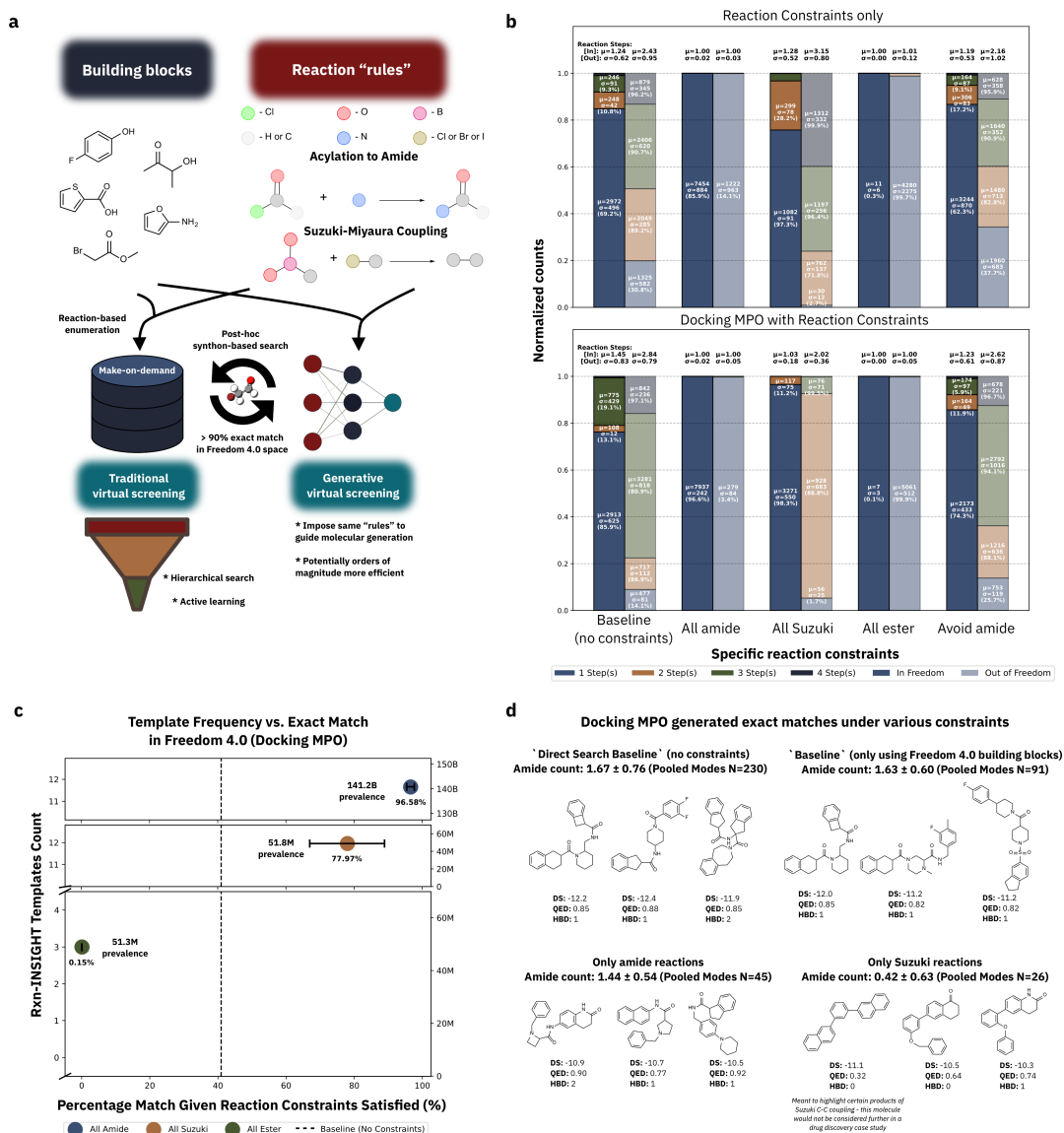


Figure 8: Generative virtual screening overview and results. **a** Ultra-large make-on-demand virtual libraries are typically enumerated with pre-selected building blocks and reaction "rules". Imposing similar reaction constraints to a generative model can loosely mimic virtual screening of these libraries. **b** Generative virtual screening results using reaction constraints to steer towards exact match in Freedom 4.0 space. The top and bottom plots are for the experiments *only* optimizing for synthesizability and the docking MPO objective, respectively. The body of the histograms are annotated with the mean and standard deviation (across 5 seeds, 0–4 inclusive) of the number of exact matches partitioned by the number of reaction steps predicted by the retrosynthesis model. Given a specific reaction step, the generated molecules are either "[In]" or "[Out]" of Freedom 4.0 so values always sum to 1. The mean and standard deviation of the overall number of reaction steps for "[In]" and "[Out]" are annotated above the histograms. **c** Selected reactions' Rxn-INSIGHT template frequencies and prevalence (estimated number of products in Freedom 4.0 using the reaction). High exact match rates are marked by high template frequency *and* prevalence. **d** Example Modes (< -10 docking score and all with < 0.5 Tanimoto similarity to each other) generated from various reaction constraint experiments. Amongst the pooled Modes (across 5 seeds), the mean and standard deviation of the number of amide bond occurrences is annotated. When not actively *detering* amide bonds, generated molecules have high prevalence of them (due to amide products being largely represented in Freedom 4.0). The *All Suzuki* reaction constraint steers away from this chemical space and can generate exact matches with markedly less amide bonds.

Thus far in this work, we have described a framework to generate molecules under various reaction constraints. In practice, many industrial early-phase drug discovery efforts focus on screening ultra-large make-on-demand libraries. This approach can be attractive as selected molecules are directly purchasable. The disadvantage is that the library is pre-defined and *may* limit novelty. Though in practice, this is often inconsequential especially if one is only interested in finding initial hits. In this section, we show that a *generalist* pre-trained generative model can *loosely* mimic ultra-large virtual screening with no overhead.

Ultra-large make-on-demand libraries continue to exponentially grow in size²⁶. As of May 2025, the largest commercial library is eXplore on the order of 10^{12} (trillion) molecules¹⁸⁴ with proprietary libraries in pharmaceutical companies many orders of magnitude larger⁸. Screening these libraries exhaustively is already infeasible and existing work reports using 5.6 million vCPUs through AWS Cloud for virtual screening²⁰. Beyond the scale of compute required, the infrastructure for data storage and transfer also requires substantial engineering efforts. Existing approaches to mitigate brute-force screening include hierarchical search (such as V-SYNTHES²¹) and active learning (such as using Thompson sampling¹⁸⁵). Very recently, Recursion proposed Scalable Active Learning via Synthon Acquisition (SALSA)¹⁸⁶. This synthon-based approach starts from an input fragment with defined exit vectors and shows scalability to search in up to 10^{12} (trillion) spaces. SALSA shows comparable or enhanced performance in identifying favourable molecules compared to existing active learning approaches such as MolPAL¹⁸⁷ and LibINVENT⁶⁶ which is a generative model that also "decorates" around a fixed scaffold. Distinct from active learning approaches, Atomwise recently proposed NeuralGenThesis (NGT) that re-frames screening as a generative task¹⁸⁸. NGT is pre-trained on a virtual space from Enamine defined based on 74,232 synthons and 21 reactions (about 3 trillion products)¹⁸⁸. The model can then *generate* molecules in this space and the authors demonstrate improved efficiency over V-SYNTHES²¹. Importantly, NGT can be run on a single GPU. However, the model was pre-trained *specifically* for the Enamine 3 trillion space which limits generalizability.

In this section, we will show that Saturn, using the *same* generalist pre-trained model can be steered to generate molecules with exact match in ultra-large make-on-demand libraries (Figure 8a). This enables leveraging Saturn’s sample-efficient optimization, where we will show that docking 15,000 molecules in total, can find docking-optimized and *diverse* molecules in ChEMSPACE’s Freedom 4.0 make-on-demand library (142 billion molecules). This amounts to screening 0.00001% of the library. We also note that no pre-defined fragments with exit vectors are required as molecules are generated completely *de novo*. To demonstrate this *generative virtual screening* (Figure 8a) capability, we adopt the same objective function as the Development experiments which we recap below:

1. **Docking:** Minimize QuickVina2-GPU^{158–160} docking scores against ATP-dependent Clp protease proteolytic subunit (ClpP)¹⁶¹.
2. **QED:** Maximize the quantitative estimate of drug-likeness (QED)¹⁶² score.
3. **Hydrogen-bond Donors:** Constrain the number of hydrogen bond donors < 4 .
4. **Synthesizability:** MEGAN⁹⁷ retrosynthesis model but instead of eMolecules stock, use the building blocks of Freedom 4.0 provided by ChEMSPACE (see Data Availability section).

Hypothesis. Virtual libraries are enumerated based on pre-selected building blocks and reactions. Conceptually, imposing the *exact same* reaction constraints on a generative model should enable generating directly in the same space. However, ensuring *exact* constraints poses some challenges: (1) Does one re-train their retrosynthesis model every time the reaction rules of a space change? (2) What if this information is not available? (3) Should one also pre-train the generative model on a similar space? (4) Can the generative model still optimize for arbitrary objective functions? Retrieving exact matches in libraries is insufficient; the molecules must also possess favourable property profiles. We continue to posit that a *generalist* model is malleable to generate in arbitrary chemical spaces through RL. Thus, we do not deviate from our PubChem¹⁴⁴ pre-trained model. Most importantly, virtual libraries are typically enumerated with relatively well-characterized reactions in order to enhance the synthesis success rates. These reactions are common and we hypothesize that out-of-the-box retrosynthesis models should have sufficiently useful coverage of the chemistry to enable guided generation in *specific* spaces.

The questions we will answer using the Freedom 4.0 space are:

1. Can *generating* exact matches be achieved using a brute-force approach?
2. How can imposing reaction constraints confer the ability to *generate* exact match molecules?
3. In addition to reaction constraints, are there characteristics of the generated molecules that increase the exact match rate?

Experimental Setup. We run two sets of experiments: (1) *Only optimizing for synthesizability* and (2) The docking MPO that also includes synthesizability. The rationale for (1) is to show that in an isolated setting, reaction constraints

directly steer generation towards Freedom 4.0 exact match. Following up with (2), this capability is retained when optimizing for an objective function. The oracle budget was fixed to 15,000 (same as Development experiments). We choose the following reaction constraints with a rough estimate of its frequency in defining the Freedom 4.0 space products in parentheses:

- Direct Search Baseline: Instead of using a retrosynthesis model, directly query Freedom 4.0 exact match for every generated molecule. Return 1.0 if matched and 0.0 otherwise
- Baseline (No Constraints): Only including the Freedom 4.0 building blocks in the retrosynthesis model
- All Amide: Only allowing amide reactions (amide reactions involved in > 100B products)
- All Suzuki: Only allowing Suzuki reactions (Suzuki reactions involved in > 50M products)
- All Ester: Only allowing Ester reactions (Ester reactions involved in > 50M products)
- Avoid Amide: Allowing *any* reaction *except* amide

The ‘Direct Search Baseline’ is essentially a brute-force approach to generate exact matches in Freedom 4.0. For the reaction constraints, all reaction labeling is performed with Rxn-INSIGHT¹⁵², which we re-iterate makes the framework end-to-end open-source. The exact reactions were chosen due to their presence and prevalence when defining the Freedom 4.0 space (this information was estimated based on data provided by Chemspace; see Data Availability for details). Lastly, to check whether generated molecules are present in Freedom 4.0, we use RDKit’s synthon-based search function, based on Cosgrove¹⁸⁹. The exact synthons and reactions used to define Freedom 4.0 were provided by Chemspace (see Data Availability). As with all experiments in this paper, we run everything across 5 seeds (0–4 inclusive) and report the mean and standard deviations.

Reaction Constraints Results. We first discuss the results when imposing reaction constraints to highlight interesting observations. Figure 8b shows the number of exact matches in Freedom 4.0, given that the reaction constraints are satisfied, and partitioned across the number of reaction steps predicted by the retrosynthesis model. In the body of individual histograms, the mean and standard deviation of the number of exact matches (given the reaction steps) is annotated. For a concrete example, see the *All Suzuki* histograms for the Docking MPO. For one-step reactions, 98.3% of molecules satisfying this reaction constraint are in Freedom 4.0. Notice that 1.7% satisfying the same reaction constraint are not in Freedom 4.0 (right-side histogram). These values *always* sum up to 1. Lastly, the mean and standard deviation of the number of reaction steps for "[In]" and "[Out]" of Freedom 4.0 are annotated at the top of the histograms. We make the following observations:

- *Just* using the Freedom 4.0 building blocks (Baseline) with no reaction constraints in the retrosynthesis model leads to considerable exact match rates
- For the baselines, there is a distribution of reaction steps. This means the retrosynthesis model predicts that the generated molecules are synthesizable over a range of reaction steps, as proposed by the retrosynthesis model. Note that we only consider molecules with up to 4 steps for figure clarity (there are few above this). Notice that the majority of exact matches are single-step reactions (quantitatively, this is annotated at the top of the histograms)
- When moving to the reaction constraints, *All Amide* and *All Suzuki* can yield very high exact match rates (> 95%) and the majority are again single-step reactions. This is consistent with *how* Freedom 4.0 is enumerated which involves many 1-2 step reaction sequences
- For *All Ester*, the majority of generated molecules are not in Freedom 4.0
- When the reaction constraints are relaxed and only enforcing to *Avoid Amide*, the exact match rates drop relative to the baseline which allows *any* reaction. This suggests that amide reactions are prevalent in defining the Freedom 4.0 space (this is true as an estimated > 100B molecules in the virtual library contain amide bonds)
- Steering for exact match using reaction constraints is still possible when performing MPO which is vital for practical applications

We follow-up with more quantitative analyses to interrogate how satisfying the imposed reaction constraints can control exact match rates (Table 7). Amongst the entire generated set of molecules, **Synth** denotes a retrosynthesis route was returned but not necessarily satisfying the reaction constraints and **Synth Match** denotes the number of exact matches in this set. **Synth (constraints)** denotes a retrosynthesis route was returned *and* satisfying the reaction constraints and **Synth (constraints) Match** denotes the number of exact matches in this set. **Exact Match Rate** denotes the percentage exact match in the **Synth (constraints)** set. Amongst the **Synth (constraints) Match** molecules, **Modes**

Table 7: Docking MPO quantitative exact match rates given various degrees of synthesizability definition. The oracle budget was fixed at 15,000. **Non-synth** denotes no retrosynthesis route was returned for the molecule. **Synth** denotes a retrosynthesis route was returned but not necessarily satisfying the reaction constraints and **Synth Match** denotes the number of exact matches in this set. **Synth (constraints)** denotes a retrosynthesis route was returned *and* satisfying the reaction constraints and **Synth (constraints) Match** denotes the number of exact matches in this set. **Exact Match Rate** denotes the percentage exact match in the **Synth (constraints)** set. Amongst the **Synth (constraints) Match** molecules, **Modes** is the number of molecules below the docking score thresholds that are also < 0.5 Tanimoto similarity to each other (radius=2, nBits=1024). **Yield** is the number of unique molecules below the docking score thresholds. All metrics are the mean and standard deviation across 5 seeds (0–4 inclusive).

^a The Search Reward Baseline is the experiment which returns a binary reward whether the generated molecules are in or out of Freedom 4.0. In this case, **Synth (constraints) Match** denotes the number of generated molecules in Freedom out of the total number of generated molecules.

Experiment	Synthesizability					Exact Match Rate	Modes (Yield) - QED	
	Non-synth	Synth	Synth Match	Synth (constraints)	Synth (constraints) Match		< -10 DS	< -9 DS
Direct Search Baseline	N/A	N/A	N/A	N/A	11123 \pm 242 ^a (15005 \pm 4)	0.74 \pm 0.02	67 \pm 15 (501 \pm 280) 0.84 \pm 0.01	255 \pm 13 (3052 \pm 769) 0.85 \pm 0.01
Baseline	5388 \pm 171	N/A	N/A	9621 \pm 174	3847 \pm 712	0.40 \pm 0.08	25 \pm 6 (70 \pm 31) 0.83 \pm 0.02	122 \pm 19 (715 \pm 176) 0.84 \pm 0.02
All Amide	5756 \pm 208	9247 \pm 207	8328 \pm 209	8220 \pm 202	7939 \pm 244	0.97 \pm 0.01	15 \pm 1 (26 \pm 5) 0.83 \pm 0.03	140 \pm 18 (980 \pm 74) 0.86 \pm 0.01
All Suzuki	9053 \pm 668	5950 \pm 670	4155 \pm 656	4452 \pm 746	3389 \pm 541	0.78 \pm 0.15	7 \pm 3 (16 \pm 10) 0.58 \pm 0.01	47 \pm 18 (229 \pm 158) 0.64 \pm 0.01
All Ester	8478 \pm 424	6527 \pm 425	175 \pm 41	5079 \pm 518	7 \pm 3	0.0015 \pm 0.0007	0 \pm 0 (0 \pm 0) N/A	0 \pm 0 (0 \pm 0) N/A
Avoid Amide	6179 \pm 737	8826 \pm 738	2630 \pm 526	8686 \pm 716	2553 \pm 515	0.29 \pm 0.04	10 \pm 4 (17 \pm 9) 0.78 \pm 0.06	69 \pm 15 (258 \pm 117) 0.81 \pm 0.03

is the number of molecules below the docking score thresholds that are also < 0.5 Tanimoto similarity to each other (radius=2, nBits=1024). **Yield** is the number of unique molecules below the docking score thresholds. We make the following observations:

- Firstly and surprisingly, the ‘Direct Search Baseline’ which simply queries whether generated molecules are exact matches results in the most number of favourable molecules generated
- The ‘Baseline’ which only uses Freedom 4.0’s building blocks without reaction constraints also performs well
- All reaction constraints lead to exact matches except *All Ester* generates almost no exact matches in agreement with the previous Figure 8b
- All reaction constraints generate exact matches with favourable docking scores but less than both Baselines, suggesting that reaction constraints can impose a trade-off
- The exact match rates of *All Amide* and *All Suzuki* are high and the standard deviation is generally low, indicating reproducibility
- Not all molecules satisfying the reaction constraints lead to exact matches, even in the case of *All Amide* which features the highest exact match rate
- In agreement with Figure 8b, *Avoid Amide* leads to lower exact match rates compared to the Baseline (allow any reaction)
- The number of Modes indicates that generated exact matches can also be diverse (based on fingerprint)

Exact Match Rate Depends on the Reaction Labeling Tool and Reaction Frequency of the Library. The results thus far convey that imposing reaction constraints can steer generation towards Freedom 4.0 exact match. However, it leads to further questions: (1) Why is *All Ester* performance so poor? (2) Why do *All Amide* and *All Suzuki* lead to such high exact match rates? We answer these questions in Figure 8c which plots the exact match rates against the number of Rxn-INSIGHT templates encoding the specific reaction and the prevalence of said reaction in enumerating the Freedom 4.0 space. We make the following observations:

- Firstly, the exact match rates are not the same as shown in Figure 8b because here, the *overall* exact match rate over all reaction steps is annotated
- *All Ester* and *All Suzuki* have similar reaction prevalence in Freedom 4.0, yet *All Ester* essentially leads to zero exact matches. A plausible explanation for this discrepancy is that Rxn-INSIGHT only has 3 and 12 templates encoding for ester and Suzuki reactions, respectively, and that the ester reaction templates are not able to cover the majority of ester forming reactions used in Freedom 4.0.
- *All Amide* is successful because it has *both* high Rxn-INSIGHT template coverage and prevalence in Freedom 4.0

The results support the observation that both template frequency in Rxn-INSIGHT and prevalence in Freedom 4.0 are important indicators for exact match rates. This is intuitive because: (1) if the reaction labeling tool cannot label the reaction, then one cannot steer to this reaction, (2) higher template frequency increases the chance that there is overlap between the reaction "rules" of the retrosynthesis model and the library, and (3) if the reaction was not used to virtually enumerate the library, then it is unlikely that enforcing said reaction would result in products present in the space. However, there are nuances to this. We have made the assumption that there is *generalizability* in the reaction "rules" used in the retrosynthesis models. We use "rules" here to encompass template and template-free retrosynthesis models. One can envision that if extremely granular reactions are used to define a virtual space, reaction *generalization* may not be expected. As a thought experiment, consider that a hypothetical virtual library and a retrosynthesis model both use a certain reaction. However, their definitions of the reactions are extremely granular (arbitrarily, one requires the presence of 2 halogens adjacent to the reaction centre and the other no halogens). If there is no overlap in the reaction definitions, then one should not expect an out-of-the-box retrosynthesis model to be able to generate exact matches in the library. However, extremely specific reaction rules also limit the number of compatible reacting partners. As such, we posit that ultra-large virtual libraries presently can have considerable *reaction generalizability* overlap with out-of-the-box retrosynthesis models, which renders our approach applicable in these settings. Thinking towards the future, one could also train a retrosynthesis model *specifically* with the reaction "rules" used to define a virtual space, which would allow matching to specific reactions.

Are there Other Advantages of Imposing Reaction Constraints? Thus far, we have mostly discussed *how* reaction constraints can steer generation towards exact matches but from a practical perspective, the glaring observation is that the 'Direct Search Baseline' results in the most property-optimal exact matches (Table 7). If this simple baseline leads to the most favourable molecules, should one care about imposing reaction constraints? We first note that while the absolute number of property-optimal exact matches are higher in the 'Direct Search Baseline', *All Amide* has a remarkably high exact match rate. Under different oracle budgets, this can lead to clear benefits. To better understand the molecular profiles from each experiment configuration, we compare and contrast the chemotypes in the property-optimal exact matches (Figure 8d). We make the following observations:

- 'Direct Search Baseline' and 'Baseline' yield molecules with high prevalence of amide bonds
- *All Amide* also results in high prevalence of amide bonds, as expected
- *All Suzuki* results in notably less amide bonds, as these can only be inherited if already present in the building blocks. The resulting molecules have a larger proportion of carbon atoms, as Suzuki is a C-C coupling reaction

Figure 8d allows us to further comment on the benefits of reaction constraints. Amide bond forming reactions are the predominant transformations used to define Freedom 4.0. It is not completely surprising that generated exact matches contain amide bonds when not *detering* for them. This can be verified with the Modes and quantitative amide bond counts. Moreover, we cross-reference Table 7 and highlight again that when *avoiding* amide reactions, the exact match rate drops. This reasonably suggests that generated molecules containing amide bonds have a higher likelihood of matching. We additionally note that an arbitrary virtual library may not, in general, have as high amide reaction prevalence. Subsequently, we highlight the example molecules from the *All Suzuki* reaction constraint which possess notably less amide bonds and can contain extensive sp²-conjugation. This demonstrates that reaction constraints can steer exact matching to different chemical spaces of the virtual libraries. When faced with an arbitrary objective function, molecules containing amide bonds *may* turn out to be unfavourable, thus being able to navigate ultra-large spaces through reaction constraints is beneficial. As a concrete example, sp²-conjugated molecules can be more suitable for functional materials design¹⁹⁰. We note, however, that in the present *drug discovery* objective function, the first-from-the-left molecule in the *All Suzuki* examples is problematic (Figure 8d) since it is fully sp²-carbon conjugated and would likely be a promiscuous binder¹⁹¹.

Overall, we have shown how *generative design* in Saturn can be re-framed to essentially perform *retrieval* in ultra-large virtual libraries in a sample-efficient manner. By assessing 15,000 molecules, which is 0.00001% of Freedom 4.0 (142 billion molecules), many property-optimal molecules are identified. We will follow up with future work in this research direction.

7 Benchmarking Against Previous Synthesizability-constrained Generative Models

Table 8: Overview of recent synthesizability-constrained generative models. **B&H** denotes the reaction templates from Button et al.²⁹ and Hartenfeller et al.²⁸. **FP** denotes molecular fingerprint.

	GFlowNets			Transformer
	RGFN ⁷¹	SynFlowNet ⁷²	RxnFlow ⁷⁵	SynFormer ⁶⁹
# Building Blocks Used in the Paper	350 or 8,350	10,000	1,193,871	223,244
Max # Blocks Tested in the Paper	64,000	221,181 "Enamine Global" (Nov. 2023)	1,193,871 "Enamine Comprehensive" (June 2024)	223,244 "Enamine US" (Oct. 2023)
Reactions	<ul style="list-style-type: none"> • 132 templates • Up to 4-steps 	<ul style="list-style-type: none"> • 105 B&H templates • Up to 4-steps 	<ul style="list-style-type: none"> • 71 B&H templates • Up to 3-steps 	<ul style="list-style-type: none"> • 115 templates • 86 that define Enamine REAL (from Jan. 2022) • 29 selected from B&H
Synthesis Routes	Linear	Linear	Linear	Linear and branched enabled by postfix notation ⁷³
Pre-training	None	None	None	Generate training data routes by randomly selecting building blocks and reactions
Methodology to Scale # Blocks	<ul style="list-style-type: none"> • MACCS FP • Action embedding scaled by FP 	<ul style="list-style-type: none"> • Morgan FP • Action embedding scaled by FP 	<ul style="list-style-type: none"> • MACCS FP & ECFP4 • Action embedding scaled by FP • Action space subsampling 	<ul style="list-style-type: none"> • Diffusion module • Scaling to longer FP (2048 vs. 256) compared to authors' previous work⁶⁷
Docking Reward Shaping Function ^a	$R = e^{(\beta * DS)}$	$R = \frac{DS + R_{\min}}{R_{\min} + R_{\max}} - 1^b$	$R = 0.1 * \max(-DS, 0)$	N/A ^c
Peak GPU Memory ^d (Block Set Size)	44 GB (350) 55 GB (50k)	2 GB (10k) 15 GB (240k)	19 GB (1.27M)	3.2 GB (225k)

^a This row shows the reward shaping functions specifically used for docking objectives in the corresponding papers.

^b The default values are $R_{\min} = -10$ and $R_{\max} = -1$. SynFlowNet's reward shaping further adds a -0.4 reward penalty if the # of heavy atoms in the generated molecule > # heavy atoms in the reference ligand + 8.

^c SynFormer did not have case studies specifically optimizing for docking scores.

^d This row reports the peak GPU memory consumption when we ran each model with varying building block set sizes. The value is *only* for the model consumption. The QuickVina2-GPU oracle additionally consumes 20-24 GB.

Recently, synthesizability-constrained generative models have grown in popularity, particularly from mid-2024 to present^{60,69–77,79,80}. The most common approach to date is by encoding explicit bias in the generation process such that molecular generation proceeds by sampling building blocks and compatible reaction templates, following early work from Gao et al.⁶⁷. The advantage of this approach is that all generated molecules are synthesizable, limited only by the reaction templates' granularity (and lack of reaction conditions, but all methods are limited by this). Specific recent works include Reaction-GFlowNet (**RGFN**)⁷¹, SynFlowNet (**SFN**)⁷², **RxnFlow**⁷⁵, and **SynFormer**⁶⁹. We highlight these specific works as the first versions of these models were proposed at a similar time with the former three building on the GFlowNet formulation^{192,193}. In this section, we compare our framework to these models with two important caveats which we discuss in the following subsections:

1. Efforts for fair benchmarking
2. Specific benchmarking challenges related to **model-intrinsic features** and **design decisions**

7.1 Efforts for Fair Benchmarking

Generative models fundamentally model distributions and algorithmic optimization shifts this distribution towards satisfying arbitrary objective functions. An exact, fair comparison should be that all methods define the same chemical space and/or start from the same distribution. This is done in the Practical Molecular Optimization (PMO) benchmark¹⁹⁴ where all methods are pre-trained (if necessary) or parent populations initialized (in the case of genetic algorithms) based on ZINC 250k¹⁹⁵. Moreover, the PMO benchmark also defines a common hyperparameter tuning procedure so no particular method may potentially benefit from more hyperparameter tuning on the specific task. These are important because it removes confounding variables. Amongst the *first pre-print versions* of the GFlowNet synthesizability-constrained models, RxnFlow (Oct. 2024) was published latest and the authors compared to RGFN (June 2024) and SFN (May 2024). In Table 8, we contrast some key features of the models. The key point we want to convey is that all methods define a different chemical space, due to different building blocks and reaction templates. In the specific case of RxnFlow, the authors introduce *action space subsampling*, which enables their method to scale to using larger

building block sets (the authors tested up to 1.2M). In contrast, RGFN and SFN have limitations scaling to this building block set size due to the GPU memory requirements which we will comment on in the Benchmarking Results section. The building block sets and reaction templates define the chemical space the GFlowNets can sample from which means it *could be* that certain defined spaces are more beneficial for specific optimization objectives.

Our framework generates molecules *freely* and "synthesizability" is assessed by a retrosynthesis model. Therefore, for an *exact* comparison with existing works, we would have to enforce the same reaction templates. However, as shown in Table 8, existing works all use different building block and template sets. RxnFlow’s formulation also enables using larger building block sets, which can be viewed as an advantage as it covers a *much* larger chemical space. If RxnFlow is able to scale to larger building block sets, we believe one should not necessarily truncate its building block set to match other works. Therefore, we *do not* make an effort to compare *amongst* the synthesizability-constrained models. Instead, we take our framework and *match* the set-up of each individual model, with still the following caveats:

1. Reward shaping function
2. Pre-training
3. What is considered "synthesizable"?

Reward Shaping Function. RGFN, SFN, RxnFlow, and SynFormer all define different *reward shaping functions*, i.e., how is the raw oracle output transformed into a reward signal for the model to learn (see Table 8). For example, in the docking objectives, RGFN defines $\beta = 4$ and takes the exponential of the absolute docking score which equates to a very large reward. By contrast, SFN and RxnFlow shape the reward such that it is upper-bounded slightly larger than 1.0 (to be precise, there is no explicit upper-bound, but the magnitude of docking scores will generally not exceed 15 and this constrains the reward). Differing reward shaping can be a confounding variable and we note that the PMO benchmark¹⁹⁴ fixed the reward functions and hence shaping. We note that our method also has its own reward shaping (though it has not been changed from our previous works^{49,125}). Therefore, we make the decision to use the reward shaping functions as defined. If the specific reward functions were defined, then it is reasonable to expect that they *work* for that model, if not also tuned.

Pre-training. As previously discussed, all methods define a different chemical space through differing building block and reaction template sets. Our method pre-trains on PubChem¹⁴⁴, thus our starting chemical space is also different. We *do not* pre-train to define the same chemical space as each individual model as we believe a generalist pre-trained model over a large chemical space is practically advantageous. We further comment on this in the next sub-section.

What is Considered "Synthesizable"? All synthesizability-constrained models, by design, output synthesizable molecules, subject to reaction template limitations. Our framework does not intrinsically generate synthesizable molecules and instead, learns to do so through feedback from a retrosynthesis model. The retrosynthesis model we use in this work is MEGAN⁹⁷ which has different reaction rules encoded. We note again that every existing work defines different reaction rules due to template set differences. For an exact comparison, we should define a retrosynthesis model with *only* the template sets of each model. We *do not* consider this and make the decision to designate every generated molecules from synthesizability-constrained models as synthesizable. For our method, every generated molecule with a retrosynthesis solved route will be considered synthesizable. Note that in all GFlowNet works, the retrosynthesis model AiZynthFinder^{99,100} is used to further verify synthesizability even though the generated molecules have been generated through reaction template combinations. In practice, retrosynthesis models can have advantages such as generating multiple potential synthesis routes for a given target molecule. A disadvantage of using retrosynthesis models over synthesizability-constrained generation is the increased compute. This is also one of the motivations of existing works to amortize the cost of training on synthesis routes^{67,69,196} such that during generation, the model has already learned to generate synthesizable molecules.

7.2 Benchmarking Design Decisions

In this sub-section, we discuss important design decisions we make when comparing our method to the existing synthesizability-constrained models.

Building Block Scaling Limitations. The building block stock, together with the reaction "rules" (we say rules here to encompass template and template-free reaction approaches), define the synthesizable chemical space. Smaller building block stocks necessarily restrict the chemical space by sheer fact that there are less unique blocks to react. Very common building block stocks (we report their sizes as of April 2025) used in synthesizability-constrained works include Enamine’s Global Stock (307,929), US Stock (258,685), EU Stock (179,401) and Comprehensive Catalog (1,415,470). If one is interested in designing synthesizable molecules, it is reasonable to use these stocks as is, because they can all be ordered and delivered within a set time-frame. We now highlight that some GFlowNet works use much more constrained building block sets (see Table 8 for a summary). RGFN uses 350 blocks (but investigate up to 64,000)

in their main experiments with the rationale being that they are cheap and accessible⁷¹. This is reasonable but defines a very narrow chemical space as even if the state space, i.e., all reachable molecules combining blocks and reactions, is large, the diversity of the space is inherently limited. SFN uses 10,000 blocks in their main experiments but investigate up to 221,181 (Enamine’s Global Stock from Nov. 2023)⁷². However, in these works, since the main experiments were not run with larger block sets, it is unclear the performance in these settings.

In this work so far, we have been using eMolecules (23,077,162 in size) stock originally from Chen et al.⁸⁶. Building blocks from eMolecules can often be delivered within days so it is reasonable to consider this entire block set¹⁹⁷. This is orders of magnitude larger than the existing synthesizability-constrained works which will have challenges scaling to this size (we will show this explicitly in the Results section). Using the eMolecules stock provides our model with access to an expanded synthesizable chemical space, which we do not believe is a disadvantage because we *can* scale to this size. However, small reaction spaces can be advantageous if one is specifically interested in that space. By contrast, SynFormer⁶⁹ introduces a diffusion module that *generates* the fingerprints enabling scaling to longer fingerprints, i.e., more bits, which mitigates situations with bit collisions. During sampling, the generated fingerprints are compared to the building block stock using L2 distance to retrieve a match. To have faster inference, the fingerprints should be stored in memory as recomputing will be slow for large stocks, which necessarily requires more memory capacity. In our benchmark experiments, we will *match* the building block sets used in the comparison works and then also show the results using our default eMolecules stock.

One final caveat, which in our opinion, is the most important point, is that if a small, constrained building block set is defined, then our model would have to first learn to generate molecules in this specific chemical space before being able to optimize the objective function. It would be practical to then pre-train *specifically* on this chemical space via enumeration using these exact blocks so that our model already can generate in this chemical space (pre-training can take as little as 1 hour on a single GPU) and is exactly what some existing works do^{67,69,73}. We *do not* consider this in our comparison because we believe a generalist model that is malleable is practically advantageous. Therefore, we do not deviate from our pre-trained PubChem¹⁴⁴ model in this section (or anywhere in this work). It would be expected that performance would improve if we pre-train specifically on the chemical space of interest.

Reaction Steps and Routes. Between GFlowNet works, the permitted number of reaction steps of generated molecules differs from 3-4 (Table 8). To match this, we cap our synthesis routes to 4 reaction steps. Moreover, all GFlowNet works only allow linear synthesis routes while our method and SynFormer allow branched pathways. We do not take any action related to this point but highlight that it is a limitation as branched routes are common in medicinal chemistry.

Objective Functions. Most generated design papers achieving experimental validation use docking so we focus on docking case studies⁴³. In the development experiments so far, we dock against ClpP¹⁶¹. For benchmarking, we instead take one protein target used in each corresponding GFlowNet paper. This means we can take their model formulation out-of-the-box with their defined reward shaping. We also intentionally choose a different protein target when comparing to each paper (as papers can have overlap) to additionally show our method is generalizable across any target. Note that the synthesizability-constrained models would also be expected to generalize. However, we believe this is still a practical and useful point as we do not change any reward shaping across all targets. For specific details on the docking objective functions, we defer to the corresponding Results section.

Lastly, generating synthesizable molecules as defined by varying building block sets is "normal" synthesizability which we tackled in our previous work⁴⁹. In that work, we showed that QuickVina2-GPU docking¹⁵⁸⁻¹⁶⁰ is not a particularly discriminative oracle, such that "good" docking compounds can generally be found in PubChem¹⁴⁴ chemical space. The synthetic accessibility (SA) score⁵⁰ is defined based on PubChem space and is very well correlated with retrosynthesis solvability. In this scenario, optimizing for SA score which is cheap to compute and then post-hoc filtering with retrosynthesis models is a better allocation of computational resources. We ignore this observation in this work since we ultimately want to show the ability to steer generation towards satisfying reaction constraints which require an explicit synthesis route. Accordingly, we run additional experiments enforcing that all reactions are amide bond-forming reactions since this is a common reaction.

7.3 Benchmarking Results

We designate separate sections to compare to each individual model since we are *matching* their case studies.

Compute Details. All models are run across 5 seeds (0-4). We compare based on **Oracle** and **Wall Time** budgets. We match the PMO benchmark¹⁹⁴ and compare under a 10,000 oracle budget. In all docking case studies, QuickVina2-GPU¹⁵⁸⁻¹⁶⁰ is used which is a cheap docking oracle (seconds to dock batches of 100 molecules). If the oracle were more expensive, it would be the bottleneck and some oracles can also have additional monetary costs, e.g., API costs. Therefore, the oracle budget is a practical consideration. We additionally set a maximum time limit for runs to be 24 hours and report the results for however many molecules were generated. We do this since different models have

different training and inference times. Next, all models, with the exception of RGFN⁷¹ were run on NVIDIA L40S GPUs which have 48 GB GPU memory. RGFN was run on NVIDIA H100 GPUs which have 94 GB GPU memory because 48 GB is insufficient. We note that H100 GPUs are faster than L40S GPUs but we ignore this in the comparison results. The code versions (GitHub hash) we used are as follows:

- **RGFN**⁷¹: e21b5cb
- **SynFlowNet**⁷²: 574f1e1
- **RxnFlow**⁷⁵: 23017e3
- **SynFormer**⁶⁹: bef02bc

We run these models *generally* out-of-the-box from the provided scripts in the codebases. As shown in Table 8, all models use specific building block stocks from specific release dates. Since we do not have access to these previous stock versions, we download the latest versions and follow the data pre-processing pipeline in the codebases. In this way, we can ensure that the building block stocks are the same when comparing to each model. See Appendix E for more details on exact data processing and small efficiency implementations we added.

Metrics. The benchmarking metrics are summarized in Table 9. In contrast to the Development Experiments, the number of synthesizable molecules is not reported because the metrics are *only* reported for the synthesizable molecules. To recap, this means:

- **Synthesizability-constrained Models:** All generated molecules are considered synthesizable
- **Our Work:** Only generated molecules with a retrosynthesis model solved pathway are considered synthesizable

The **Modes** metric is newly defined in this section and follows the GFlowNet works⁷¹. This is defined as the number of molecules with < -10 docking score (sort the molecules first based on better docking scores) that are additionally < 0.5 Tanimoto similarity to each other. We also report **Yield** which removes the Tanimoto similarity constraint. All Tanimoto similarity calculations are computed with Morgan fingerprints with radius 2 and 1024 bits. For case studies which also optimize for QED, we filter the generated molecules for $QED > 0.5$. Finally, we report **Peak GPU Memory** of the models and note that QuickVina2-GPU^{158–160} which is used for all docking, consumes 20-24GB GPU memory under the fixed parameters. We make sure to report the GPU memory consumption of the model only (excluding the docking). This metric will help convey scaling limitations of existing synthesizability-constrained models.

7.3.1 RGFN

Objective Function. Minimize QuickVina2-GPU docking scores against TBLR1¹⁹⁸. Optimizing only for docking scores will exploit the docking algorithm and reward generating large, greasy molecules^{49,191}. Since RGFN uses a large reward magnitude (see Table 8), we do not want to impose a reward shaping transformation, though likely multiplying the reward by QED would work since $QED \in [0, 1]$. However, we make the decision to follow the objective function exactly. The docking box follows the original work and is defined as $18\text{\AA} \times 18\text{\AA} \times 18\text{\AA}$ ⁷¹. The reward shaping follows the original work as shown in Table 8. RGFN allows up to 4 reaction steps⁷¹.

Results. The RGFN/Saturn comparison results are shown in Table 10. RGFN’s⁷¹ out-of-the-box building block stock is 350 curated fragments. We did not run this configuration because with such a constrained chemical space, it would be *much* more practical to pre-train Saturn on this enumerated space. In this way, Saturn would not need to first learn to generate molecules in this chemical space before being able to optimize the objective. In the RGFN work, the authors scaled up their building block set up to 64,000 by sampling from Enamine stock. We do the same and use Enamine Global from Feb. 2025 but did not follow their specific building block selection procedure described in their Appendix E⁷¹, which curates blocks to be maximally compatible with their defined reactions. Using this 64,000 building block stock, our efforts to run RGFN led to GPU out-of-memory on an H100 with 94 GB GPU memory. As a result, we truncated the 64,000 building blocks to 50,000. With 50,000 blocks, we sometimes still experienced GPU out-of-memory due to gradient accumulation, but we re-ran the experiment if this occurred. For Saturn, we run experiments with the 64,000 stock with and without enforcing all amide reactions using NameRxn¹⁵⁷. We also run Saturn with the default (in this work) eMolecules stock (23,077,162 in size). We summarize the results and **bold the metric that supports the observation**:

- With 350 fragments, RGFN generates many Modes - **RGFN Modes (Yield)**
- For RGFN, scaling the block set from 350 to 50,000 leads to a notable performance drop, somewhat unintuitively - **RGFN Modes (Yield) comparing 350/50,000 blocks**

Table 9: Summary of benchmarking evaluation metrics. All metrics are reported as the average and standard deviation across 5 seeds (0–4 inclusive).

Category	Metric (averaged across all 5 seeds)
Compute	Oracle Calls: # unique generated molecules scored by the objective function. ^a <i>This is fixed at 10,000 following the PMO benchmark</i> ¹⁹⁴ Wall Time: Compute time on a shared NVIDIA L40S GPU cluster. <i>This is fixed at 24h</i> Peak GPU Memory: Peak GPU memory consumption by the model
Molecule Set Quality	Modes: Set of molecules with QuickVina2-GPU docking score < -10 ^{158–160} against a given protein target. Molecules must also have Tanimoto similarity < 0.5 to each other, following the RGFN work ⁷¹ Yield: Set of molecules with docking score < -10 against a given protein target The metrics below are reported for the ‘Yield’ set of generated molecules: QED ¹⁶² : Quantitative estimate of drug-likeness. (Not reported for RGFN as it was not part of the objective function) Bemis–Murcko Scaffolds ¹⁶⁵ : # unique Bemis–Murcko scaffolds IntDiv1 ¹⁶⁶ : Pairwise Morgan fingerprint similarity (radius = 2, nBits = 1024) #Circles ¹⁶⁷ : Sphere packing number (0.75 similarity threshold) Molecular Weight (MW): Comments on molecular size Ligand Efficiency (LE): Docking score divided by # heavy atoms

^a For RGFN⁷¹, RxnFlow⁷⁵, and SynFormer⁶⁹, we implement checks to ensure that only unique *and* not previously generated molecules are scored by the objective function. This removes any repeated scoring of molecules, for maximum efficiency. For SynFlowNet⁷², these extra checks were not implemented due to requiring more involved changes in the codebase which we will implement in a later version of this work.

- RGFN accumulates GPU memory consumption, limiting scalability. 50,000 blocks consumes 55 GB - **RGFN Peak GPU Memory**
- In general, Saturn generates less Modes than RGFN, which also means less diverse molecules - **Compare RGFN and Saturn Modes, IntDiv1, #Circles**
- Saturn is much more sample-efficient under the oracle budget, with much higher Yield - **Compare RGFN 50,000 and Saturn 64,000 Yield (RGFN 350 has higher Yield)**
- RGFN exploits the docking oracle and generates large molecules with much lower ligand efficiency - **Compare RGFN and Saturn MW and LE**
- Saturn generates higher quality molecules (MW and LE) even under the only amide reaction constraint - **Saturn Only Amide results**
- Saturn demonstrates scalability as using the eMolecules stock results in the most sample-efficient (under the 10,000 oracle budget) configuration. The generated molecules have better property profiles across all metrics - **Saturn eMolecules**

We further comment on RGFN’s most performant configuration which uses 350 fragments. Based on our previous work⁴⁹, QuickVina2-GPU docking is a permissive oracle, where *many* molecules can receive good docking scores¹⁹⁹. This diminished capability to distinguish between molecules is a limitation in real-world drug discovery, and the industry standard uses docking algorithms, e.g., Glide¹⁶⁸, which are more expensive to run but can lead to much better enrichment¹⁷². The main point we want to highlight is that with oracles that are more discriminative, one may need to access a much larger and diverse chemical space to generate property-optimized molecules and we have shown that RGFN has scaling limitations. Furthermore, existing ultra-large make-on-demand libraries which are enumerated with different building blocks, cover different chemical spaces¹⁸⁴. There is demand for these distinct libraries because varying design objectives require different chemotypes. The ability to scale to much larger building block sets, like we have shown, is a practical advantage.

Table 10: RGFN-Saturn comparison results. The mean and standard deviation are reported across 5 seeds (0–4 inclusive). Results are reported for both the 24h wall time limit and 10,000 oracle calls budget. RGFN was run on an NVIDIA H100 (94 GB GPU memory), while Saturn was run on an NVIDIA L40S (48 GB GPU memory). **DS** denotes QuickVina2-GPU docking score. **Scaffs** denotes the number of unique Bemis-Murcko scaffolds. Only amide reactions used NameRxn labeling. **Saturn out-of-the-box outperforms RGFN under the oracle budget.**

Blocks	Modes \uparrow (Yield) \uparrow	DS \downarrow	Scaffs \uparrow	IntDiv1 \uparrow	#Circles \uparrow	MW \downarrow	LE \uparrow
Reaction-GFlowNet (RGFN) ⁷¹							
Peak GPU Memory: 350 blocks = 44 GB 50,000 blocks = 55 GB							
350							
Time Limit (24h)	10843 \pm 188 (51868 \pm 2371)	−10.99 \pm 0.01	48559 \pm 2593	0.751 \pm 0.005	57 \pm 1	654.08 \pm 4.94	0.23 \pm 0.00
Oracle Limit (10,000 Calls)	1516 \pm 122 (2265 \pm 140)	−10.75 \pm 0.03	2260 \pm 138	0.780 \pm 0.008	32 \pm 2	643.96 \pm 4.05	0.23 \pm 0.00
50,000							
Time Limit (24h)	14996 \pm 1698 (19898 \pm 4535)	−10.95 \pm 0.06	19861 \pm 4519	0.817 \pm 0.008	413 \pm 79	739.47 \pm 10.80	0.21 \pm 0.00
Oracle Limit (10,000 Calls)	341 \pm 58 (431 \pm 99)	−10.58 \pm 0.03	426 \pm 94	0.822 \pm 0.013	87 \pm 10	637.46 \pm 10.09	0.24 \pm 0.01
This Work (Saturn)							
Peak GPU Memory: All Configurations = 5.5 GB							
64,000							
Time Limit (24h)	302 \pm 63 (27982 \pm 5813)	−11.27 \pm 0.45	25867 \pm 4995	0.681 \pm 0.025	11 \pm 1	562.49 \pm 30.63	0.27 \pm 0.01
Oracle Limit (10,000 Calls)	90 \pm 14 (1992 \pm 406)	−11.11 \pm 0.32	1879 \pm 440	0.675 \pm 0.013	7 \pm 2	510.43 \pm 29.28	0.30 \pm 0.02
64,000 Only Amide (NameRxn)							
Time Limit (24h)	293 \pm 108 (8843 \pm 3206)	−10.82 \pm 0.17	7965 \pm 2876	0.717 \pm 0.038	11 \pm 2	540.34 \pm 20.21	0.27 \pm 0.01
Oracle Limit (10,000 Calls)	60 \pm 17 (486 \pm 288)	−10.65 \pm 0.10	436 \pm 255	0.727 \pm 0.019	7 \pm 1	482.54 \pm 42.64	0.31 \pm 0.02
eMolecules							
Time Limit (24h)	1143 \pm 399 (14151 \pm 5977)	−12.43 \pm 0.43	13267 \pm 5625	0.717 \pm 0.029	36 \pm 5	517.68 \pm 16.65	0.31 \pm 0.01
Oracle Limit (10,000 Calls)	694 \pm 161 (4844 \pm 942)	−12.04 \pm 0.30	4415 \pm 857	0.702 \pm 0.053	33 \pm 3	503.51 \pm 12.08	0.31 \pm 0.00

7.3.2 SynFlowNet

Objective Function. Minimize QuickVina2-GPU docking scores against KRAS²⁰⁰ and maximize QED. In certain case studies in the SFN work, maximum reward (1.0) can be obtained by achieving QED = 0.7⁷². This is reasonable as drug molecules do not necessarily need to have "perfect" (1.0) QED. However, we do not adopt this clipping and maximize QED, as is. The docking box follows the original work and is defined as 18Å x 18Å x 18Å⁷². The reward shaping follows the original work as shown in Table 8. The SFN work tested two configurations allowing reactions routes of up to 3 or 4 steps⁷². In general, 3 performed better and is the default in the codebase. Therefore, we used this default value.

Results. The SynFlowNet/Saturn comparison results are shown in Table 11. SFN’s⁷² out-of-the-box building block stock is 10,000 molecules from Enamine Global. We highlight that it would also likely be *much* more practical to pre-train Saturn on this enumerated space. However, we retain our pre-trained model on PubChem and directly use the same block set. SFN further showed the capability to scale the building block set up to the entire Enamine Global stock (we downloaded the version from Feb. 2025). We also match this block set and run Saturn with and without enforcing all amide reactions using NameRxn¹⁵⁷. Lastly, we continue to run Saturn with the default eMolecules stock (23,077,162 in size). We summarize the results and **bold the metric that supports the observation**:

Table 11: SynFlowNet-Saturn comparison results. The mean and standard deviation are reported across 5 seeds (0–4 inclusive). Results are reported for both the 24h wall time limit and 10,000 oracle calls budget. Both models were run on an NVIDIA L40S (48 GB GPU memory). **DS** denotes QuickVina2-GPU docking score. **Scafs** denotes the number of unique Bemis-Murcko scaffolds. Only amide reactions used NameRxn labeling. **N=2** for Saturn with 10,000 blocks indicates that under the Oracle Limit, only 2/5 seeds successfully generated ≥ 1 molecule(s) with $DS < -10$ and $QED > 0.5$. **Saturn out-of-the-box outperforms SynFlowNet under the oracle budget.**

Blocks	Modes \uparrow (Yield) \uparrow	DS \downarrow (QED) \uparrow	Scafs \uparrow	IntDiv1 \uparrow	#Circles \uparrow	MW \downarrow	LE \uparrow
SynFlowNet (SFN) ⁷²							
Peak GPU Memory: 10,000 blocks = 2.0 GB Enamine Global (Feb. 2025) 240,254 blocks = 15 GB							
10,000							
Time Limit (24h)	741 \pm 132 (2233 \pm 447)	-10.37 \pm 0.01 (0.77 \pm 0.01)	1850 \pm 384	0.834 \pm 0.001	117 \pm 11	359.33 \pm 2.74	0.41 \pm 0.00
Oracle Limit (10,000 Calls)	119 \pm 30 (148 \pm 43)	-10.35 \pm 0.03 (0.67 \pm 0.03)	144 \pm 36	0.843 \pm 0.004	51 \pm 3	379.47 \pm 7.34	0.39 \pm 0.01
Enamine Global (Feb. 2025)							
Time Limit (24h)	1721 \pm 718 (13362 \pm 6857)	-10.35 \pm 0.01 (0.86 \pm 0.05)	6695 \pm 3179	0.795 \pm 0.020	121 \pm 17	347.79 \pm 17.67	0.42 \pm 0.01
Oracle Limit (10,000 Calls)	107 \pm 40 (128 \pm 51)	-10.36 \pm 0.03 (0.66 \pm 0.02)	126 \pm 51	0.829 \pm 0.014	46 \pm 16	396.58 \pm 6.20	0.38 \pm 0.01
This Work (Saturn)							
Peak GPU Memory: All Configurations = 5.5 GB							
10,000							
Time Limit (24h)	28 \pm 24 (107 \pm 131)	-10.37 \pm 0.09 (0.60 \pm 0.04)	105 \pm 130	0.545 \pm 0.275	3 \pm 1	405.05 \pm 22.24	0.36 \pm 0.02
Oracle Limit (N=2) (10,000 Calls)	4 \pm 3 (7 \pm 6)	-10.41 \pm 0.17 (0.63 \pm 0.06)	7 \pm 6	0.328 \pm 0.328	2 \pm 1	390.89 \pm 31.94	0.38 \pm 0.03
Enamine Global							
Time Limit (24h)	863 \pm 181 (30061 \pm 10828)	-10.58 \pm 0.03 (0.88 \pm 0.01)	26451 \pm 8659	0.732 \pm 0.011	25 \pm 4	364.96 \pm 4.56	0.39 \pm 0.01
Oracle Limit (10,000 Calls)	237 \pm 32 (1960 \pm 364)	-10.59 \pm 0.06 (0.86 \pm 0.02)	1776 \pm 389	0.729 \pm 0.023	16 \pm 4	346.15 \pm 2.97	0.43 \pm 0.01
Enamine Global Only Amide (NameRxn)							
Time Limit (24h)	402 \pm 14 (6297 \pm 505)	-10.41 \pm 0.02 (0.89 \pm 0.00)	5905 \pm 490	0.750 \pm 0.003	16 \pm 2	325.91 \pm 3.46	0.44 \pm 0.00
Oracle Limit (10,000 Calls)	135 \pm 8 (1207 \pm 244)	-10.42 \pm 0.05 (0.89 \pm 0.01)	1118 \pm 210	0.722 \pm 0.006	11 \pm 2	325.03 \pm 2.83	0.43 \pm 0.00
eMolecules							
Time Limit (24h)	539 \pm 50 (7004 \pm 675)	-10.61 \pm 0.04 (0.88 \pm 0.01)	5789 \pm 402	0.737 \pm 0.023	26 \pm 2	345.45 \pm 5.42	0.42 \pm 0.01
Oracle Limit (10,000 Calls)	341 \pm 16 (2487 \pm 170)	-10.57 \pm 0.03 (0.87 \pm 0.01)	2128 \pm 134	0.746 \pm 0.006	26 \pm 2	346.85 \pm 3.72	0.43 \pm 0.00

- With 10,000 blocks, SFN outperforms Saturn across all metrics - **Compare SFN and Saturn 10,000 blocks all metrics**
- For SFN, scaling the block set from 10,000 to Enamine Global (240,254 blocks) improves performance under the time limit but not under the oracle budget - **SFN Modes (Yield) comparing the Time and Oracle Limits**
- SFN also has scaling limitations as going from 10,000 to 240,254 blocks increases GPU memory consumption from 2 to 15 GB. Further increasing the block sizes by factors of 10 or 100 (as in eMolecules) would likely not be possible on a single GPU -**SFN Peak GPU Memory**
- In general, Saturn generates less Modes than SFN, (though this is not as notable as when comparing to RGFN) which also means less diverse molecules - **Compare RGFN and Saturn Modes, IntDiv1, #Circles**

- With Enamine Global stock, Saturn largely outperforms SFN under both Time and Oracle Limits. Many more property-optimized molecules are generated with a trade-off on diversity - **Compare SFN and Saturn Enamine Global metrics**
- Under an oracle budget, SFN can struggle to perform multi-parameter optimization - **SFN QED which is not optimized yet**
- Saturn with eMolecules finds less Modes and has lower Yield than Enamine Global because the search over 23M building blocks takes longer than over 240k - **Compare Saturn Enamine Global and eMolecules Modes (Yield)**
- Saturn with eMolecules under the oracle budget generates the highest quality molecules - **Saturn eMolecules LE**
- Saturn generates higher quality molecules (MW and LE) even under the only amide reaction constraint (within the Oracle Limit) - **Saturn Only Amide results**

When using the Enamine Global stock (240,254 blocks) and eMolecules (23,077,162 blocks), all Saturn configurations outperform SFN under the 10,000 oracle budget with a trade-off in diversity for enhanced sample efficiency. Very recent GFlowNet work proposes the same diversity trade-off to improve sample efficiency²⁰¹. SFN’s metrics drastically improve under the 24h time limit compared to the oracle budget, suggesting that a large number of oracle calls is required for optimization. In the original work, the authors used a 300,000 oracle budget when comparing to REINVENT^{40,147,148}. With more expensive oracles, one cannot freely call the oracle for a large number of molecules, making such a budget potentially infeasible.

7.3.3 RxnFlow

Objective Function. Minimize QuickVina2-GPU docking scores against ADRB2 which is from the LIT-PCBA dataset²⁰² with 15 protein targets and maximize QED. We chose ADRB2 arbitrarily (it is the first target in LIT-PCBA when sorted in alphabetical order). The docking box follows the original work and is defined as 22.5Å x 22.5Å x 22.5Å⁷⁵. The reward shaping follows the original work as shown in Table 8. RxnFlow allows up to 4 reaction steps⁷⁵.

Results. The RxnFlow/Saturn comparison results are shown in Table 12. RxnFlow’s⁷⁵ out-of-the-box building block stock is Enamine Comprehensive (we downloaded the version from Feb. 2025). After following RxnFlow’s building blocks pre-processing pipeline for Enamine Comprehensive, 1,273,563 building blocks were left. With this building block size, we believe it would not necessarily be more practical to pre-train Saturn on this enumerated chemical space because the space is enormous. Therefore, in contrast to our comparison experiments with RGFN and SFN which featured small out-of-the-box building block sets, we *do not* believe it is likely that pre-training on this specific space would improve Saturn’s performance appreciably. Similar to before, we match this building block set and run Saturn with and without enforcing all amide reactions using NameRxn¹⁵⁷. We continue to run Saturn with the default eMolecules stock (23,077,162 in size). We summarize the results and **bold the metric that supports the observation**:

- Under the 10,000 oracle budget, Saturn notably outperforms RxnFlow across all configurations, even when enforcing only amide reactions. Under the oracle budget, RxnFlow generates almost no molecules passing the docking (< -10) and QED (> 0.5) filters - **Compare all metrics across the Oracle Limit**
- Under the 24h time limit, RxnFlow generates many Modes, though the Yield is essentially the same as Saturn. Therefore, RxnFlow can generate more diverse results than Saturn - **See RxnFlow Time Limit IntDiv1 and #Circles**
- Saturn generates higher quality molecules compared to RxnFlow - **Compare docking scores and LE between RxnFlow and all Saturn configurations**
- RxnFlow introduced *action space subsampling* (we used the default 2% in the codebase) to enable scaling to 1.27M blocks. However, further scaling to the eMolecules stock (23M), for example, would be likely prohibitive as 1.27M blocks already takes 19 GB GPU memory - **RxnFlow Peak GPU Memory**

RxnFlow introduces *action space subsampling* to accommodate larger building block sets. The motivation, as stated by the authors is that existing works restrict the search space (via less building blocks) for optimization efficiency, which trades off chemical space diversity⁷⁵. Action space subsampling estimates the GFlowNet forward transition probability by considering only a sub-set of the action space. This mitigates memory requirements for large building block sets, at the expense of variance, since the transition probabilities are more noisy. Empirically, we show in the comparison results in Table 12 that the sample efficiency with the Enamine Comprehensive (1,273,563 blocks) stock is notably diminished.

Table 12: RxnFlow-Saturn comparison results. The mean and standard deviation are reported across 5 seeds (0–4 inclusive). Results are reported for both the 24h wall time limit and 10,000 oracle calls budget. Both models were run on an NVIDIA L40S (48 GB GPU memory). **DS** denotes QuickVina2-GPU docking score. **Scaffs** denotes the number of unique Bemis-Murcko scaffolds. Only amide reactions used NameRxn labeling. **Saturn out-of-the-box outperforms RxnFlow under the oracle budget.**

Blocks	Modes \uparrow (Yield) \uparrow	DS \downarrow (QED) \uparrow	Scaffs \uparrow	IntDiv1 \uparrow	#Circles \uparrow	MW \downarrow	LE \uparrow
RxnFlow							
Peak GPU Memory: Enamine Comprehensive (Feb. 2025) 1,273,563 blocks = 19 GB							
Enamine Comprehensive (Feb. 2025)							
Time Limit (24h)	12812 \pm 589 (39606 \pm 7164)	−10.64 \pm 0.05 (0.85 \pm 0.01)	26701 \pm 3154	0.817 \pm 0.014	690 \pm 9	336.36 \pm 0.82	0.44 \pm 0.00
Oracle Limit (10,000 Calls)	18 \pm 2 (18 \pm 2)	−10.50 \pm 0.04 (0.63 \pm 0.02)	18 \pm 2	0.810 \pm 0.009	15 \pm 2	384.21 \pm 10.55	0.39 \pm 0.01
This Work (Saturn)							
Peak GPU Memory: All Configurations = 5.5 GB							
Enamine Comprehensive							
Time Limit (24h)	1179 \pm 116 (39796 \pm 4600)	−11.51 \pm 0.19 (0.91 \pm 0.00)	36977 \pm 4359	0.732 \pm 0.012	37 \pm 3	338.92 \pm 8.91	0.46 \pm 0.01
Oracle Limit (10,000 Calls)	528 \pm 41 (4433 \pm 332)	−11.15 \pm 0.05 (0.89 \pm 0.00)	3756 \pm 305	0.737 \pm 0.012	32 \pm 4	331.07 \pm 4.94	0.46 \pm 0.01
Enamine Comprehensive Only Amide (NameRxn)							
Time Limit (24h)	744 \pm 71 (19721 \pm 2249)	−11.06 \pm 0.02 (0.91 \pm 0.00)	17928 \pm 2361	0.743 \pm 0.005	26 \pm 2	321.66 \pm 0.49	0.47 \pm 0.00
Oracle Limit (10,000 Calls)	375 \pm 40 (4008 \pm 274)	−11.03 \pm 0.08 (0.90 \pm 0.00)	3463 \pm 264	0.733 \pm 0.015	22 \pm 1	318.88 \pm 2.44	0.47 \pm 0.00
eMolecules							
Time Limit (24h)	829 \pm 143 (10612 \pm 837)	−11.36 \pm 0.13 (0.90 \pm 0.00)	9419 \pm 618	0.730 \pm 0.013	38 \pm 7	336.73 \pm 2.25	0.46 \pm 0.01
Oracle Limit (10,000 Calls)	636 \pm 70 (4582 \pm 216)	−11.10 \pm 0.11 (0.89 \pm 0.00)	3762 \pm 317	0.742 \pm 0.010	35 \pm 7	332.46 \pm 1.95	0.45 \pm 0.00

7.3.4 SynFormer

Objective Function. Minimize QuickVina2-GPU docking scores against ALDH1 which is also from the LIT-PCBA dataset²⁰² and maximize QED. We chose ALDH1 arbitrarily (it is the second target in LIT-PCBA when sorted in alphabetical order and we already used the first target for RxnFlow). The docking box follows the RxnFlow work and is defined as 22.5Å x 22.5Å x 22.5Å⁷⁵. We used a docking task from RxnFlow because the SynFormer work⁶⁹ does not have case studies optimizing for docking scores. We define the reward shaping for SynFormer as our own reward shaping where $r \in [0, 1]$. There is reason to believe this works well because SynFormer performs optimization tasks from Therapeutics Data Commons (TDC) which often has this reward normalization. During pre-training, SynFormer⁶⁹ follows the authors’ previous ChemProjector work⁷³ which generates training data up to 5 reaction steps. Therefore, it is reasonable to assume the model generates molecules with up to 5 reaction steps (though this could change during optimization).

Results. The SynFormer/Saturn comparison results are shown in Table 13. SynFormer⁶⁹ pre-trains on enumerated routes based on Enamine US (Oct. 2023)¹⁹⁶. We obtain the Enamine US (Oct. 2023) stock directly from Enamine and were sent 5 different sub-versions (there were 5 version dumps in Oct. 2023). We use the earliest one from Oct. 2, 2023 which is the smallest stock. SynFormer features two variants: an encoder-decoder and decoder-only where the former takes generated molecules by GraphGA²⁰³ and projects out synthesizability analogs. We chose to compare to this encoder-decoder variant (SynFormer-ED) because the authors state that the decoder-only variant (SynFormer-D) currently requires a lot of oracle calls. Moreover, in the paper, the merged GraphGA and SynFormer-ED model is named GraphGA-SF and features sample-efficient optimization results across several benchmark tasks. Therefore, we compare to GraphGA-SF. As GraphGA requires an initial population of molecules, we randomly sample from Saturn’s processed PubChem dataset¹⁴⁴. As with before, we match the stock (Enamine US Oct. 2023 in this case) and run Saturn

Table 13: SynFormer-Saturn comparison results. The mean and standard deviation are reported across 5 seeds (0–4 inclusive). Results are reported for both the 24h wall time limit and 10,000 oracle calls budget. Both models were run on an NVIDIA L40S (48 GB GPU memory). **DS** denotes QuickVina2-GPU docking score. **Scaffs** denotes the number of unique Bemis-Murcko scaffolds. Only amide reactions used NameRxn labeling. **Saturn out-of-the-box outperforms SynFormer under the time and oracle budgets.**

Blocks	Modes \uparrow (Yield) \uparrow	DS \downarrow (QED) \uparrow	Scaffs \uparrow	IntDiv1 \uparrow	#Circles \uparrow	MW \downarrow	LE \uparrow
SynFormer (GraphGA-SF) ⁶⁹							
Peak GPU Memory: Enamine US (Oct. 2023) 225,824 blocks = 3.2 GB							
Enamine US (Oct. 2023)							
Time Limit (24h)	361 \pm 68 (651 \pm 190)	−10.62 \pm 0.09 (0.66 \pm 0.01)	632 \pm 187	0.849 \pm 0.011	103 \pm 13	406.03 \pm 9.90	0.37 \pm 0.01
Oracle Limit (10,000 Calls)	357 \pm 68 (645 \pm 192)	−10.62 \pm 0.09 (0.66 \pm 0.01)	625 \pm 189	0.849 \pm 0.011	104 \pm 11	405.91 \pm 9.90	0.37 \pm 0.01
This Work (Saturn)							
Peak GPU Memory: All Configurations = 5.5 GB							
Enamine US							
Time Limit (24h)	1111 \pm 133 (43661 \pm 2193)	−10.93 \pm 0.16 (0.88 \pm 0.00)	37745 \pm 1488	0.748 \pm 0.013	30 \pm 2	360.60 \pm 7.05	0.41 \pm 0.01
Oracle Limit (10,000 Calls)	330 \pm 25 (3331 \pm 105)	−10.86 \pm 0.18 (0.88 \pm 0.01)	2861 \pm 242	0.727 \pm 0.009	21 \pm 3	349.18 \pm 9.95	0.42 \pm 0.01
Enamine US Only Amide (NameRxn)							
Time Limit (24h)	455 \pm 71 (14150 \pm 669)	−10.60 \pm 0.02 (0.89 \pm 0.00)	12138 \pm 789	0.731 \pm 0.007	16 \pm 4	332.09 \pm 3.62	0.43 \pm 0.00
Oracle Limit (10,000 Calls)	196 \pm 19 (2924 \pm 335)	−10.66 \pm 0.06 (0.90 \pm 0.00)	2567 \pm 274	0.705 \pm 0.009	13 \pm 2	325.10 \pm 5.18	0.44 \pm 0.00
eMolecules							
Time Limit (24h)	770 \pm 38 (10538 \pm 1137)	−11.17 \pm 0.24 (0.88 \pm 0.01)	9159 \pm 861	0.728 \pm 0.008	40 \pm 4	349.32 \pm 11.07	0.43 \pm 0.01
Oracle Limit (10,000 Calls)	571 \pm 46 (4079 \pm 303)	−10.91 \pm 0.07 (0.87 \pm 0.01)	3463 \pm 255	0.741 \pm 0.016	36 \pm 2	345.58 \pm 6.26	0.43 \pm 0.01

with and without enforcing all amide reactions using NameRxn¹⁵⁷. We also show results for Saturn with the default eMolecules stock (23,077,162 in size). We summarize the results and **bold the metric that supports the observation**:

- Under the 10,000 oracle budget, Saturn notably outperforms SynFormer across all configurations, even when enforcing only amide reactions - **Compare all metrics across the Oracle Limit**
- While SynFormer does not need to run an explicit retrosynthesis search on every molecule, the projection operation takes a notable amount of time. This is the reason that the Oracle Limit and Time Limit results are almost identical, as it takes almost 24h to generate 10,000 unique molecules - **Compare SynFormer Time Limit and Oracle Limit results**
- Saturn generates higher quality molecules compared to SynFormer, optimizing all properties in the objective function - **Compare QED and LE between SynFormer and all Saturn configurations**
- SynFormer can generate more diverse results than Saturn but Saturn generates many more property-optimized molecules - **Compare SynFormer and Saturn IntDiv1 and #Circles**
- SynFormer results under the Time and Oracle Limits are almost identical because the 10,000 oracle budget took about 24h to exhaust - **Compare SynFormer Time and Oracle Limit Modes (Yield)**

7.4 Post-benchmark General Observations

After benchmarking against RGFN⁷¹, SFN⁷², RxnFlow⁷⁵, and SynFormer⁶⁹, we highlight some general observations and add more discussion.

Diverse Molecules and Property Optimization. The GFlowNet models can generate diverse molecules (Modes) but can have diminished sample efficiency. This has been shown in the PMO benchmark¹⁹⁴ and also in the Benchmark Results here. By design, GFlowNets sample trajectories (molecules in this case) with probability proportional to the reward in order to sample diverse solutions¹⁹³. However, we believe that diverse results need to also be property-optimized. Very recently, Atomic GFlowNets (A-GFNs)²⁰¹ were proposed which perform pre-training for about 2 weeks on 4 NVIDIA A100 GPUs with pre-computed inexpensive oracles such as QED score. This pre-trained model was then tasked to optimize objectives and the most exploitative setting tested resulted in the highest sample efficiency. These results demonstrate the trade-off between sample efficiency and diversity which has been previously reported¹⁹⁴. The A-GFN formulation could be potentially applied to the synthesizability-constrained GFlowNets for improved sample efficiency.

GFlowNet Models with Reaction Constraints. The synthesizability-constrained GFlowNets could conceivably also be tasked with reaction constraints, such as allowing only amide reactions by masking the actions. Since this is not natively implemented, we do not implement it ourselves.

Scalability. We observe that with larger action spaces (increasing building block set size), GFlowNets become less sample-efficient, which limits the scalability, even if there was sufficient GPU memory. Consequently, we find that the smallest building block sets, e.g., 350 for RGFN and 10,000 for SFN (for SFN, increasing the block set does not improve the oracle limit performance), were the best performing configurations in the respective models. As stated previously, this can be advantageous if one is interested in a specific chemical space. However, a constrained space can limit the ability to find favourable molecules when considering arbitrary objective functions. We believe a generalist pre-trained model that can be moulded towards arbitrary objective functions in an enormous chemical space is practically advantageous. In all experiments so far (and in this paper), we use the same model out-of-the-box. Moreover, under constrained chemical spaces, we believe a comparison with enumeration-based approaches such as SYNOPSIS²⁷ or DINGOS²⁹ would be interesting. We leave this for future work.

Time and Oracle Limits. We ran every single benchmark experiment under 24h Time and 10,000 Oracle Budget Limits. We did this because our framework has the overhead of running an explicit retrosynthesis search on every generated molecule. By contrast, all GFlowNet models generate synthesizable molecules directly and SynFormer projects a synthesizable analog from GraphGA generated molecules. The objective function for all models used QuickVina2-GPU docking which is a computationally inexpensive oracle. In terms of docking, QuickVina2-GPU can be permissive, offering poor (or even none as is common with docking) correlation with actual binding affinity^{172,199,204}. This is the reason more expensive, higher-fidelity oracles are used. We give specific examples of such oracles:

1. More expensive docking such as Schrödinger Glide¹⁶⁸ which is one of the industry standards
2. Ensemble docking where a single molecule is docked against multiple protein receptors²⁰⁵. This can be a valuable compromise between static docking and molecular dynamics as multiple protein receptors feature different residue positions
3. Direct molecular dynamic simulations to estimate binding free energy, such as MMPB(GB)SA^{204,206}
4. Quantum-mechanical descriptors where semi-empirical or DFT calculations are performed^{122,207,208}

In these settings, the simulation oracle itself would be the bottleneck, and it would not be possible to evaluate over 100,000-300,000 generated molecules like in the GFlowNet works in under 24h. This is why the 10,000 Oracle Limit is a practical consideration and is also the motivation in the PMO benchmark¹⁹⁴.

8 Conclusion

This work introduces a small molecule generative framework capable of generating molecules predicted to be synthesizable using specific reactions and/or avoiding other reactions. Previously, we described a sample-efficient molecular generative framework named ‘Saturn’ capable of multi-parameter optimization¹⁴¹. In follow-up work, we demonstrated that Saturn can generate synthesizable molecules by coupling a retrosynthesis model to the reinforcement learning optimization loop⁴⁹. Subsequently, we proposed the ‘TANGO’ reward function that enables generating molecules whose synthesis routes incorporate specific pre-defined building blocks¹²⁵. Here, we abstract the problem one-step higher and demonstrate *steerable and granular* synthesizability control. We demonstrate molecular generation under various and stringent reaction constraints with the continued capability to enforce specific building blocks in the synthesis routes, as described in our previous TANGO work¹²⁵. We summarize and highlight the new capabilities:

(1) Enforcing the Presence, Avoiding, or Only Allowing Specific Reactions. In Sections 4.1 and 4.1.3, we show that generated molecules have synthesis routes enforcing the presence and/or avoiding specific reactions. We observed the emergence of specific reaction tandems in the synthetic routes when avoiding certain undesired reactions to satisfy the MPO objective. Furthermore, we show the capability to enforce that all reactions in the synthesis routes belong to a pre-defined set of reactions. In addition to making the synthesis of generated molecules more tractable, this opens the opportunity to *design* batches of property-optimized molecules that can be synthesized using the same reaction procedures and/or equipment.

(2) Incentivizing Short Synthesis Routes. In Section 4.1.4, we show that Saturn can be *incentivized* to generate property-optimized molecules with shorter synthesis routes. We highlighted interesting observations where shorter synthesis routes implicitly use larger building blocks, so as to satisfy the docking objective (larger molecules, on average, have better docking scores). Shorter synthesis routes naturally place less synthesis burden on chemists and opens the opportunity for faster ‘make’ cycles and decreased costs.

(3) Industrial Waste Valorization. In Section 5, we draw inspiration from Wołos et al.¹⁷⁷ demonstrating the ability to transform industrial waste into valuable known medicines or agrochemicals. We abstract the problem one-step higher and show that the combination of our TANGO work¹²⁵ and this work, enables the *de novo* design of property-optimized molecules derived from industrial waste. For maximal practicality, we demonstrate that industrial waste from the US and the EU can be combined by geographical origin with their respective building block stocks, as supplied by Enamine, to design potential COX2¹⁷⁸ inhibitors. The designed potential inhibitors possess optimized property profiles but more importantly, their synthesis routes incorporate industrial waste building blocks and pre-defined reactions. This opens the opportunity to valorize arbitrary *specific* building blocks or byproducts towards arbitrary design objectives while guaranteeing the molecule’s supply chain.

(4) Generative Virtual Screening. In Section 6, we demonstrate the interplay between ultra-large virtual screening and generative design. Ultra-large libraries are constructed using a set of building blocks and specific reactions. Enforcing similar synthesizability constraints enables *generating* molecules with exact matches in the library. We show that *just using* the same building block stock allows our *generalist model* to be steered to generate molecules with a 40% exact match rate in Freedom 4.0 containing 142 billion molecules, while optimizing a docking multi-parameter optimization objective. Going further, by enforcing the same reactions in the generative framework as the ones used to enumerate Freedom 4.0, we can achieve over 90% exact match rate. Moreover, and as expected, we show that enforcing reactions that are less represented in Freedom 4.0, results in less exact matches, and vice versa. Ultra-large libraries will continue to grow and as of May 2025, the largest commercial library to the best of our knowledge is ‘eXplore’ which is on the order of 10^{12} ¹⁸⁴. Our framework opens the opportunity to overcome the exponential scaling. We generated and docked 15,000 molecules which amounts to 0.00001% of Freedom 4.0 (142 billion) to find docking-optimized molecules.

Beyond these new capabilities, we benchmark against recently proposed synthesizability-constrained generative models including Reaction GFlowNet (RGFN)⁷¹, SynFlowNet (SFN)⁷², RxnFlow⁷⁵, and SynFormer⁶⁹. These models directly generate synthesizable molecules by combining building blocks and reaction templates. In Section 7, we show that Saturn is the most sample-efficient model and notably outperforms the synthesizability-constrained models under a 10,000 oracle budget, generating more property-optimized molecules. However, this comes with a trade-off in diversity but as synthesis and experimental validation will continue to be the major bottleneck, generating *excellent* candidate molecules under limited computational budgets is practically important. We highlight that the synthesizability-constrained GFlowNet models (RGFN, SFN, and RxnFlow) generate diverse molecules when allowing a large number of oracle calls. This makes the models performant when the oracle is computationally inexpensive, but limits application to higher-fidelity oracle settings that confer enhanced predictive accuracy. Lastly, the GFlowNet models currently only generate linear synthesis routes while we note that SynFormer and our framework can propose branched synthesis routes.

We conclude with general higher-level observations around our framework and future work. The main theme of this paper is taking a *generalist* pre-trained model and *incentivizing* desired behaviours through reinforcement learning. However, reinforcement learning can be data-demanding²⁰⁹, requiring a large number of interactions with the environment, which in our problem setting means generating molecules and evaluating their property profiles. This epitomizes the sample efficiency problem where we want to label as few molecules as possible, while finding property-optimized molecules in an enormous state space. Our earlier work focused on improving sample efficiency and proposed Saturn¹⁴¹. In our follow-up works around synthesizability^{49,125} (including this work), we show that a sample-efficient model can directly tackle synthesizability out-of-the-box, without any explicit inductive biases in the generation process. However, there are important challenges that we want to acknowledge:

(1) Reaction Feasibility. All synthesis routes proposed by the retrosynthesis model are subject to limitations in the training data. Presently, these models sometimes output synthesis routes with selectivity issues and hallucinated reactions due to the lack of consideration of incompatibilities²¹⁰. Moreover, reaction conditions have not been provided in any synthesis routes in this work. We have since integrated automatic annotation of predicted conditions using Reacon which uses templates and clustering²¹¹. In a future version of this work, we will discuss and show explicit examples of this functionality in prioritizing generated molecules.

(2) Reward Formulation. We use a binary reward to learn various reaction constraints but this can be a problem in more complex reward landscapes where the inefficiency of initial exploration can be computational prohibitive. We discussed the use of reaction-based enumeration to seed the initial learning (see Appendix H). While we only observed benefits in *some* settings, we envision it will be strictly beneficial when the reward function imposes many troughs. Specifically, if favourable chemical spaces are highly discontinuous, it would be challenging to rely on free exploration to solve the optimization problem. In this scenario, a potential solution could be leveraging diversity-maximizing reaction-based enumeration to "map out" potential chemical spaces of interest.

(3) Optimization. Real-world drug discovery necessitates multi-parameter objective functions that impose a much harsher and challenging optimization problem. In these settings, it can be disadvantageous, given the current optimization algorithm, to include a retrosynthesis model in the optimization loop. If the model struggles to navigate the multi-parameter objective function, then generated molecules could possess sub-optimal property profiles. In this case, additionally adding a retrosynthesis solvability objective could make the reward landscape prohibitively challenging. One existing method that may help such settings is curriculum learning^{212,213} which decomposes a complex objective function into sequential, simpler ones. However, it is not always obvious *how* a curriculum should be defined.

Overall, we have demonstrated a framework for *steerable and granular* synthesizability control in small molecule generation. We envision that Saturn with these new capabilities will lower the barrier for experimental validation.

Data Availability

For experiments using open-source data, all relevant files are deposited here: <https://doi.org/10.6084/m9.figshare.29040977.v1>. For the Generative Virtual Screening section, we were provided access to Chemspace's Freedom space 4.0 building blocks and synthons. This information can be requested from cs_sales@chem-space.com. The synthon-based search script to search for exact match in Freedom 4.0 is based on Cosgrove¹⁸⁹.

Code Availability

The code is available at: <https://github.com/schwallergroup/saturn>. There are provided files to reproduce the experiments with an associated README with installation details.

Author Contributions

JG and VSG proposed the idea to impose reaction constraints. JG conceptualized the generative virtual screening capability. JG developed the generative model code. VSG developed the reaction-based enumeration code. JG developed the analysis code with feedback from VSG. JG performed the development and benchmarking experiments. VSG performed the waste valorization experiment with docking validation. VSG and JG performed the generative virtual screening experiment. ZJ and VSG oversaw the chemical plausibility of generated molecules and synthesis routes. VSG and PS designed the figures with feedback from all authors. PS and JSL supervised the project. All authors contributed to writing the manuscript.

Acknowledgements

We thank Anna Kapeliukha for discussions and assistance around searching Freedom Space 4.0. JG acknowledges funding from NSERC. JG, VSG, JSL and PS acknowledge support from the NCCR Catalysis (grant number 225147), a National Centre of Competence in Research funded by the Swiss National Science Foundation. VSG acknowledges support from the European Union's Horizon 2020 research and innovation program under the Marie Skłodowska-Curie grant agreement N° 945363. ZJ acknowledges funding by the Swiss National Science Foundation (SNSF) [214915].

Appendix

The Appendix contains additional details and discussion on:

- Saturn (Appendix A)
- PubChem pre-training details (Appendix B)
- Rxn-INSIGHT templates (Appendix C)
- Rxn-INSIGHT vs. NameRxn (Appendix D)
- Data pre-processing for the benchmarking experiments (Appendix E)
- Docking validation for the waste valorization case study (Appendix F)
- Additional example routes of generated molecules (Appendix G)
- Reaction-based Enumeration in Saturn (Appendix H)
- Further scaling the building block set (Appendix I)

A Saturn: Architecture and Reinforcement Learning Algorithm

In this section, we add high-level information about Saturn and how the reinforcement learning (RL) algorithm guides the model to generated property-optimized molecules. For more details about Saturn, we refer to our original work¹⁴¹.

Saturn. Saturn is a molecular generative model that can use various language-based backbones. The specific backbone we use is Mamba¹⁴³. In our problem setting, molecules are represented as SMILES¹⁴⁵ and the task is to generate new SMILES in an autoregressive manner. We define a SMILES sequence by x and adopt the notation from the original Mamba¹⁴³ and a technical blog²¹⁴ to describe the key operations:

$$\begin{aligned}h_t &= \bar{\mathbf{A}}h_{t-1} + \bar{\mathbf{B}}(x_t)x_t \\ y_t &= \bar{\mathbf{C}}(x_t)h_t + \bar{\mathbf{D}}x_t\end{aligned}$$

Mamba features four learnable matrices (A, B, C, D) and processes sequence information in an input-dependent manner. This is important as it enables a *selective* mechanism to control how information is propagated, similar to the self-attention mechanism in transformers²¹⁵. In the equations above, h is the state and y is the output. As with any language-modeling task, the output from the backbone (Mamba in this case) is subject to a linear projection to obtain a probability distribution over SMILES tokens.

Reinforcement Learning. The general framework of Saturn is to take a pre-trained model on a corpus of molecules (PubChem¹⁴⁴) in this case and apply RL fine-tuning. For pre-training details, see Appendix B. The RL algorithm is based on REINVENT^{40,147,148} with modifications (see next section). The pre-trained model is defined as the Prior which has frozen weights. Every SMILES sequence, when passed through the Prior, returns a log-likelihood. Next, the Agent is also initialized as the pre-trained model but in contrast to the Prior, its weights are updated during RL. Following REINVENT, the Augmented Likelihood (augmented log-likelihood but we denote this as Augmented Likelihood to match the original REINVENT work) is defined as follows:

$$\log \pi_{\text{Augmented}}(x) = \log \pi_{\text{Prior}}(x) + \sigma R(x) \quad (1)$$

where R is an arbitrary reward function that takes as input a SMILES, x , and returns a scalar reward $\in [0, 1]$. σ is a scalar factor that can up-weight the contribution of the reward signal. Taken together, the Augmented Likelihood is a linear combination of the log-likelihood of the SMILES under the Prior modulated by its reward. RL proceeds by defining the following loss function:

$$L(\theta) = (\log \pi_{\text{Augmented}} - \log \pi_{\theta_{\text{Agent}}})^2 \quad (2)$$

where the squared distance between the Augmented and Agent log-likelihoods is minimized. Since the Augmented log-likelihood is a linear combination of the Prior which is frozen and the reward function, the objective is to maximize the reward while regularizing the Agent to not deviate too far from the pre-trained distribution. θ denotes that the Agent is parameterized by the Mamba network.

Augmented Memory. The specific RL algorithm is Augmented Memory¹⁴⁶ which we previously proposed and is a modified version of REINVENT’s algorithm. During RL, a replay buffer stores the top-100 highest reward SMILES generated so far. At each epoch, the Agent is updated not only based on the newly generated batch of SMILES but also every SMILES in the replay buffer. This is done N times and is denoted an Augmentation Round. Specifically, every SMILES in the replay buffer is augmented (randomized²¹⁶) which generates an alternative sequence form of the same molecule. Consequently, the Agent is updated with different sequence (SMILES) representations of the same molecules and is a mechanism that enhances sample efficiency. Finally, following REINVENT, a Diversity Filter (DF)²¹⁷ stores the Bemis-Murcko¹⁶⁵ scaffolds of all generated molecules. If a particular scaffold has been generated above a threshold number of times (10 in this work), its reward is truncated to 0.0. This mechanism enables improved exploration by the Agent.

B Saturn PubChem Pre-training

All experiments in this work used the same pre-trained model from our previous TANGO work on constrained synthesizability¹²⁵. This section contains a copy of the information from our TANGO work for completeness.

The full data pre-processing and pre-training pipeline started from the raw PubChem which was downloaded from <https://ftp.ncbi.nlm.nih.gov/pubchem/Compound/Extras/>. The exact file is "CID-SMILES.gz". **Note that there is now a new version of PubChem. We previously downloaded the version close to Aug. 7, 2024.**

The exact pre-processing steps along with the SMILES remaining after each step are:

1. Raw PubChem - 118,563,810
2. De-duplication - 118,469,904
3. Standardization (charge and isotope handling) based on https://github.com/MolecularAI/ReinventCommunity/blob/master/notebooks/Data_Preparation.ipynb. All SMILES that could not be parsed by RDKit were removed - 109,128,315
4. Tokenize all SMILES based on REINVENT’s tokenizer: https://github.com/MolecularAI/reinvent-models/blob/main/reinvent_models/reinvent_core/models/vocabulary.py
5. Keep SMILES ≤ 80 tokens, $150 \leq$ molecular weight ≤ 650 , number of heavy atoms ≤ 40 , number of rings ≤ 8 , Size of largest ring ≤ 8 , longest aliphatic carbon chain ≤ 4 - 97,667,549
6. Removed SMILES containing the following tokens (due to undesired chemistry, low token frequency, and redundancy): [Br+2], [Br+3], [Br+], [C+], [C-], [CH+], [CH-], [CH2+], [CH2-], [CH2], [CH], [C], [Cl+2], [Cl+3], [Cl+], [ClH+2], [ClH2+2], [ClH3+3], [N-], [N@+], [N@@+], [NH+], [NH-], [NH2+], [NH3+], [NH], [N], [O+], [OH+], [OH2+], [O], [S+], [S-], [S@+], [S@@+], [S@@], [S@], [SH+], [SH-], [SH2], [SH4], [SH], [S], [c+], [c-], [cH+], [cH-], [c], [n+], [n-], [nH+], [nH], [o+], [s+], [sH+], [sH-], [sH2], [sH4], [sH], [s] - **88,618,780**

The final vocabulary contained 35 tokens (2 extra tokens were added, indicating <START> and <END>) and carbon stereochemistry tokens were kept. Saturn¹⁴¹ uses the Mamba¹⁴³ architecture and we used the default hyperparameters in the code-base. With the vocabulary size of 35, the model has 5,265,408 parameters. Saturn was pre-trained for 5 steps, with each step consisting of a full pass through the dataset. The model was pre-trained on a workstation with an NVIDIA RTX 3090 GPU and AMD Ryzen 9 5900X 12-Core CPU. The pre-training parameters were:

1. Training steps = 5
2. Seed = 0
3. Batch size = 512
4. Learning rate = 0.0001
5. Randomize²¹⁶ every batch of SMILES

Relevant metrics of the pre-trained model (final model checkpoint) are:

1. Average negative log-likelihood (NLL) = 30.914
2. Validity (10k) = 98.74%
3. Uniqueness (10k) = 98.73%
4. Wall time = 106 hours (takes a relatively long time, but pre-training only needs to be done once)

C Rxn-INSIGHT: Reaction Name Definitions

The reaction names that the synthesizability oracle considers depend on the reaction classification software in the framework (in this case, Rxn-INSIGHT¹⁵²). Here, specific SMIRKS are used to name different reactions, and this affects the oracle output when the labelled reactions are evaluated in the synthesis routes. From a user perspective, one would select a list of reaction name keywords that wants to enforce or avoid, and the oracle will consider them as matched if the labelled reactions in the synthesis routes contain these keywords. This can lead to differences between the desired transformation and the matched reaction if the keywords are not properly defined or the SMIRKS used for classification are not named properly. For example, we show one of the matched templates for the experiments enforcing the presence of a Wittig reaction (Figure C9). In this case, the matched template is technically a Horner-Wadsworth-Emmons (HWE) reaction, which is a modification of the Wittig reaction where an alkene is formed from a phosphonate and a carbonyl group²¹⁸. This transformation can be considered a variant of the Wittig reaction, although it has a different mechanism. The specific template name for this example in Rxn-INSIGHT is "Wittig with Phosphonium", and therefore when enforcing the presence of a Wittig reaction in the experiments (enforced using the "Wittig" keyword), any HWE reaction in the synthesis route matching this template will be considered as a Wittig reaction according to the selected keyword. However, this may not be an issue from the synthesis point of view, as both transformations yield the same product (an alkene from a carbonyl).

Rxn-INSIGHT name: "Wittig with Phosphonium"

SMIRKS:

```
[#6:1]-[#6;+0:2](=O).O-P(=O)(-O)-[C;H2;D2;+0:3]-[*:4]
>>[#6:1]-[#6;+0:2]=[C;H1;D2;+0:3]-[*:4]
```

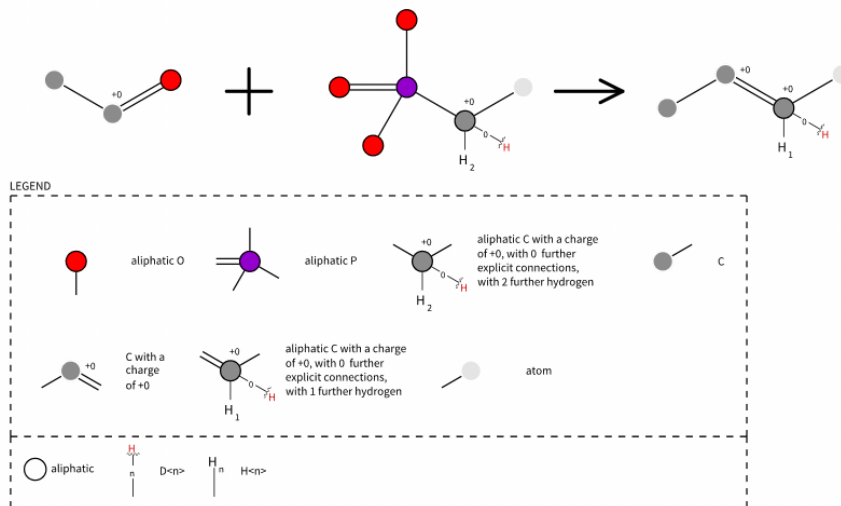


Figure C9: Horner-Wadsworth-Emmons (HWE) SMIRKS visualization. The template corresponds to a HWE reaction, although it is labeled as "Wittig with Phosphonium" in Rxn-INSIGHT. The SMIRKS pattern is visualized using SMARTSplus²¹⁹

Another example that has been commented in the main text is the stereospecificity in the Mitsunobu transformation. The associated template in Rxn-INSIGHT ("Mitsunobu aryl ether") does not consider the inversion of the stereocentre, and therefore any reaction matching this non-chiral template would be considered as a Mitsunobu reaction. We note that this problem can be solved by having a more granular naming of the reaction templates used for reaction name labelling, or by expanding the collection of templates to cover more transformations.

D Rxn-INSIGHT vs. NameRxn

In this section, we discuss nuance details about Rxn-INSIGHT¹⁵² compared to NameRxn¹⁵⁷ and their implications on the wall time of our framework. In this work, every generated molecule is passed to Synthesus¹⁴² to generate an explicit predicted synthesis route. Each reaction SMILES from Synthesus is then labeled with both the reaction

class and *name*. In Rxn-INSIGHT, obtaining the reaction class requires atom mapping of the reaction SMILES using RXNMapper¹⁵⁵. The mapped reaction SMILES is then subject to comparisons of bond-electron matrices to output a 10-class classification. Obtaining the reaction name only requires comparing the reaction SMILES to a set of 527 SMIRKS. Therefore, most of the computational burden of Rxn-INSIGHT is from atom mapping. In this work, all experiments we ran generally only enforced reaction names. As such, we did not necessarily need to perform atom mapping using Rxn-INSIGHT to obtain the class but we do it anyways and use Rxn-INSIGHT out-of-the-box in case the class, e.g., "Aromatic heterocycle formation", is of interest. By contrast, NameRxn does not require running RXNMapper and thus, labeling the reaction *class* requires a negligible amount of time. The implications of this in our framework is that all experiments using Rxn-INSIGHT require a notably longer wall time than NameRxn. To be precise, we could have avoided the computational burden of reaction mapping since we generally only enforced *named* reactions in this work. In the future, we will de-couple the class and name labeling in case one only cares about *specific* reactions. Lastly, we highlight that reaction name labeling by SMIRKS matching like in the case of Rxn-INSIGHT requires that there is a match at all to the SMIRKS set. In the event that there are no matches, the bond matrix workflow with atom mapping could provide useful reaction class information, where the alternative is no label at all.

We next provide additional details on our choice of using MEGAN⁹⁷ as the retrosynthesis model which is not template-based. Since MEGAN is not template-based, the reaction *name* needs to be labeled. If a template-based retrosynthesis model were used, the matched template could directly return the reaction name, avoiding any external calls to tools like Rxn-INSIGHT or NameRxn. However, labeling the class, if wanting to leverage Rxn-INSIGHT's bond-electron matrix workflow, would still require atom mapping. As stated in the main text, we opted to use this approach of external tool calling to make our framework compatible with *any* retrosynthesis model. In the future, we will streamline all workflows and provide control over the need to label reaction *classes* and/or *names*.

Finally, see Table 14 for a side-by-side comparison of wall times using Rxn-INSIGHT and NameRxn.

E Benchmarking Experiments Additional Details

In this section, we provide additional details related to our efforts in running RGFN⁷¹, SFN⁷², RxnFlow⁷⁵, and SynFormer⁶⁹. Most details will be related to preparing the building block stocks according to each paper's procedure. Since we do not, in general, have access to the original building block stocks used in the respective papers, we download the latest versions and follow the pre-processing pipeline described in each model's GitHub. We do this so that our framework can use the exact same building block stock. We first recap the GitHub versions we used:

- **RGFN**⁷¹: e21b5cb
- **SynFlowNet**⁷²: 574f1e1
- **RxnFlow**⁷⁵: 23017e3
- **SynFormer**⁶⁹: bef02bc

RGFN. For RGFN⁷¹, we used the default 350 curated building blocks provided in the GitHub: <https://github.com/koziarskilab/RGFN/blob/main/data/chemistry.xlsx>. In the paper, the authors scaled up to 64,000 building blocks but this was not provided. Therefore, we downloaded Enamine Global (Feb. 2025) and randomly sampled blocks to add to the default 350 to get 64,000 blocks. We note that in Appendix E of the RGFN work, the authors describe their specific building block selection procedure which we did not follow in this work. With 64,000 blocks, we experienced GPU out-of-memory on an NVIDIA H100 with 94 GB GPU. Therefore, we truncated the 64,000 blocks to 50,000 (arbitrarily removing the last 14,000). We used this block set as is in the main text experiments.

SFN. For SFN⁷², we downloaded the Enamine Global (Feb. 2025) stock and pre-processed it by removing invalid molecules and SMILES with ".", leading to 240,254 blocks from 303,018. Next, we followed the instructions provided in the GitHub README: https://github.com/mirunacrt/synflownet/tree/main/src/synflownet/data/building_blocks to create the "10,000" blocks stock. Following all the processing steps as described in the README, the final stocks used were:

- "10,000" stock: After processing, this had **9,984** blocks left
- The entire Enamine Global: After processing, this had **208,129** blocks left

We lastly note that SFN only keeps building blocks with less than total 20 atoms.

RxnFlow. For RxnFlow⁷⁵, we downloaded Enamine Comprehensive Catalog (Feb. 2025) and pre-processed it by removing invalid molecules and SMILES with ".". Additionally, following the RxnFlow paper, we only kept blocks

Table 14: Wall times of main text experiments. The mean and standard deviation are reported across 5 seeds (0–4 inclusive). For all Rxn-INSIGHT experiments, eMolecules stock was used. For NameRxn experiments, we scaled up to 40 million building blocks. See Appendix I for more details.

Experiment	Wall Time
Rxn-INSIGHT - eMolecules Stock (23,077,162 Building Blocks)	
Enforce Reaction Presence	
Amide	46h 40m \pm 3h 2m
Amide Blocks	49h 56m \pm 2h 6m
Suzuki	59h 19m \pm 2h 49m
Suzuki-Block	54h 17m \pm 2h 1m
Mitsunobu	58h 14m \pm 3h 29m
Mitsunobu-Blocks	58h 36m \pm 5h 22m
Heck	59h 34m \pm 4h 22m
Heck-Blocks	52h 28m \pm 6h 15m
Wittig	60h 3m \pm 4h 22m
Wittig-Blocks	62h 10m \pm 1h 46m
Enforce Only Specific Reactions	
Amide	36h 7m \pm 1h 25m
Amide-Blocks	41h45m \pm 3h11m
Amide-Suzuki	38h 5m \pm 2h 41m
Amide-Suzuki-Blocks	43h 18m \pm 1h 46m
NameRxn - "Aggregated Stock" (40,429,262 Building Blocks)	
Enforce Only Specific Reactions	
Amide	23h 28m \pm 1h 36m
Amide-Blocks	26h 57m \pm 2h 18m

with the following atom types: B, C, N, O, F, P, S, Cl, Br, I. There were 1,306,561 molecules remaining from 1,404,227 after this. Next, RxnFlow constructs the ‘Molecule Environment’ before running the model and we do this following the instructions in the GitHub: <https://github.com/SeonghwanSeo/RxnFlow/blob/master/data/README.md>. After running the scripts following the instructions, **1,273,536** blocks remained.

SynFormer. SynFormer⁶⁹ was pre-trained using enumerated synthesis routes from the authors’ previous ChemProjector work¹⁹⁶. The building block stock used was Enamine US (Oct. 2023). We obtain this previous stock version from Enamine directly. In Oct. 2023, there were 5 versions of Enamine US and we take the earliest one which is the smallest in size from Oct. 2, 2023. We remove any duplicates resulting in **225,824** molecules from 225,970. The pre-trained SynFormer model was downloaded from: <https://huggingface.co/whgao/synformer/tree/main>. This is the link provided in the authors’ code repository.

F Waste Valorization Additional Details

In this section, we provide additional details related to the waste valorization experiments.

Waste Building Blocks. Waste building blocks and their geographical location were extracted from the Supplementary Information S1 of Wołos et al.¹⁷⁷. In this Supplementary Information, lists of industrial waste molecules are classified by the continent in which they are produced. Some molecules are produced in both continents. We extracted these waste building blocks by geographical location. NCC(=O)O was removed from the US waste list and O=CO, Nc1ccccc1 and

O=C(O)CCC(=O)O were removed from the EU list after preliminary runs to promote higher diversity on the enforced waste blocks routes. The SMILES of the final waste blocks are provided below:

- US waste: O=C1CCCCC1, CC(C)=O, O=C(O)Cc1ccc(O)cc1, OCC(O)CO, CC#N, CC(O)C(=O)O, CCO, CO, C=O, O=C(O)CCC(=O)O, CCCCC(=O)O, CCCCC(=O)O, CCCO, CCCCO, CC(=O)O, O=C(O)/C=C/C=C/C(=O)O, C=Cc1ccccc1, O=C=O, O=C(O)CCCC(=O)O, Oc1ccccc1, CCCC(O)CO, CC(C)O, C=CC(=O)O, O=C
- EU waste: CC(C)=O, OCC(O)c1ccc(O)c(O)c1, OCC(O)CO, CC=O, CC#N, CC(O)C(=O)O, CCO, CC(C)(C)C(=O)O, NCC(=O)O, C=O, Nc1ccccc1C(=O)O, Oc1ccccc(O)c1, C=C, CCCCO, CC(=O)O, O=C(O)/C=C/C=C/C(=O)O, O=C=O, Oc1ccccc1, CC(C)O, O=C(O)c1ccc(C(=O)O)cc1, CO

Docking Validation. Docking scores commonly do not correlate with actual binding affinity¹⁷². For the waste valorization experiments, we make an effort to *validate* the docking protocol to mimic a real-world use case. Docking was performed using Gnina¹⁷⁹ against COX2 (PDB ID: 1CX2 target¹⁷⁸), implicated in inflammation. Validation was done in two steps:

- *Ligand Re-docking:* The 1CX2 protein structure was prepared for docking following the Dockstream¹⁷² standard pipeline which uses PDBFixer²²⁰. The co-crystallized ligand was re-docked using Gnina with standard parameters (exhaustiveness=8, flexdist=0, random seed=0) to reproduce the original pose. The docked pose possessed < 0.75 Å RMSD and the geometry can conceivably recover the co-crystallized ligand’s pocket interactions (Figure F10).
- *Decoys Set Binding:* A set of decoys and active molecules for 1CX2 was extracted from DEKOIS 2.0¹⁸⁰. These molecules represent a challenging set with similar physico-chemical properties to assess the scoring power of Gnina: how well does the docking score distinguish between active and decoys? We docked all active and inactive molecules with the same parameters that were used to reproduce the binding pose. The enrichment factor of the top 1% docked molecules was 28.4, showing that Gnina was able to separate active molecules from decoys with some resolution. After inspecting the docking scores distribution of actives and decoys (despite a large number of actives also possessing > 0 docking score), we use Gnina docking in Saturn with a reverse sigmoid reward shaping function with min=-20, max=0 (see Figure F11).

These results verified that the Gnina could be used in a meaningful way to design potential inhibitors to COX2.

G Additional Example Synthesis Routes

In this section, we show more example routes with property profiles annotated across the Development experiments (Figure G12 and G13).

H Reaction-based Enumeration to Seed Generative Experiments

In this section we report the results for the Development experiments where the initial Replay buffer is seeded with reaction-based enumerated molecules. These enumerated molecules satisfy the imposed reaction constraints. The hypothesis is that this may guide initial learning and mitigate early non-productivity of RL. In general, we did not observe an improvement with respect to the baselines. However, it may be possible that for very constrained or challenging optimization scenarios, an initial seeding maximizing the diversity of the enumerated molecules may be beneficial for learning. We will investigate this in future work. The quantitative results for the reaction constraints without and with also enforcing block constraints are shown in Tables 15 and 16, respectively.

I Experiments with 40M Building Blocks

In this section, we move beyond eMolecules stock (23,077,162 Building Blocks) and aggregate it with Enamine Comprehensive and ZINC Frag-Reac Subsets stock (about 17.7 million molecules) which we used in our previous work⁴⁹ and is used in the AiZynthFinder retrosynthesis model^{99,100}. After de-duplication this "**Aggregated stock**" contains 40,429,262 building blocks.

Using the Aggregated stock, we run the following experiments with arbitrarily chosen reaction constraints: all enforcing *only* amide reactions:

1. Enforce only amide reactions

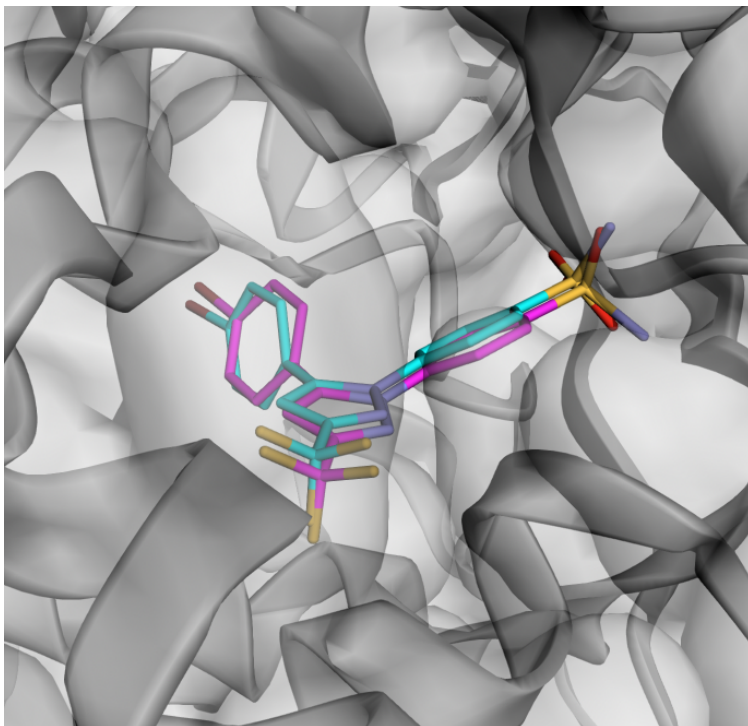


Figure F10: Re-docked co-crystallized ligand (PDB ID: 1CX2) using Gnina (RMSD: 0.72 Å).

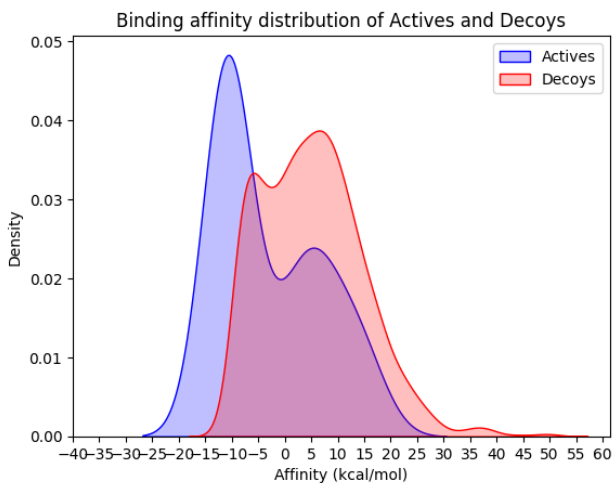


Figure F11: Gnina docking score distribution for the actives and decoys from the DEKOIS 2.0 1CX2 set. Gnina provides some resolution to distinguish between actives and decoys based on the docking scores.

2. Enforce only amide reactions and blocks

The results are shown in Table 17. Overall, these experiments show that it is straightforward to use even larger building block stocks, if desired.

J Development Enforce Block Experiments

The Development experiments enforcing blocks were run with an earlier version of the code. We found a bug where if the generated molecule is *exactly* one of the enforced blocks, the reward of the batch is set to 0 (due to a try and

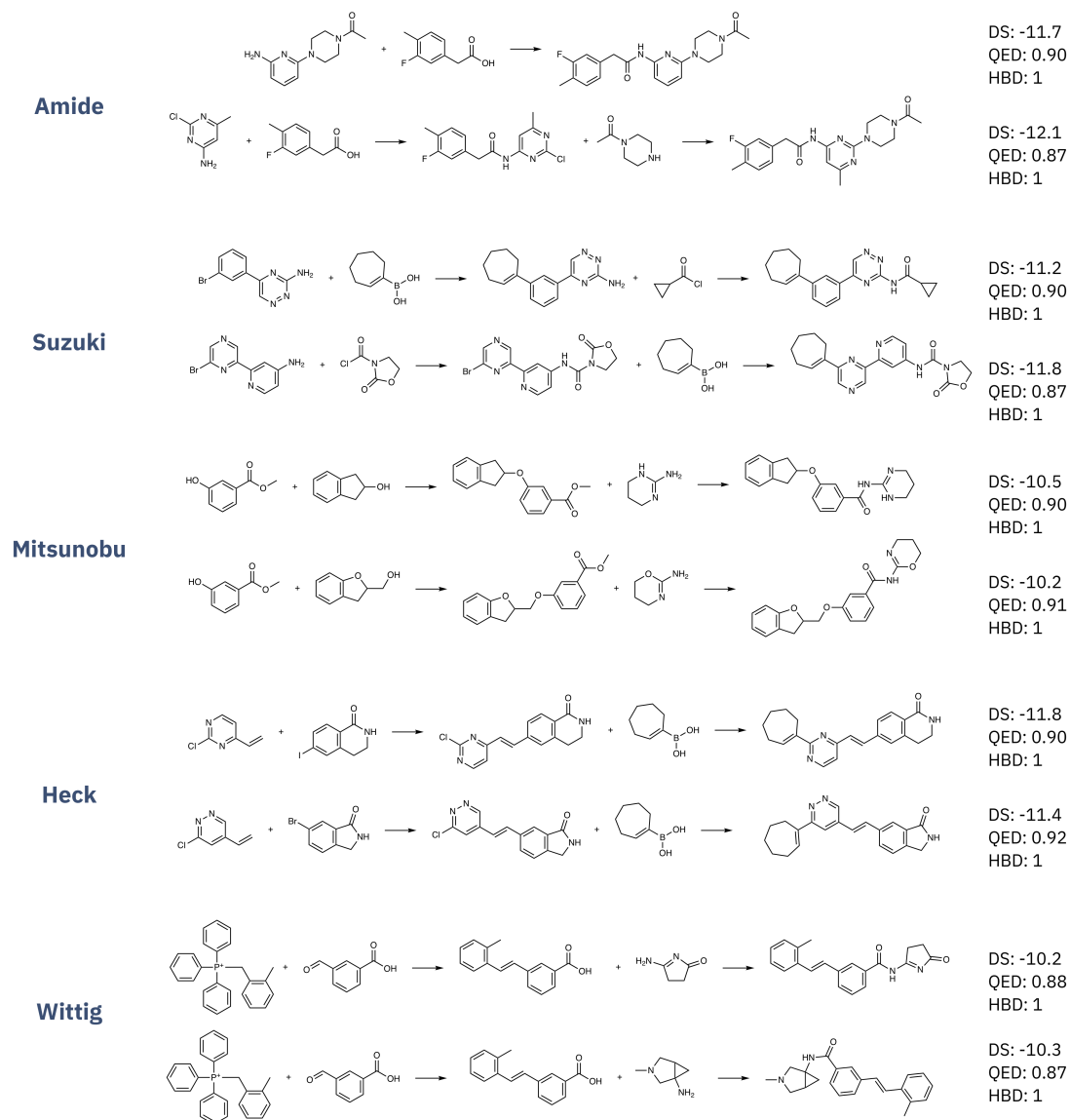


Figure G12: Additional synthetic routes to optimized molecules enforcing the presence of a given chemical reaction.

except code block). This happens a handful of times in the enforce block runs and therefore, does not affect the results significantly. we highlight this for transparency and note that this has since been fixed.

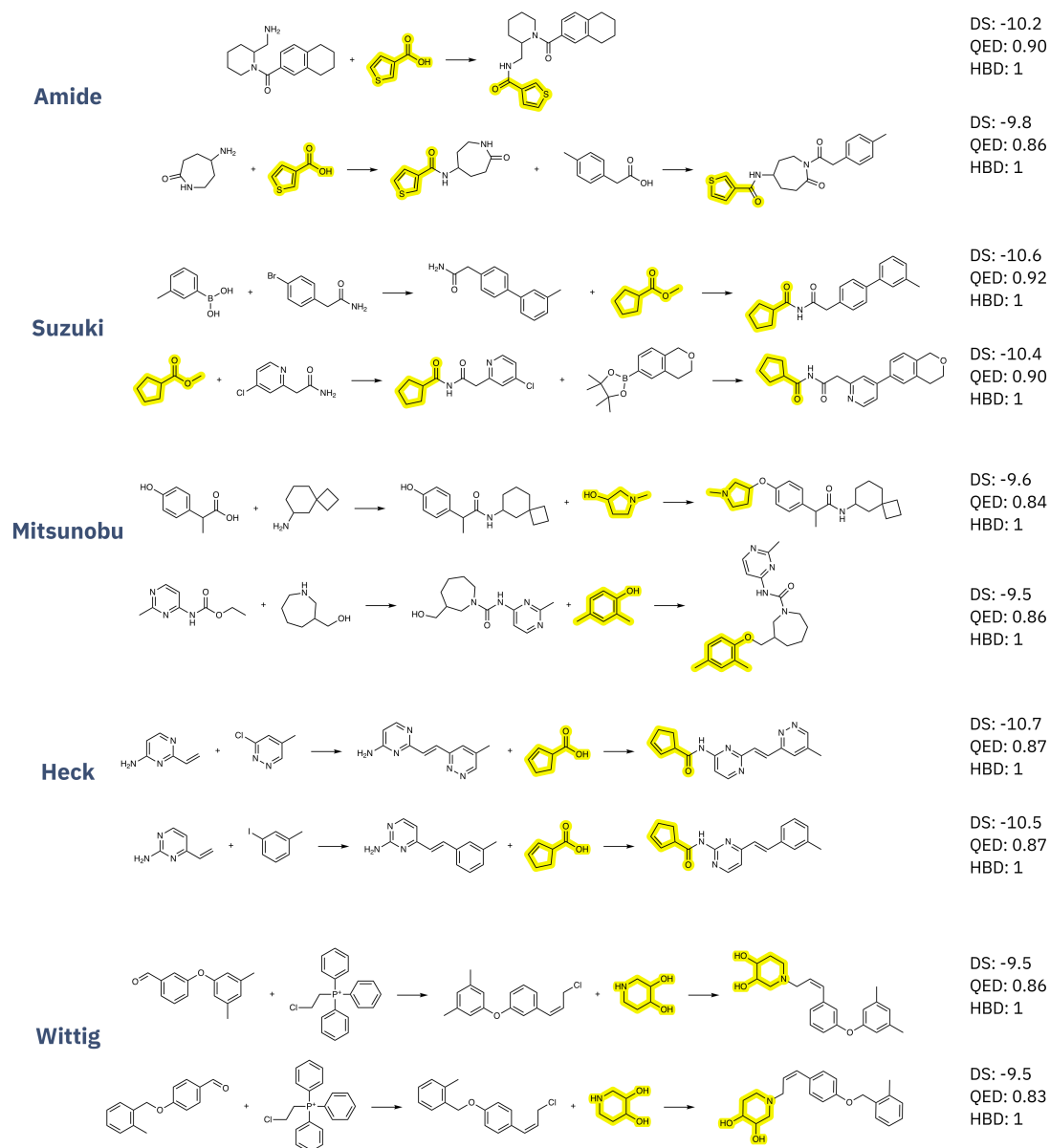


Figure G13: Additional synthetic routes to optimized molecules enforcing the presence of a given chemical reaction and enforcing the presence of a building block from a set.

Table 15: **Enumeration experiments.** The enforced reaction is present in ≥ 1 step(s) of the predicted route. The mean and standard deviation across 5 seeds are reported. The total number of molecules in each docking score interval pooled across all 5 seeds is denoted by **M**. Within each of these docking score intervals, the **QED** and number of hydrogen-bond donors (**HBD**) are annotated, ligand efficiency (**LE**), number of Bemis-Murcko scaffolds (**BMS**), internal diversity (**IntDiv1**), and number of circles (**#Circles (0.75)**) are annotated. The oracle budget was fixed at 15,000.

Enforced	Synthesizability			Rxn Steps	Docking Score Intervals		
	Non-synth	Synth	Synth (constraints)		DS < -10	-10 < DS < -9	-9 < DS < -8
Amide (N=5)	2427 \pm 382	12576 \pm 383	10640 \pm 534	2.19 \pm 1.40	-10.55 \pm 0.42 (M=7428) 0.87 \pm 0.07 (QED) 1.06 \pm 0.24 (HBD) 0.39 \pm 0.03 (LE) 6319 (BMS) 0.737 (IntDiv1) 22 (#Circles)	-9.52 \pm 0.28 (M=16824) 0.89 \pm 0.07 1.07 \pm 0.27 0.37 \pm 0.03 12423 0.758 38	-8.58 \pm 0.29 (M=16187) 0.88 \pm 0.09 1.14 \pm 0.38 0.35 \pm 0.04 12815 0.781 78
Amide-Enumerate (N=5)	2163 \pm 314	12852 \pm 314	10855 \pm 403	2.1 \pm 1.21	-10.51 \pm 0.38 (M=10858) 0.88 \pm 0.06 1.04 \pm 0.19 0.39 \pm 0.02 5907 0.710 9	-9.55 \pm 0.28 (M=17950) 0.90 \pm 0.06 1.06 \pm 0.24 0.38 \pm 0.03 10941 0.746 31	-8.60 \pm 0.28 (M=13212) 0.88 \pm 0.07 1.15 \pm 0.39 0.36 \pm 0.04 9484 0.787 89
Suzuki (N=5)	3369 \pm 436	11637 \pm 438	10078 \pm 401	3.00 \pm 1.32	-10.49 \pm 0.36 (M=7788) 0.86 \pm 0.08 1.00 \pm 0.36 0.40 \pm 0.03 7258 0.758 17	-9.52 \pm 0.28 (M=18568) 0.87 \pm 0.08 1.00 \pm 0.43 0.37 \pm 0.03 17053 0.766 52	-8.61 \pm 0.28 (M=15037) 0.85 \pm 0.11 0.94 \pm 0.56 0.35 \pm 0.04 12389 0.788 105
Suzuki-Enumerate (N=5)	3971 \pm 296	11035 \pm 294	9931 \pm 330	3.14 \pm 1.28	-10.51 \pm 0.38 (M=6825) 0.87 \pm 0.07 0.95 \pm 0.38 0.40 \pm 0.02 6512 0.712 17	-9.52 \pm 0.28 (M=16462) 0.88 \pm 0.07 0.99 \pm 0.45 0.37 \pm 0.03 15053 0.750 44	-8.60 \pm 0.28 (M=14022) 0.87 \pm 0.09 0.99 \pm 0.56 0.35 \pm 0.04 11585 0.787 106
Mitsunobu (N=5)	3860 \pm 1353	11148 \pm 1352	8861 \pm 1321	3.17 \pm 1.48	-10.32 \pm 0.24 (M=1516) -10.38 \pm 0.29 (M=2659) 0.84 \pm 0.09 0.89 \pm 0.42 0.38 \pm 0.02 2486 0.720 11	-9.41 \pm 0.27 (M=3076) -9.48 \pm 0.27 (M=13152) 0.85 \pm 0.11 0.88 \pm 0.45 0.36 \pm 0.03 10913 0.742 28	-8.48 \pm 0.27 (M=5882) -8.57 \pm 0.28 (M=16435) 0.82 \pm 0.15 0.86 \pm 0.51 0.33 \pm 0.04 13332 0.771 49
Mitsunobu-Enumerate (N=5)	3397 \pm 359	11613 \pm 358	8566 \pm 505	3.04 \pm 1.27	-10.38 \pm 0.30 (M=1027) 0.83 \pm 0.08 0.85 \pm 0.50 0.36 \pm 0.02 971 0.670 9	-9.42 \pm 0.26 (M=7760) 0.85 \pm 0.08 0.97 \pm 0.44 0.35 \pm 0.03 6152 0.748 24	-8.54 \pm 0.28 (M=17501) 0.86 \pm 0.09 0.98 \pm 0.46 0.34 \pm 0.04 12579 0.773 76
Heck (N=5)	3993 \pm 675	11014 \pm 674	8691 \pm 970	3.29 \pm 1.38	-10.47 \pm 0.35 (M=5372) 0.86 \pm 0.08 0.97 \pm 0.48 0.40 \pm 0.03 5218 0.755 11	-9.52 \pm 0.28 (M=13284) 0.86 \pm 0.08 1.04 \pm 0.45 0.37 \pm 0.03 11833 0.777 19	-8.57 \pm 0.28 (M=13774) 0.85 \pm 0.09 1.06 \pm 0.53 0.34 \pm 0.04 11930 0.787 35
Heck-Enumerate (N=5)	3682 \pm 619	11322 \pm 618	9379 \pm 491	3.09 \pm 1.30	-10.33 \pm 0.24 (M=1910) 0.88 \pm 0.07 0.97 \pm 0.34 0.42 \pm 0.02 1784 0.738 12	-9.47 \pm 0.27 (M=12409) 0.89 \pm 0.07 0.99 \pm 0.36 0.39 \pm 0.03 10152 0.770 29	-8.57 \pm 0.28 (M=16195) 0.89 \pm 0.08 0.99 \pm 0.45 0.36 \pm 0.04 12325 0.781 55
Wittig (N=5)	4478 \pm 929	10528 \pm 931	8491 \pm 664	3.64 \pm 1.46	1.02 \pm 0.25 0.40 \pm 0.03 7303 0.757 12	1.04 \pm 0.27 0.37 \pm 0.03 17169 0.764 31	1.10 \pm 0.29 0.34 \pm 0.04 12478 0.786 59
Wittig-Enumerate (N=5)	4478 \pm 929	10528 \pm 931	8491 \pm 664	3.64 \pm 1.46	-10.58 \pm 0.42 (M=4554) 0.78 \pm 0.08 0.84 \pm 0.46 0.37 \pm 0.02 3181 0.680 12	-9.50 \pm 0.28 (M=10078) 0.82 \pm 0.09 0.95 \pm 0.40 0.36 \pm 0.03 8339 0.780 31	-8.55 \pm 0.29 (M=12702) 0.83 \pm 0.10 0.94 \pm 0.40 0.34 \pm 0.04 10310 0.807 47

Table 16: **Enumeration experiments also enforcing blocks.** The enforced reaction is present in ≥ 1 step(s) of the predicted route. The mean and standard deviation across 5 seeds are reported. The total number of molecules in each docking score interval pooled across all 5 seeds is denoted by **M**. Within each of these docking score intervals, the **QED** and number of hydrogen-bond donors (**HBD**) are annotated, ligand efficiency (**LE**), number of Bemis-Murcko scaffolds (**BMS**), internal diversity (**IntDiv1**), and number of circles (**#Circles (0.75)**) are annotated. The oracle budget was fixed at 15,000.

Reaction	Synthesizability			Rxn Steps	Docking Score Intervals			Enforced Blocks in Top 5% Molecules
	Non-synth	Synth	Synth (constraints)		DS < -10	-10 < DS < -9	-9 < DS < -8	
Amide (N=5)	3036 \pm 171	11969 \pm 173	6041 \pm 722	2.33 \pm 1.28	-10.47 \pm 0.35 (M=828) 0.82 \pm 0.07 (QED) 1.10 \pm 0.30 (HBD) 0.40 \pm 0.03 (LE) 762 (BMS) 0.630 (IntDiv1) 4 (Circles)	-9.44 \pm 0.27 (M=3301) 0.84 \pm 0.07 1.12 \pm 0.33 0.37 \pm 0.03 2969 0.732 6	-8.49 \pm 0.28 (M=9698) 0.85 \pm 0.07 1.13 \pm 0.35 0.33 \pm 0.03 7634 0.710 7	5/100
Amide-Enumerate (N=5)	2534 \pm 233	12473 \pm 232	5589 \pm 392	2.40 \pm 1.25	-10.28 \pm 0.21 (M=219) 0.84 \pm 0.08 1.13 \pm 0.36 0.38 \pm 0.03 199 0.713 4	-9.39 \pm 0.25 (M=3240) 0.86 \pm 0.07 1.30 \pm 0.51 0.36 \pm 0.02 2403 0.737 5	-8.52 \pm 0.28 (M=10264) 0.86 \pm 0.07 1.35 \pm 0.53 0.33 \pm 0.03 6974 0.739 8	4/100
Suzuki (N=4)	3354 \pm 532	11654 \pm 533	2841 \pm 1698	2.71 \pm 1.26	-10.33 \pm 0.24 (M=1278) 0.71 \pm 0.09 0.85 \pm 0.48 0.37 \pm 0.03 1199 0.679 2	-9.52 \pm 0.28 (M=5485) 0.74 \pm 0.09 0.91 \pm 0.47 0.35 \pm 0.03 4839 0.714 7	-8.60 \pm 0.28 (M=4638) 0.78 \pm 0.10 0.94 \pm 0.44 0.32 \pm 0.04 4044 0.750 5	4/100
Suzuki-Enumerate (N=5)	3138 \pm 710	11869 \pm 708	2375 \pm 2298	2.88 \pm 1.21	-10.39 \pm 0.29 (M=1002) 0.81 \pm 0.08 1.34 \pm 0.49 0.40 \pm 0.04 942 0.670 4	-9.51 \pm 0.27 (M=4356) 0.82 \pm 0.07 1.22 \pm 0.45 0.36 \pm 0.04 3886 0.713 5	-8.59 \pm 0.29 (M=3896) 0.83 \pm 0.08 1.05 \pm 0.42 0.32 \pm 0.04 3061 0.740 7	3/100
Mitsunobu (N=5)	4762 \pm 1292	10245 \pm 1288	5648 \pm 1800	3.17 \pm 1.51	-10.37 \pm 0.30 (M=79) 0.75 \pm 0.12 0.85 \pm 0.48 0.35 \pm 0.02 75 0.530 3	-9.34 \pm 0.24 (M=1644) 0.81 \pm 0.10 0.85 \pm 0.46 0.34 \pm 0.02 1490 0.683 4	-8.46 \pm 0.27 (M=11593) 0.84 \pm 0.10 0.87 \pm 0.44 0.33 \pm 0.03 9705 0.735 4	4/100
Mitsunobu-Enumerate (N=5)	3519 \pm 164	11485 \pm 164	6279 \pm 301	3.08 \pm 1.35	-10.29 \pm 0.21 (M=98) 0.80 \pm 0.07 1.09 \pm 0.50 0.37 \pm 0.02 96 0.601 2	-9.37 \pm 0.25 (M=1647) 0.83 \pm 0.08 1.07 \pm 0.51 0.35 \pm 0.02 1375 0.631 4	-8.46 \pm 0.27 (M=10108) 0.86 \pm 0.08 0.95 \pm 0.51 0.33 \pm 0.03 6897 0.641 8	4/100
Heck (N=5)	3963 \pm 649	11044 \pm 642	1295 \pm 1598	2.78 \pm 1.27	-10.27 \pm 0.16 (M=27) 0.84 \pm 0.08 1.00 \pm 0.00 0.43 \pm 0.02 23 0.571 2	-9.36 \pm 0.25 (M=411) 0.83 \pm 0.08 1.07 \pm 0.25 0.39 \pm 0.04 299 0.645 5	-8.47 \pm 0.27 (M=2188) 0.80 \pm 0.07 1.11 \pm 0.32 0.34 \pm 0.04 1852 0.717 6	4/100
Heck-Enumerate (N=5)	3155 \pm 434	11853 \pm 434	599 \pm 1196	2.82 \pm 1.18	-10.19 \pm 0.09 (M=11) 0.85 \pm 0.10 1.00 \pm 0.00 0.38 \pm 0.03 9 0.445 1	-9.36 \pm 0.24 (M=221) 0.87 \pm 0.08 1.16 \pm 0.37 0.35 \pm 0.03 147 0.562 1	-8.46 \pm 0.27 (M=1128) 0.91 \pm 0.05 1.06 \pm 0.24 0.33 \pm 0.02 624 0.585 2	1/100
Wittig (N=5)	4504 \pm 454	10501 \pm 450	2320 \pm 1757	3.63 \pm 1.62	-10.40 \pm 0.28 (M=400) 0.72 \pm 0.08 0.82 \pm 0.60 0.34 \pm 0.02 399 0.551 3	-9.43 \pm 0.27 (M=2585) 0.74 \pm 0.08 0.92 \pm 0.73 0.33 \pm 0.03 2307 0.696 7	-8.55 \pm 0.28 (M=5380) 0.77 \pm 0.09 1.09 \pm 0.81 0.33 \pm 0.04 4280 0.756 7	5/100
Wittig-Enumerate (N=5)	3816 \pm 353	11192 \pm 356	3250 \pm 1228	3.62 \pm 1.48	-10.40 \pm 0.29 (M=157) 0.74 \pm 0.10 0.97 \pm 0.37 0.36 \pm 0.04 150 0.727 7	-9.39 \pm 0.26 (M=1715) 0.78 \pm 0.09 0.98 \pm 0.40 0.34 \pm 0.04 1411 0.780 10	-8.50 \pm 0.28 (M=6323) 0.80 \pm 0.08 0.95 \pm 0.39 0.32 \pm 0.03 5147 0.786 11	9/100

Table 17: **Aggregated stock experiments.** Only amide reactions are permitted. The mean and standard deviation across 5 seeds are reported. **N** denotes the number of replicates (out of 5) that have at least one generated molecule satisfying all reaction constraints. The total number of molecules in each docking score interval pooled across all 5 seeds is denoted by **M** (only molecules satisfying all reaction constraints are considered). Within each of these docking score intervals, the **QED**, number of hydrogen-bond donors (**HBD**), ligand efficiency (**LE**), number of Bemis-Murcko scaffolds (**BMS**), internal diversity (**IntDiv1**), and number of circles (**#Circles (0.75)**) are annotated. The oracle budget was fixed at 15,000.

Experiment	Synthesizability			Rxn Steps	Docking Score Intervals for Synth (constraints)		
	Non-synth	Synth	Synth (constraints)		DS < -10	-10 < DS < -9	-9 < DS < -8
No Blocks (N=5)	2911 \pm 409	12097 \pm 411	8130 \pm 232	1.45 \pm 1.06	-10.37 \pm 0.29 (M=1176) 0.87 \pm 0.07 (QED) 1.04 \pm 0.24 (HBD) 0.40 \pm 0.03 (LE) 1006 (BMS) 0.746 (IntDiv1) 16 (#Circles)	-9.43 \pm 0.26 (M=9406) 0.90 \pm 0.06 1.04 \pm 0.27 0.38 \pm 0.03 7159 0.760 29	-8.57 \pm 0.28 (M=16979) 0.90 \pm 0.06 1.04 \pm 0.33 0.36 \pm 0.04 13127 0.780 55
Blocks (N=5) Enforced Blocks in Top 5% Molecules = 2	4574 \pm 466	10429 \pm 464	2577 \pm 1077	1.72 \pm 1.25	-10.17 \pm 0.09 (M=3) 0.78 \pm 0.06 0.67 \pm 0.47 0.38 \pm 0.01 3 0.449 1	-9.28 \pm 0.18 (M=182) 0.84 \pm 0.06 1.12 \pm 0.41 0.36 \pm 0.03 163 0.636 2	-8.42 \pm 0.26 (M=2061) 0.86 \pm 0.06 1.14 \pm 0.48 0.35 \pm 0.03 1555 0.644 3

References

- [1] Luca Monari. Molecule icon generator!
- [2] Bruce D Roth. 1 the discovery and development of atorvastatin, a potent novel hypolipidemic agent. *Progress in medicinal chemistry*, 40:1–22, 2002.
- [3] Wei Wang, Zhuyifan Ye, Hanlu Gao, and Defang Ouyang. Computational pharmaceutics-a new paradigm of drug delivery. *Journal of Controlled Release*, 338:119–136, 2021.
- [4] Lingle Wang, Jennifer Chambers, and Robert Abel. Protein–ligand binding free energy calculations with fep+. *Biomolecular simulations: methods and protocols*, pages 201–232, 2019.
- [5] Yuriy Khalak, Gary Tresadern, David F Hahn, Bert L de Groot, and Vytutas Gapsys. Chemical space exploration with active learning and alchemical free energies. *Journal of Chemical Theory and Computation*, 18(10):6259–6270, 2022.
- [6] Filipp Gusev, Evgeny Gutkin, Maria G Kurnikova, and Olexandr Isayev. Active learning guided drug design lead optimization based on relative binding free energy modeling. *Journal of Chemical Information and Modeling*, 63(2):583–594, 2023.
- [7] David C Blakemore, Luis Castro, Ian Churcher, David C Rees, Andrew W Thomas, David M Wilson, and Anthony Wood. Organic synthesis provides opportunities to transform drug discovery. *Nature chemistry*, 10(4):383–394, 2018.
- [8] Wendy Warr. Report on an nih workshop on ultralarge chemistry databases. *ChemRxiv*, 2021.
- [9] Oleksandr O Grygorenko, Dmytro S Radchenko, Igor Dziuba, Alexander Chuprina, Kateryna E Gubina, and Yurii S Moroz. Generating multibillion chemical space of readily accessible screening compounds. *Iscience*, 23(11), 2020.
- [10] Atanu Acharya, Rupesh Agarwal, Matthew B Baker, Jerome Baudry, Debsindhu Bhowmik, Swen Boehm, Kendall G Byler, SY Chen, Leighton Coates, Connor J Cooper, et al. Supercomputer-based ensemble docking drug discovery pipeline with application to covid-19. *Journal of chemical information and modeling*, 60(12):5832–5852, 2020.
- [11] Jiankun Lyu, Sheng Wang, Trent E Balius, Isha Singh, Anat Levit, Yurii S Moroz, Matthew J O’Meara, Tao Che, Enkhjargal Alгаа, Kateryna Tolmachova, et al. Ultra-large library docking for discovering new chemotypes. *Nature*, 566(7743):224–229, 2019.
- [12] Stefan Gahbauer, Chelsea DeLeon, Joao M Braz, Veronica Craik, Hye Jin Kang, Xiaobo Wan, Xi-Ping Huang, Christian B Billesbølle, Yongfeng Liu, Tao Che, et al. Docking for ep4r antagonists active against inflammatory pain. *Nature communications*, 14(1):8067, 2023.
- [13] Fangyu Liu, Cheng-Guo Wu, Chia-Ling Tu, Isabella Glenn, Justin Meyerowitz, Anat Levit Kaplan, Jiankun Lyu, Zhiqiang Cheng, Olga O Tarkhanova, Yurii S Moroz, et al. Large library docking identifies positive allosteric modulators of the calcium-sensing receptor. *Science*, 385(6715):ead01868, 2024.
- [14] Tia A Tummino, Christos Iliopoulos-Tsoutsouvas, Joao M Braz, Evan S O’Brien, Reed M Stein, Veronica Craik, Ngan K Tran, Suthakar Ganapathy, Fangyu Liu, Yuki Shiimura, et al. Large library docking for cannabinoid-1 receptor agonists with reduced side effects. *bioRxiv*, pages 2023–02, 2024.
- [15] Shannon T Smith, Jackson B Cassada, Lukas Von Bredow, Kevin Erreger, Emma M Webb, Trevor A Trombley, Jacob J Kalbfleisch, Brian J Bender, Irene Zagol-Ikapitte, Valerie M Kramlinger, et al. Discovery of protease-activated receptor 4 (par4)-tethered ligand antagonists using ultralarge virtual screening. *ACS Pharmacology & Translational Science*, 7(4):1086–1100, 2024.
- [16] Jiankun Lyu, Nicholas Kapolka, Ryan Gumpfer, Assaf Alon, Liang Wang, Manish K Jain, Ximena Barros-Álvarez, Kensuke Sakamoto, Yoojoong Kim, Jeffrey DiBerto, et al. Alphafold2 structures guide prospective ligand discovery. *Science*, page eadn6354, 2024.
- [17] Fangyu Liu, Cheng-Guo Wu, Chia-Ling Tu, Isabella Glenn, Justin Meyerowitz, Anat Levit Kaplan, Jiankun Lyu, Zhiqiang Cheng, Olga O Tarkhanova, Yurii S Moroz, et al. Large library docking identifies positive allosteric modulators of the calcium-sensing receptor. *Science*, 385(6715):ead01868, 2024.
- [18] Bryan Fraser, Nicholas Young, Brian Bender, Stefan Gahbauer, Olzhas Ilyassov, Ryan Wilson, Yanjun Li, Almagul Seitova, André Luiz Lourenço, Dong-Hee Chung, et al. Large library docking and biophysical analysis of small molecule tmprss2 inhibitors. *ChemRxiv*, 2024.
- [19] Christoph Gorgulla, Andras Boeszoermenyi, Zi-Fu Wang, Patrick D Fischer, Paul W Coote, Krishna M Padmanabha Das, Yehor S Malets, Dmytro S Radchenko, Yurii S Moroz, David A Scott, et al. An open-source drug discovery platform enables ultra-large virtual screens. *Nature*, 580(7805):663–668, 2020.

- [20] Christoph Gorgulla, AkshatKumar Nigam, Matt Koop, Suleyman S Cinaroglu, Christopher Secker, Mohammad Haddadnia, Abhishek Kumar, Yehor Malets, Alexander Hasson, Roni Levin-Konigsberg, et al. Virtualflow 2.0-the next generation drug discovery platform enabling adaptive screens of 69 billion molecules, 2023. Preprint at <https://doi.org/10.1101/2023.04.25.537981>.
- [21] Arman A Sadybekov, Anastasiia V Sadybekov, Yongfeng Liu, Christos Iliopoulos-Tsoutsouvas, Xi-Ping Huang, Julie Pickett, Blake Houser, Nilkanth Patel, Ngan K Tran, Fei Tong, et al. Synthon-based ligand discovery in virtual libraries of over 11 billion compounds. *Nature*, 601(7893):452–459, 2022.
- [22] Fangyu Liu, Olivier Mailhot, Isabella S Glenn, Seth F Vigneron, Viola Bassim, Xinyu Xu, Karla Fonseca-Valencia, Matthew S Smith, Dmytro S Radchenko, James S Fraser, et al. The impact of library size and scale of testing on virtual screening. *bioRxiv*, pages 2024–07, 2024.
- [23] François Sindt, Anthony Seyller, Merveille Eguida, and Didier Rognan. Protein structure-based organic chemistry-driven ligand design from ultralarge chemical spaces. *ACS Central Science*, 10(3):615–627, 2024.
- [24] Álvaro Serrano-Morrás, Andrea Bertran-Mostazo, Marina Miñarro-Lleonar, Arnau Comajuncosa-Creus, Adrià Cabello, Carme Labranya, Carmen Escudero, Tian Tian, Inna Khutorianska, Dmytro S Radchenko, et al. A novel bottom-up approach to find lead-compounds in billion-sized libraries. *ChemRxiv*, 2025.
- [25] Andreas Lutten, Israel Cabeza de Vaca, Leonard Sparring, José Brea, Antón Leandro Martínez, Nour Aldin Kahlous, Dmytro S Radchenko, Yuri S Moroz, María Isabel Loza, Ulf Norinder, et al. Rapid traversal of vast chemical space using machine learning-guided docking screens. *Nature Computational Science*, pages 1–12, 2025.
- [26] Artem Cherkasov. The ‘big bang’ of the chemical universe. *Nat. Chem. Biol.*, 19(6):667–668, June 2023.
- [27] H Maarten Vinkers, Marc R de Jonge, Frederik FD Daeyaert, Jan Heeres, Lucien MH Koymans, Joop H van Lenthe, Paul J Lewi, Henk Timmerman, Koen Van Aken, and Paul AJ Janssen. Synopsis: synthesize and optimize system in silico. *Journal of medicinal chemistry*, 46(13):2765–2773, 2003.
- [28] Markus Hartenfeller, Heiko Zettl, Miriam Walter, Matthias Rupp, Felix Reisen, Ewgenij Proschak, Sascha Weggen, Holger Stark, and Gisbert Schneider. Dogs: reaction-driven de novo design of bioactive compounds. *PLoS computational biology*, 8(2):e1002380, 2012.
- [29] Alexander Button, Daniel Merk, Jan A Hiss, and Gisbert Schneider. Automated de novo molecular design by hybrid machine intelligence and rule-driven chemical synthesis. *Nature machine intelligence*, 1(7):307–315, 2019.
- [30] Gian Marco Ghiandoni, Michael J Bodkin, Beining Chen, Dimitar Hristozov, James EA Wallace, James Webster, and Valerie J Gillet. Renate: a pseudo-retrosynthetic tool for synthetically accessible de novo design. *Molecular Informatics*, 41(4):2100207, 2022.
- [31] Gian Marco Ghiandoni, Stuart R Flanagan, Michael J Bodkin, Maria Giulia Nizi, Albert Galera-Prat, Annalaura Brai, Beining Chen, James EA Wallace, Dimitar Hristozov, James Webster, et al. Synthetically accessible de novo design using reaction vectors: Application to parp1 inhibitors. *Molecular Informatics*, 43(4):e202300183, 2024.
- [32] Laurent Batiste, Andrea Unzue, Aymeric Dolbois, Fabrice Hassler, Xuan Wang, Nicholas Deearain, Jian Zhu, Dimitrios Spiliotopoulos, Cristina Nevado, and Amedeo Caflisch. Chemical space expansion of bromodomain ligands guided by in silico virtual couplings (autocouple). *ACS central science*, 4(2):180–188, 2018.
- [33] Florent Chevillard, Helena Rimmer, Cecilia Betti, Els Pardon, Steven Ballet, Niek van Hilten, Jan Steyaert, Wibke E Diederich, and Peter Kolb. Binding-site compatible fragment growing applied to the design of β 2-adrenergic receptor ligands. *Journal of Medicinal Chemistry*, 61(3):1118–1129, 2018.
- [34] Kai Sommer, Florian Flachsenberg, and Matthias Rarey. Naominext—synthetically feasible fragment growing in a structure-based design context. *European Journal of Medicinal Chemistry*, 163:747–762, 2019.
- [35] Jacob O Spiegel and Jacob D Durrant. Autogrow4: an open-source genetic algorithm for de novo drug design and lead optimization. *Journal of cheminformatics*, 12:1–16, 2020.
- [36] Tianfan Fu, Wenhao Gao, Connor Coley, and Jimeng Sun. Reinforced genetic algorithm for structure-based drug design. *Advances in Neural Information Processing Systems*, 35:12325–12338, 2022.
- [37] Pieter H Bos, Fabio Ranalli, Emelie Flood, Shawn Watts, Daigo Inoyama, Jennifer L Knight, Anthony J Clark, Andrew Placzek, Jiashi Wang, Aleksey I Gerasyuto, et al. Autodesigner-core design, a de novo design algorithm for chemical scaffolds: Application to the design and synthesis of novel selective weel inhibitors. *Journal of Chemical Information and Modeling*, 64(19):7513–7524, 2024.

- [38] Artur Kadurin, Alexander Aliper, Andrey Kazennov, Polina Mamoshina, Quentin Vanhaelen, Kuzma Khrabrov, and Alex Zhavoronkov. The cornucopia of meaningful leads: Applying deep adversarial autoencoders for new molecule development in oncology. *Oncotarget*, 8(7):10883, 2017.
- [39] Esben Jannik Bjerrum and Richard Threlfall. Molecular generation with recurrent neural networks (rnns). *arXiv preprint arXiv:1705.04612*, 2017.
- [40] Marcus Olivecrona, Thomas Blaschke, Ola Engkvist, and Hongming Chen. Molecular de-novo design through deep reinforcement learning. *Journal of cheminformatics*, 9:1–14, 2017.
- [41] Mariya Popova, Olexandr Isayev, and Alexander Tropsha. Deep reinforcement learning for de novo drug design. *Science advances*, 4(7):eaap7885, 2018.
- [42] Marwin HS Segler, Thierry Kogej, Christian Tyrchan, and Mark P Waller. Generating focused molecule libraries for drug discovery with recurrent neural networks. *ACS central science*, 4(1):120–131, 2018.
- [43] Yuanqi Du, Arian R Jamasb, Jeff Guo, Tianfan Fu, Charles Harris, Yingheng Wang, Chenru Duan, Pietro Liò, Philippe Schwaller, and Tom L Blundell. Machine learning-aided generative molecular design. *Nature Machine Intelligence*, pages 1–16, 2024.
- [44] Frank W Pun, Ivan V Ozerov, and Alex Zhavoronkov. Ai-powered therapeutic target discovery. *Trends in Pharmacological Sciences*, 2023.
- [45] <https://github.com/guojeff/generative-drug-design-with-experimental-validation>, 2025.
- [46] Wenhao Gao and Connor W Coley. The synthesizability of molecules proposed by generative models. *Journal of chemical information and modeling*, 60(12):5714–5723, 2020.
- [47] Camille Bilodeau, Wengong Jin, Tommi Jaakkola, Regina Barzilay, and Klavs F Jensen. Generative models for molecular discovery: Recent advances and challenges. *Wiley Interdisciplinary Reviews: Computational Molecular Science*, 12(5):e1608, 2022.
- [48] Megan Stanley and Marwin Segler. Fake it until you make it? generative de novo design and virtual screening of synthesizable molecules. *Current Opinion in Structural Biology*, 82:102658, 2023.
- [49] Jeff Guo and Philippe Schwaller. Directly optimizing for synthesizability in generative molecular design using retrosynthesis models. *Chemical Science*, 2025.
- [50] Peter Ertl and Ansgar Schuffenhauer. Estimation of synthetic accessibility score of drug-like molecules based on molecular complexity and fragment contributions. *Journal of cheminformatics*, 1:1–11, 2009.
- [51] Shuan Chen and Yousung Jung. Estimating the synthetic accessibility of molecules with building block and reaction-aware sascore. *Journal of Cheminformatics*, 2024.
- [52] Connor W Coley, Luke Rogers, William H Green, and Klavs F Jensen. Scscore: synthetic complexity learned from a reaction corpus. *Journal of chemical information and modeling*, 58(2):252–261, 2018.
- [53] Milan Voršilák, Michal Kolář, Ivan Čmelo, and Daniel Svozil. Syba: Bayesian estimation of synthetic accessibility of organic compounds. *Journal of cheminformatics*, 12:1–13, 2020.
- [54] Casper Steinmann and Jan H Jensen. Using a genetic algorithm to find molecules with good docking scores. *PeerJ Physical Chemistry*, 3:e18, 2021.
- [55] Zhe Xue, Chenwei Sun, Wenhao Zheng, Jiancheng Lv, and Xianggen Liu. Targetsa: adaptive simulated annealing for target-specific drug design. *Bioinformatics*, 41(1):btac730, 2025.
- [56] Seul Lee, Seanie Lee, and Sung Ju Hwang. Drug discovery with dynamic goal-aware fragments. *arXiv preprint arXiv:2310.00841*, 2023.
- [57] Oh-Hyeon Choung, Riccardo Vianello, Marwin Segler, Nikolaus Stiefl, and José Jiménez-Luna. Extracting medicinal chemistry intuition via preference machine learning. *Nature Communications*, 14(1):6651, 2023.
- [58] Rebecca M Neeser, Bruno Correia, and Philippe Schwaller. Fsscore: A personalized machine learning-based synthetic feasibility score. *Chemistry-Methods*, page e202400024, 2024.
- [59] Alan Kai Hassen, Martin Šícho, Yorick J van Aalst, Mirjam CW Huizenga, Darcy NR Reynolds, Sohvi Luukkonen, Andrius Bernatavicius, Djork-Arné Clevert, Antonius Janssen, Gerard JP van Westen, et al. Generate what you can make: achieving in-house synthesizability with readily available resources in de novo drug design. *Journal of Cheminformatics*, 17(1):1–16, 2025.
- [60] Matthew Medcalf, Varsha Jain, Stefani Gamboa, Brian Atwood, Maoussi Lhuillier-Akakpo, Victoire Cachoux, and Quentin Perron. Overcoming dmta cycle challenges: A unified ai-driven system for efficient drug design. *ChemRxiv*, 2024.

- [61] John Bradshaw, Brooks Paige, Matt J Kusner, Marwin Segler, and José Miguel Hernández-Lobato. A model to search for synthesizable molecules. *Advances in Neural Information Processing Systems*, 32, 2019.
- [62] John Bradshaw, Brooks Paige, Matt J Kusner, Marwin Segler, and José Miguel Hernández-Lobato. Barking up the right tree: an approach to search over molecule synthesis dags. *Advances in neural information processing systems*, 33:6852–6866, 2020.
- [63] Ksenia Korovina, Sailun Xu, Kirthevasan Kandasamy, Willie Neiswanger, Barnabas Poczos, Jeff Schneider, and Eric Xing. Chembo: Bayesian optimization of small organic molecules with synthesizable recommendations. In *International Conference on Artificial Intelligence and Statistics*, pages 3393–3403. PMLR, 2020.
- [64] Sai Krishna Gottipati, Boris Sattarov, Sufeng Niu, Yashaswi Pathak, Haoran Wei, Shengchao Liu, Simon Blackburn, Karam Thomas, Connor Coley, Jian Tang, et al. Learning to navigate the synthetically accessible chemical space using reinforcement learning. In *International conference on machine learning*, pages 3668–3679. PMLR, 2020.
- [65] Julien Horwood and Emmanuel Noutahi. Molecular design in synthetically accessible chemical space via deep reinforcement learning. *ACS omega*, 5(51):32984–32994, 2020.
- [66] Vendy Fialková, Jiayi Zhao, Kostas Papadopoulos, Ola Engkvist, Esben Jannik Bjerrum, Thierry Kogej, and Atanas Patronov. Libinvent: reaction-based generative scaffold decoration for in silico library design. *Journal of Chemical Information and Modeling*, 62(9):2046–2063, 2021.
- [67] Wenhao Gao, Rocío Mercado, and Connor W Coley. Amortized tree generation for bottom-up synthesis planning and synthesizable molecular design. *Proc. 10th International Conference on Learning Representations*, 2022.
- [68] Seonghwan Seo, Jaechang Lim, and Woo Youn Kim. Molecular generative model via retrosynthetically prepared chemical building block assembly. *Advanced Science*, 10(8):2206674, 2023.
- [69] Wenhao Gao, Shitong Luo, and Connor W Coley. Generative artificial intelligence for navigating synthesizable chemical space. *arXiv preprint arXiv:2410.03494*, 2024.
- [70] Kyle Swanson, Gary Liu, Denise B Catacutan, Autumn Arnold, James Zou, and Jonathan M Stokes. Generative ai for designing and validating easily synthesizable and structurally novel antibiotics. *Nature Machine Intelligence*, 6(3):338–353, 2024.
- [71] Michał Koziarski, Andrei Rekish, Dmytro Shevchuk, Almer van der Sloot, Piotr Gaiński, Yoshua Bengio, Cheng-Hao Liu, Mike Tyers, and Robert A Batey. Rgfn: Synthesizable molecular generation using gflownets. *arXiv preprint arXiv:2406.08506*, 2024.
- [72] Miruna Cretu, Charles Harris, Julien Roy, Emmanuel Bengio, and Pietro Liò. Synflownet: Towards molecule design with guaranteed synthesis pathways. *arXiv preprint arXiv:2405.01155*, 2024.
- [73] Shitong Luo, Wenhao Gao, Zuofan Wu, Jian Peng, Connor W Coley, and Jianzhu Ma. Projecting molecules into synthesizable chemical spaces. *Proc. 41st International Conference on Machine Learning*, 2024.
- [74] Zygimantas Jocys, Henriette MG Willems, and Katayoun Farrahi. Synthformer: Equivariant pharmacophore-based generation of molecules for ligand-based drug design. *arXiv preprint arXiv:2410.02718*, 2024.
- [75] Seonghwan Seo, Minsu Kim, Tony Shen, Martin Ester, Jinkyoo Park, Sungsoo Ahn, and Woo Youn Kim. Generative flows on synthetic pathway for drug design. *arXiv preprint arXiv:2410.04542*, 2024.
- [76] Mingyang Wang, Shuai Li, Jike Wang, Odin Zhang, Hongyan Du, Dejun Jiang, Zhenxing Wu, Yafeng Deng, Yu Kang, Peichen Pan, et al. Clickgen: Directed exploration of synthesizable chemical space via modular reactions and reinforcement learning. *Nature Communications*, 15(1):10127, 2024.
- [77] João Correia, Vítor Pereira, and Miguel Rocha. Combining evolutionary algorithms with reaction rules towards focused molecular design. In *Proceedings of the Genetic and Evolutionary Computation Conference*, pages 900–909, 2023.
- [78] Shogo Nakamura, Nobuaki Yasuo, and Masakazu Sekijima. Molecular optimization using a conditional transformer for reaction-aware compound exploration with reinforcement learning. *Commun. Chem.*, 8(1), 2025.
- [79] Xiaodan Yin, Xiaorui Wang, Zhenxing Wu, Qin Li, Yu Kang, Yafeng Deng, Pei Luo, Huanxiang Liu, Guqin Shi, Zheng Wang, et al. Syn-molopt: a synthesis planning-driven molecular optimization method using data-derived functional reaction templates. *Journal of Cheminformatics*, 17(1):1–14, 2025.
- [80] Clarisse Descamps, Vincent Bouttier, Juan Sanz García, Quentin Perron, and Hamza Tajmouati. Growing and linking optimizers: Synthesis-driven molecule design. *ChemRxiv*, 2025.
- [81] Piotr Gaiński, Oussama Boussif, Dmytro Shevchuk, Andrei Rekish, Ali Parviz, Mike Tyers, Robert A Batey, and Michał Koziarski. Scalable and cost-efficient de novo template-based molecular generation. In *ICLR 2025 Workshop on Generative and Experimental Perspectives for Biomolecular Design*, 2025.

- [82] Elias James Corey and W Todd Wipke. Computer-assisted design of complex organic syntheses: Pathways for molecular synthesis can be devised with a computer and equipment for graphical communication. *Science*, 166(3902):178–192, 1969.
- [83] Elias James Corey, Alan K Long, and Stewart D Rubenstein. Computer-assisted analysis in organic synthesis. *Science*, 228(4698):408–418, 1985.
- [84] Marwin HS Segler, Mike Preuss, and Mark P Waller. Planning chemical syntheses with deep neural networks and symbolic ai. *Nature*, 555(7698):604–610, 2018.
- [85] Yemin Yu, Ying Wei, Kun Kuang, Zhengxing Huang, Huaxiu Yao, and Fei Wu. Grasp: Navigating retrosynthetic planning with goal-driven policy. *Advances in Neural Information Processing Systems*, 35:10257–10268, 2022.
- [86] Binghong Chen, Chengtao Li, Hanjun Dai, and Le Song. Retro*: learning retrosynthetic planning with neural guided a* search. In *International conference on machine learning*, pages 1608–1616. PMLR, 2020.
- [87] Daniel Armstrong, Zlatko Joncev, Jeff Guo, and Philippe Schwaller. Tango*: Constrained synthesis planning using chemically informed value functions. *arXiv preprint arXiv:2412.03424*, 2024.
- [88] Guoqing Liu, Di Xue, Shufang Xie, Yingce Xia, Austin Tripp, Krzysztof Maziarz, Marwin Segler, Tao Qin, Zongzhang Zhang, and Tie-Yan Liu. Retrosynthetic planning with dual value networks. In *International Conference on Machine Learning*, pages 22266–22276. PMLR, 2023.
- [89] Kevin Yu, Jihye Roh, Ziang Li, Wenhao Gao, Runzhong Wang, and Connor W Coley. Double-ended synthesis planning with goal-constrained bidirectional search. *arXiv preprint arXiv:2407.06334*, 2024.
- [90] Sara Szymkuć, Ewa P Gajewska, Tomasz Klucznik, Karol Molga, Piotr Dittwald, Michał Startek, Michał Bajczyk, and Bartosz A Grzybowski. Computer-assisted synthetic planning: the end of the beginning. *Angewandte Chemie International Edition*, 55(20):5904–5937, 2016.
- [91] Bartosz A Grzybowski, Sara Szymkuć, Ewa P Gajewska, Karol Molga, Piotr Dittwald, Agnieszka Wołos, and Tomasz Klucznik. Chematica: a story of computer code that started to think like a chemist. *Chem*, 4(3):390–398, 2018.
- [92] Shuan Chen and Yousung Jung. Deep retrosynthetic reaction prediction using local reactivity and global attention. *JACS Au*, 1(10):1612–1620, 2021.
- [93] Shufang Xie, Rui Yan, Junliang Guo, Yingce Xia, Lijun Wu, and Tao Qin. Retrosynthesis prediction with local template retrieval. In *Proceedings of the AAAI Conference on Artificial Intelligence*, volume 37, pages 5330–5338, 2023.
- [94] Bowen Liu, Bharath Ramsundar, Prasad Kawthekar, Jade Shi, Joseph Gomes, Quang Luu Nguyen, Stephen Ho, Jack Sloane, Paul Wender, and Vijay Pande. Retrosynthetic reaction prediction using neural sequence-to-sequence models. *ACS central science*, 3(10):1103–1113, 2017.
- [95] Marwin HS Segler and Mark P Waller. Neural-symbolic machine learning for retrosynthesis and reaction prediction. *Chemistry—A European Journal*, 23(25):5966–5971, 2017.
- [96] Yuqiang Han, Xiaoyang Xu, Chang-Yu Hsieh, Keyan Ding, Hongxia Xu, Renjun Xu, Tingjun Hou, Qiang Zhang, and Huajun Chen. Retrosynthesis prediction with an iterative string editing model. *Nature Communications*, 15(1):6404, 2024.
- [97] Mikołaj Sacha, Mikołaj Błaz, Piotr Byrski, Paweł Dabrowski-Tumanski, Mikołaj Chrominski, Rafał Loska, Paweł Włodarczyk-Pruszyński, and Stanisław Jastrzebski. Molecule edit graph attention network: modeling chemical reactions as sequences of graph edits. *Journal of Chemical Information and Modeling*, 61(7):3273–3284, 2021.
- [98] Weihe Zhong, Ziduo Yang, and Calvin Yu-Chian Chen. Retrosynthesis prediction using an end-to-end graph generative architecture for molecular graph editing. *Nature Communications*, 14(1):3009, 2023.
- [99] Samuel Genheden, Amol Thakkar, Veronika Chadimová, Jean-Louis Reymond, Ola Engkvist, and Esben Bjerrum. Aizynthfinder: a fast, robust and flexible open-source software for retrosynthetic planning. *Journal of cheminformatics*, 12(1):70, 2020.
- [100] Lakshidaa Saigiridharan, Alan Kai Hassen, Helen Lai, Paula Torren-Peraire, Ola Engkvist, and Samuel Genheden. Aizynthfinder 4.0: developments based on learnings from 3 years of industrial application. *Journal of Cheminformatics*, 16(1):57, 2024.
- [101] Ross Irwin, Spyridon Dimitriadis, Jiazhen He, and Esben Jannik Bjerrum. Chemformer: a pre-trained transformer for computational chemistry. *Machine Learning: Science and Technology*, 3(1):015022, 2022.
- [102] Connor W Coley, Luke Rogers, William H Green, and Klavs F Jensen. Computer-assisted retrosynthesis based on molecular similarity. *ACS central science*, 3(12):1237–1245, 2017.

- [103] Hanjun Dai, Chengtao Li, Connor Coley, Bo Dai, and Le Song. Retrosynthesis prediction with conditional graph logic network. *Advances in Neural Information Processing Systems*, 32, 2019.
- [104] Shoichi Ishida, Kei Terayama, Ryosuke Kojima, Kiyosei Takasu, and Yasushi Okuno. Prediction and interpretable visualization of retrosynthetic reactions using graph convolutional networks. *Journal of chemical information and modeling*, 59(12):5026–5033, 2019.
- [105] Shuangjia Zheng, Jiahua Rao, Zhongyue Zhang, Jun Xu, and Yuedong Yang. Predicting retrosynthetic reactions using self-corrected transformer neural networks. *Journal of chemical information and modeling*, 60(1):47–55, 2019.
- [106] Michael E Fortunato, Connor W Coley, Brian C Barnes, and Klavs F Jensen. Data augmentation and pretraining for template-based retrosynthetic prediction in computer-aided synthesis planning. *Journal of chemical information and modeling*, 60(7):3398–3407, 2020.
- [107] Philipp Seidl, Philipp Renz, Natalia Dyubankova, Paulo Neves, Jonas Verhoeven, Jorg K Wegner, Marwin Segler, Sepp Hochreiter, and Gunter Klambauer. Improving few-and zero-shot reaction template prediction using modern hopfield networks. *Journal of chemical information and modeling*, 62(9):2111–2120, 2022.
- [108] Connor W Coley, Dale A Thomas III, Justin AM Lummiss, Jonathan N Jaworski, Christopher P Breen, Victor Schultz, Travis Hart, Joshua S Fishman, Luke Rogers, Hanyu Gao, et al. A robotic platform for flow synthesis of organic compounds informed by ai planning. *Science*, 365(6453):eaax1566, 2019.
- [109] Ian A Watson, Jibo Wang, and Christos A Nicolaou. A retrosynthetic analysis algorithm implementation. *Journal of cheminformatics*, 11:1–12, 2019.
- [110] Molecule.one. The m1 platform.
- [111] IBM. Rxn for chemistry.
- [112] Iktos. Spaya.
- [113] PostEra. Manifold.
- [114] CAS. Cas scifinder.
- [115] Philippe Schwaller, Riccardo Petraglia, Valerio Zullo, Vishnu H Nair, Rico Andreas Haeuselmann, Riccardo Pisoni, Costas Bekas, Anna Iuliano, and Teodoro Laino. Predicting retrosynthetic pathways using transformer-based models and a hyper-graph exploration strategy. *Chemical science*, 11(12):3316–3325, 2020.
- [116] Amol Thakkar, Alain C Vaucher, Andrea Byekwaso, Philippe Schwaller, Alessandra Toniato, and Teodoro Laino. Unbiasing retrosynthesis language models with disconnection prompts. *ACS Central Science*, 9(7):1488–1498, 2023.
- [117] Krzysztof Maziarz, Guoqing Liu, Hubert Misztela, Aleksei Kornev, Piotr Gaiński, Holger Hoeffling, Mike Fortunato, Rishi Gupta, and Marwin Segler. Chimera: Accurate retrosynthesis prediction by ensembling models with diverse inductive biases. *arXiv preprint arXiv:2412.05269*, 2024.
- [118] Andres M Bran, Theo A Neukomm, Daniel P Armstrong, Zlatko Jončev, and Philippe Schwaller. Chemical reasoning in llms unlocks steerable synthesis planning and reaction mechanism elucidation. *arXiv preprint arXiv:2503.08537*, 2025.
- [119] Yaxia Yuan, Jianfeng Pei, and Luhua Lai. Ligbuilder 2: a practical de novo drug design approach. *Journal of chemical information and modeling*, 51(5):1083–1091, 2011.
- [120] Yaxia Yuan, Jianfeng Pei, and Luhua Lai. Ligbuilder v3: a multi-target de novo drug design approach. *Frontiers in chemistry*, 8:142, 2020.
- [121] Jason D Shields, Rachel Howells, Gillian Lamont, Yin Leilei, Andrew Madin, Christopher E Reimann, Hadi Rezaei, Tristan Reuillon, Bryony Smith, Clare Thomson, et al. Aizynth impact on medicinal chemistry practice at astrazeneca. *RSC Medicinal Chemistry*, 15(4):1085–1095, 2024.
- [122] Cheng-Han Li and Daniel P Tabor. Generative organic electronic molecular design informed by quantum chemistry. *Chemical Science*, 14(40):11045–11055, 2023.
- [123] Albin Ekborg. De novo molecular generation of molecules with consistent synthetic strategy. Master’s thesis, Chalmers University of Technology, 2024.
- [124] Maud Parrot, Hamza Tajmouati, Vinicius Barros Ribeiro da Silva, Brian Ross Atwood, Robin Fourcade, Yann Gaston-Mathé, Nicolas Do Huu, and Quentin Perron. Integrating synthetic accessibility with ai-based generative drug design. *Journal of Cheminformatics*, 15(1):83, 2023.
- [125] Jeff Guo and Philippe Schwaller. It takes two to tango: Directly optimizing for constrained synthesizability in generative molecular design. *arXiv preprint arXiv:2410.11527*, 2024.

- [126] Ewa P Gajewska, Sara Szymkuć, Piotr Dittwald, Michał Startek, Oskar Popik, Jacek Mlynarski, and Bartosz A Grzybowski. Algorithmic discovery of tactical combinations for advanced organic syntheses. *Chem*, 6(1):280–293, 2020.
- [127] Gary Tom, Stefan P Schmid, Sterling G Baird, Yang Cao, Kourosh Darvish, Han Hao, Stanley Lo, Sergio Pablo-García, Ella M Rajaonson, Marta Skreta, et al. Self-driving laboratories for chemistry and materials science. *Chemical Reviews*, 2024.
- [128] Joshua W Sin, Siu Lun Chau, Ryan P Burwood, Kurt Püntener, Raphael Bigler, and Philippe Schwaller. Highly parallel optimisation of nickel-catalysed suzuki reactions through automation and machine intelligence. *ChemRxiv*, 2024.
- [129] Anne-Catherine Bédard, Andrea Adamo, Kosi C Aroh, M Grace Russell, Aaron A Bedermann, Jeremy Torosian, Brian Yue, Klavs F Jensen, and Timothy F Jamison. Reconfigurable system for automated optimization of diverse chemical reactions. *Science*, 361(6408):1220–1225, 2018.
- [130] Sebastian Steiner, Jakob Wolf, Stefan Glatzel, Anna Andreou, Jarosław M Granda, Graham Keenan, Trevor Hinkley, Gerardo Aragon-Camarasa, Philip J Kitson, Davide Angelone, et al. Organic synthesis in a modular robotic system driven by a chemical programming language. *Science*, 363(6423):eaav2211, 2019.
- [131] Nicholas H Angello, Vandana Rathore, Wiktor Beker, Agnieszka Wołos, Edward R Jira, Rafał Roszak, Tony C Wu, Charles M Schroeder, Alán Aspuru-Guzik, Bartosz A Grzybowski, et al. Closed-loop optimization of general reaction conditions for heteroaryl suzuki-miyaura coupling. *Science*, 378(6618):399–405, 2022.
- [132] Wesley Wang, Nicholas H Angello, Daniel J Blair, Theodore Tyrikos-Ergas, William H Krueger, Kameron NS Medine, Antonio J LaPorte, Joshua M Berger, and Martin D Burke. Rapid automated iterative small-molecule synthesis. *Nature Synthesis*, pages 1–8, 2024.
- [133] Nicholas H Angello, David M Friday, Changhyun Hwang, Seungjoo Yi, Austin H Cheng, Tiara C Torres-Flores, Edward R Jira, Wesley Wang, Alán Aspuru-Guzik, Martin D Burke, et al. Closed-loop transfer enables artificial intelligence to yield chemical knowledge. *Nature*, 633(8029):351–358, 2024.
- [134] Felix Strieth-Kalthoff, Han Hao, Vandana Rathore, Joshua Derasp, Théophile Gaudin, Nicholas H Angello, Martin Seifrid, Ekaterina Trushina, Mason Guy, Junliang Liu, et al. Delocalized, asynchronous, closed-loop discovery of organic laser emitters. *Science*, 384(6697):eadk9227, 2024.
- [135] Connor W Coley, Natalie S Eyke, and Klavs F Jensen. Autonomous discovery in the chemical sciences part i: Progress. *Angewandte Chemie International Edition*, 59(51):22858–22893, 2020.
- [136] Connor W Coley, Natalie S Eyke, and Klavs F Jensen. Autonomous discovery in the chemical sciences part ii: outlook. *Angewandte Chemie International Edition*, 59(52):23414–23436, 2020.
- [137] Jenna C Fromer and Connor W Coley. An algorithmic framework for synthetic cost-aware decision making in molecular design. *Nature Computational Science*, 4(6):440–450, 2024.
- [138] Jenna C Fromer, Alexandra D Volkova, and Connor W Coley. Optimal compound downselection to promote diversity and parallel chemistry. *arXiv preprint arXiv:2503.13627*, 2025.
- [139] Sepp Hochreiter and Jürgen Schmidhuber. Long short-term memory. *Neural computation*, 9(8):1735–1780, 1997.
- [140] Daniel Neil, Marwin Segler, Laura Guasch, Mohamed Ahmed, Dean Plumbley, Matthew Sellwood, and Nathan Brown. Exploring deep recurrent models with reinforcement learning for molecule design. In *Proc. 6th International Conference on Learning Representations*, 2018.
- [141] Jeff Guo and Philippe Schwaller. Saturn: Sample-efficient generative molecular design using memory manipulation. *arXiv preprint arXiv:2405.17066*, 2024.
- [142] Krzysztof Maziarz, Austin Tripp, Guoqing Liu, Megan Stanley, Shufang Xie, Piotr Gaiński, Philipp Seidl, and Marwin HS Segler. Re-evaluating retrosynthesis algorithms with syntheseus. *Faraday Discussions*, 256:568–586, 2025.
- [143] Albert Gu and Tri Dao. Mamba: Linear-time sequence modeling with selective state spaces. *arXiv preprint arXiv:2312.00752*, 2023.
- [144] Sunghwan Kim, Jie Chen, Tiejun Cheng, Asta Gindulyte, Jia He, Siqian He, Qingliang Li, Benjamin A Shoemaker, Paul A Thiessen, Bo Yu, et al. Pubchem 2023 update. *Nucleic acids research*, 51(D1):D1373–D1380, 2023.
- [145] David Weininger. Smiles, a chemical language and information system. 1. introduction to methodology and encoding rules. *Journal of chemical information and computer sciences*, 28(1):31–36, 1988.

- [146] Jeff Guo and Philippe Schwaller. Augmented memory: Sample-efficient generative molecular design with reinforcement learning. *JACS Au*, 2024.
- [147] Thomas Blaschke, Josep Arús-Pous, Hongming Chen, Christian Margreitter, Christian Tyrchan, Ola Engkvist, Kostas Papadopoulos, and Atanas Patronov. Reinvent 2.0: an ai tool for de novo drug design. *Journal of chemical information and modeling*, 60(12):5918–5922, 2020.
- [148] Hannes H Loeffler, Jiazhen He, Alessandro Tibo, Jon Paul Janet, Alexey Voronov, Lewis H Mervin, and Ola Engkvist. Reinvent 4: Modern ai-driven generative molecule design. *Journal of Cheminformatics*, 16(1):20, 2024.
- [149] Ronald J Williams. Simple statistical gradient-following algorithms for connectionist reinforcement learning. *Machine learning*, 8:229–256, 1992.
- [150] Nadine Schneider, Nikolaus Stiefl, and Gregory A Landrum. What’s what: The (nearly) definitive guide to reaction role assignment. *Journal of chemical information and modeling*, 56(12):2336–2346, 2016.
- [151] Hanjun Dai, Chengtao Li, Connor Coley, Bo Dai, and Le Song. Retrosynthesis prediction with conditional graph logic network. *Advances in Neural Information Processing Systems*, 32, 2019.
- [152] Maarten R Dobbelaere, István Lengyel, Christian V Stevens, and Kevin M Van Geem. Rxn-insight: fast chemical reaction analysis using bond-electron matrices. *Journal of Cheminformatics*, 16(1):37, 2024.
- [153] John S Carey, David Laffan, Colin Thomson, and Mike T Williams. Analysis of the reactions used for the preparation of drug candidate molecules. *Organic & biomolecular chemistry*, 4(12):2337–2347, 2006.
- [154] Inc. Daylight Chemical Information Systems. Smirks - a reaction transform language.
- [155] Philippe Schwaller, Benjamin Hoover, Jean-Louis Reymond, Hendrik Strobelt, and Teodoro Laino. Extraction of organic chemistry grammar from unsupervised learning of chemical reactions. *Science Advances*, 7(15): eabe4166, 2021.
- [156] Steven M Kearnes, Michael R Maser, Michael Wlekinski, Anton Kast, Abigail G Doyle, Spencer D Dreher, Joel M Hawkins, Klavs F Jensen, and Connor W Coley. The open reaction database. *Journal of the American Chemical Society*, 143(45):18820–18826, 2021.
- [157] NextMove Software. Namrxn.
- [158] Oleg Trott and Arthur J Olson. Autodock vina: improving the speed and accuracy of docking with a new scoring function, efficient optimization, and multithreading. *Journal of computational chemistry*, 31(2):455–461, 2010.
- [159] Amr Alhossary, Stephanus Daniel Handoko, Yuguang Mu, and Chee-Keong Kwoh. Fast, accurate, and reliable molecular docking with quickvina 2. *Bioinformatics*, 31(13):2214–2216, 2015.
- [160] Shidi Tang, Ji Ding, Xiangyu Zhu, Zheng Wang, Haitao Zhao, and Jiansheng Wu. Vina-gpu 2.1: towards further optimizing docking speed and precision of autodock vina and its derivatives. *bioRxiv*, pages 2023–11, 2023.
- [161] Mark F Mabanglo, Keith S Wong, Marim M Barghash, Elisa Leung, Stephanie HW Chuang, Afshan Ardalan, Emily M Majaesic, Cassandra J Wong, Shen Zhang, Henk Lang, et al. Potent clpp agonists with anticancer properties bind with improved structural complementarity and alter the mitochondrial n-terminome. *Structure*, 31(2):185–200, 2023.
- [162] G Richard Bickerton, Gaia V Paolini, Jérémy Besnard, Sorel Muresan, and Andrew L Hopkins. Quantifying the chemical beauty of drugs. *Nature chemistry*, 4(2):90–98, 2012.
- [163] Scott E Lazerwith, Gina Bahador, Eda Canales, Guofeng Cheng, Lee Chong, Michael O Clarke, Edward Doerffler, Eugene J Eisenberg, Jaclyn Hayes, Bing Lu, et al. Optimization of pharmacokinetics through manipulation of physicochemical properties in a series of hcv inhibitors. *ACS Medicinal Chemistry Letters*, 2(10):715–719, 2011.
- [164] Peter W Kenny. Hydrogen-bond donors in drug design. *Journal of medicinal chemistry*, 65(21):14261–14275, 2022.
- [165] Guy W Bemis and Mark A Murcko. The properties of known drugs. 1. molecular frameworks. *Journal of medicinal chemistry*, 39(15):2887–2893, 1996.
- [166] Daniil Polykovskiy, Alexander Zhebrak, Benjamin Sanchez-Lengeling, Sergey Golovanov, Oktai Tatanov, Stanislav Belyaev, Rauf Kurbanov, Aleksey Artamonov, Vladimir Aladinskiy, Mark Veselov, et al. Molecular sets (moses): a benchmarking platform for molecular generation models. *Frontiers in pharmacology*, 11:565644, 2020.
- [167] Yutong Xie, Ziqiao Xu, Jiaqi Ma, and Qiaozhu Mei. How much space has been explored? measuring the chemical space covered by databases and machine-generated molecules. In *Proc. 11th International Conference on Learning Representations*, 2023.

- [168] Richard A Friesner, Jay L Banks, Robert B Murphy, Thomas A Halgren, Jasna J Klicic, Daniel T Mainz, Matthew P Repasky, Eric H Knoll, Mee Shelley, Jason K Perry, et al. Glide: a new approach for rapid, accurate docking and scoring. 1. method and assessment of docking accuracy. *Journal of medicinal chemistry*, 47(7):1739–1749, 2004.
- [169] Dean G Brown and Jonas Bostrom. Analysis of past and present synthetic methodologies on medicinal chemistry: where have all the new reactions gone? miniperspective. *Journal of medicinal chemistry*, 59(10):4443–4458, 2016.
- [170] Christopher A Lipinski, Franco Lombardo, Beryl W Dominy, and Paul J Feeney. Experimental and computational approaches to estimate solubility and permeability in drug discovery and development settings. *Advanced drug delivery reviews*, 64:4–17, 2012.
- [171] Sriram Mahesh, Kuei-Chien Tang, and Monika Raj. Amide bond activation of biological molecules. *Molecules*, 23(10):2615, 2018.
- [172] Jeff Guo, Jon Paul Janet, Matthias R Bauer, Eva Nittinger, Kathryn A Giblin, Kostas Papadopoulos, Alexey Voronov, Atanas Patronov, Ola Engkvist, and Christian Margreitter. Dockstream: a docking wrapper to enhance de novo molecular design. *Journal of cheminformatics*, 13:1–21, 2021.
- [173] Bowen Gao, Haichuan Tan, Yanwen Huang, Minsi Ren, Xiao Huang, Wei-Ying Ma, Ya-Qin Zhang, and Yanyan Lan. From theory to therapy: Reframing sbdd model evaluation via practical metrics. In *Proc. 13th International Conference on Learning Representations*, 2025.
- [174] Anita Ivanković, Ana Dronjić, Anita Martinović Bevanda, and Stanislava Talić. Review of 12 principles of green chemistry in practice. *International Journal of Sustainable and Green Energy*, 6(3):39–48, 2017.
- [175] Ian S Young and Phil S Baran. Protecting-group-free synthesis as an opportunity for invention. *Nature chemistry*, 1(3):193–205, 2009.
- [176] Stéphane Caron. *Practical synthetic organic chemistry: reactions, principles, and techniques*. John Wiley & Sons, 2020.
- [177] Agnieszka Wołos, Dominik Koszelewski, Rafał Roszak, Sara Szymkuć, Martyna Moskal, Ryszard Ostaszewski, Brenden T Herrera, Josef M Maier, Gordon Brezicki, Jonathon Samuel, et al. Computer-designed repurposing of chemical wastes into drugs. *Nature*, 604(7907):668–676, 2022.
- [178] R G Kurumbail, A M Stevens, J K Gierse, J J McDonald, R A Stegeman, J Y Pak, D Gildehaus, J M Miyashiro, T D Penning, K Seibert, P C Isakson, and W C Stallings. Structural basis for selective inhibition of cyclooxygenase-2 by anti-inflammatory agents. *Nature*, 384(6610):644–648, 1996.
- [179] Andrew T McNutt, Paul Francoeur, Rishal Aggarwal, Tomohide Masuda, Rocco Meli, Matthew Ragoza, Jocelyn Sunseri, and David Ryan Koes. GNINA 1.0: molecular docking with deep learning. *J. Cheminform.*, 13(1):43, June 2021.
- [180] Matthias R Bauer, Tamer M Ibrahim, Simon M Vogel, and Frank M Boeckler. Evaluation and optimization of virtual screening workflows with DEKOIS 2.0—a public library of challenging docking benchmark sets. *J. Chem. Inf. Model.*, 53(6):1447–1462, June 2013.
- [181] T V Tony Phan, Cyril Gallardo, and Jean Mane. GREEN MOTION: a new and easy to use green chemistry metric from laboratories to industry. *Green Chem.*, 17(5):2846–2852, 2015.
- [182] Rodolfo I Teixeira, Michael Andresini, Renzo Luisi, and Brahim Benyahia. Computer-aided retrosynthesis for greener and optimal total synthesis of a helicase-primase inhibitor active pharmaceutical ingredient. *JACS Au*, 4(11):4263–4272, November 2024.
- [183] Filippo Brienza, David Cannella, Diego Montesdeoca, Iwona Cybulska, and Damien P Debecker. A guide to lignin valorization in biorefineries: traditional, recent, and forthcoming approaches to convert raw lignocellulose into valuable materials and chemicals. *RSC Sustain.*, 2023.
- [184] Alexander Neumann, Lester Marrison, and Raphael Klein. Relevance of the trillion-sized chemical space “explore” as a source for drug discovery. *ACS Medicinal Chemistry Letters*, 14(4):466–472, 2023.
- [185] Kathryn Klarich, Brian Goldman, Trevor Kramer, Patrick Riley, and W Patrick Walters. Thompson sampling - an efficient method for searching ultralarge synthesis on demand databases. *Journal of Chemical Information and Modeling*, 64(4):1158–1171, 2024.
- [186] Tom George Grigg, Mason Burlage, Oliver Brook Scott, Dominique Sydow, and Liam Wilbraham. Active learning on synthons for molecular design. In *ICLR 2025 Workshop on Generative and Experimental Perspectives for Biomolecular Design*, 2025.

- [187] David E Graff, Eugene I Shakhnovich, and Connor W Coley. Accelerating high-throughput virtual screening through molecular pool-based active learning. *Chemical science*, 12(22):7866–7881, 2021.
- [188] Saulo H P de Oliveira, Aryan Pedawi, Victor Kenyon, and Henry van den Bedem. Ngt: Generative ai with synthesizability guarantees discovers mc2r inhibitors from a tera-scale virtual screen. *Journal of Medicinal Chemistry*, 67(21):19417–19427, 2024.
- [189] Dave Cosgrove. Introducing synthon searching, 2024.
- [190] Qi Yuan, Alejandro Santana-Bonilla, Martijn A Zwijnenburg, and Kim E Jelfs. Molecular generation targeting desired electronic properties via deep generative models. *Nanoscale*, 12(12):6744–6758, 2020.
- [191] John A Arnott and Sonia Lobo Planey. The influence of lipophilicity in drug discovery and design. *Expert opinion on drug discovery*, 7(10):863–875, 2012.
- [192] Yoshua Bengio, Salem Lahlou, Tristan Deleu, Edward J Hu, Mo Tiwari, and Emmanuel Bengio. Gflownet foundations. *Journal of Machine Learning Research*, 24(210):1–55, 2023.
- [193] Emmanuel Bengio, Moksh Jain, Maksym Korablyov, Doina Precup, and Yoshua Bengio. Flow network based generative models for non-iterative diverse candidate generation. *Advances in Neural Information Processing Systems*, 34:27381–27394, 2021.
- [194] Wenhao Gao, Tianfan Fu, Jimeng Sun, and Connor Coley. Sample efficiency matters: a benchmark for practical molecular optimization. *Advances in neural information processing systems*, 35:21342–21357, 2022.
- [195] Teague Sterling and John J Irwin. Zinc 15–ligand discovery for everyone. *Journal of chemical information and modeling*, 55(11):2324–2337, 2015.
- [196] Shitong Luo, Wenhao Gao, Zuofan Wu, Jian Peng, Connor W Coley, and Jianzhu Ma. Projecting molecules into synthesizable chemical spaces. In *International Conference on Machine Learning*, pages 33289–33304. PMLR, 2024.
- [197] eMolecules. Chemical building blocks.
- [198] Xin-Min Zhang, Qing Chang, Lin Zeng, Judy Gu, Stuart Brown, and Ross S Basch. Tblr1 regulates the expression of nuclear hormone receptor co-repressors. *BMC cell biology*, 7:1–17, 2006.
- [199] Bowen Gao, Haichuan Tan, Yanwen Huang, Minsi Ren, Xiao Huang, Wei-Ying Ma, Ya-Qin Zhang, and Yanyan Lan. From theory to therapy: Reframing sbdd model evaluation via practical metrics. *arXiv preprint arXiv:2406.08980*, 2024.
- [200] Dongsung Kim, Lorenz Herdeis, Dorothea Rudolph, Yulei Zhao, Jark Böttcher, Alberto Vides, Carlos I Ayala-Santos, Yasin Pourfarjam, Antonio Cuevas-Navarro, Jenny Y Xue, et al. Pan-kras inhibitor disables oncogenic signalling and tumour growth. *Nature*, 619(7968):160–166, 2023.
- [201] Mohit Pandey, Gopeshh Subbaraj, Artem Cherkasov, and Emmanuel Bengio. Pretraining generative flow networks with inexpensive rewards for molecular graph generation. *arXiv preprint arXiv:2503.06337*, 2025.
- [202] Viet-Khoa Tran-Nguyen, Célien Jacquemard, and Didier Rognan. Lit-pcba: an unbiased data set for machine learning and virtual screening. *Journal of chemical information and modeling*, 60(9):4263–4273, 2020.
- [203] Jan H Jensen. A graph-based genetic algorithm and generative model/monte carlo tree search for the exploration of chemical space. *Chemical science*, 10(12):3567–3572, 2019.
- [204] Jordan E Crivelli-Decker, Zane Beckwith, Gary Tom, Ly Le, Sheenam Khuttan, Romelia Salomon-Ferrer, Jackson Beall, Rafael Gómez-Bombarelli, and Andrea Bortolato. Machine learning guided aqfep: A fast and efficient absolute free energy perturbation solution for virtual screening. *Journal of Chemical Theory and Computation*, 20(16):7188–7198, 2024.
- [205] J Harry Moore, Matthias R Bauer, Jeff Guo, Atanas Patronov, Ola Engkvist, and Christian Margreitter. Icolos: a workflow manager for structure-based post-processing of de novo generated small molecules. *Bioinformatics*, 38(21):4951–4952, 2022.
- [206] Hannes H Loeffler, Shunzhou Wan, Marco Kl"ahn, Agastya P Bhati, and Peter V Coveney. Optimal molecular design: Generative active learning combining reinvent with precise binding free energy ranking simulations. *Journal of Chemical Theory and Computation*, 20(18):8308–8328, 2024.
- [207] Shopnil Akash, Farjana Islam Aovi, Md AK Azad, Ajoy Kumer, Unesco Chakma, Md Rezaul Islam, Nobendu Mukerjee, Md Mominur Rahman, Imren Bayıl, Summya Rashid, et al. A drug design strategy based on molecular docking and molecular dynamics simulations applied to development of inhibitor against triple-negative breast cancer by scutellarein derivatives. *PLoS One*, 18(10):e0283271, 2023.

- [208] Julius Seumer and Jan H Jensen. Beyond predefined ligand libraries: A genetic algorithm approach for de novo discovery of catalysts for the suzuki coupling reactions. *PeerJ Physical Chemistry*, 7:e34, 2025.
- [209] Yang Yu. Towards sample efficient reinforcement learning. In *IJCAI*, pages 5739–5743, 2018.
- [210] Karol Molga, Ewa P Gajewska, Sara Szymkuć, and Bartosz A Grzybowski. The logic of translating chemical knowledge into machine-processable forms: a modern playground for physical-organic chemistry. *Reaction Chemistry & Engineering*, 4(9):1506–1521, 2019.
- [211] Zihan Wang, Kangjie Lin, Jianfeng Pei, and Luhua Lai. Reacon: a template-and cluster-based framework for reaction condition prediction. *Chemical Science*, 16(2):854–866, 2025.
- [212] Jeff Guo, Vendy Fialková, Juan Diego Arango, Christian Margreitter, Jon Paul Janet, Kostas Papadopoulos, Ola Engkvist, and Atanas Patronov. Improving de novo molecular design with curriculum learning. *Nature Machine Intelligence*, 4(6):555–563, 2022.
- [213] Maranga Mokaya, Fergus Imrie, Willem P van Hoorn, Aleksandra Kalisz, Anthony R Bradley, and Charlotte M Deane. Testing the limits of smiles-based de novo molecular generation with curriculum and deep reinforcement learning. *Nature Machine Intelligence*, 5(4):386–394, 2023.
- [214] James Chen. Mamba no. 5 (a little bit of...). 2024.
- [215] Ashish Vaswani, Noam Shazeer, Niki Parmar, Jakob Uszkoreit, Llion Jones, Aidan N Gomez, Łukasz Kaiser, and Illia Polosukhin. Attention is all you need. *Advances in neural information processing systems*, 30, 2017.
- [216] Esben Jannik Bjerrum. Smiles enumeration as data augmentation for neural network modeling of molecules. *arXiv preprint arXiv:1703.07076*, 2017.
- [217] Thomas Blaschke, Ola Engkvist, Jürgen Bajorath, and Hongming Chen. Memory-assisted reinforcement learning for diverse molecular de novo design. *Journal of cheminformatics*, 12(1):68, 2020.
- [218] Kaori Ando. A mechanistic study of the horner–wadsworth–emmons reaction: Computational investigation on the reaction pass and the stereochemistry in the reaction of lithium enolate derived from trimethyl phosphonoacetate with acetaldehyde. *The Journal of Organic Chemistry*, 64(18):6815–6821, 1999. doi:10.1021/jo9909150.
- [219] Christiane Ehrt, Bennet Krause, Robert Schmidt, Emanuel S. R. Ehmki, and Matthias Rarey. Smarts.plus – a toolbox for chemical pattern design. *Molecular Informatics*, 39(12), October 2020. ISSN 1868-1751. doi:10.1002/minf.202000216.
- [220] Peter Eastman, Mark S Friedrichs, John D Chodera, Randall J Radmer, Christopher M Bruns, Joy P Ku, Kyle A Beauchamp, Thomas J Lane, Lee-Ping Wang, Diwakar Shukla, et al. Openmm 4: a reusable, extensible, hardware independent library for high performance molecular simulation. *Journal of chemical theory and computation*, 9(1):461–469, 2013.